JPRS-JST-91-030
10 SEPTEMBER 1991

Foreign Broadcast Information Service 50 ANNIVERSARY 1941 - 1991

JPRS Report

Science & Technology

Japan

NEW MANUFACTURING TECHNOLOGY FOR CERAMICS

JPRS-JST-91-030
10 SEPTEMBER 1991

SCIENCE & TECHNOLOGY
JAPAN

NEW MANUFACTURING TECHNOLOGY FOR CERAMICS

916C0033 Osaka DAI 18 KAI NYU SERAMIKKUSU SEMINA TEKISUTO in Japanese 2 Mar 91 pp 1-110

[Selected papers from the 18th New Ceramics Seminar on New Ceramics Manufacturing Technology held 28 Feb-1 Mar 91 in Osaka and sponsored by New Ceramics Konwakai, Osaka Prefectural Technology Association]

CONTENTS

New Slip Casting Technology

916C0033A Osaka DAI 18 KAI NYU SERAMIKKUSU SEMINA TEKISUTO in Japanese
2 Mar 91 pp 11-31

[Article by Sumihiko Kurita, Koransha Co., Ltd.: "NK and K Processes"]

[Text] **K Process**

With the conventional slip casting methods using plaster mold, the mold for some complicated shapes must be designed so as to divide them into several parts, and the drawing taper of the mold must be taken into account. Cracks or distortion problems sometimes occur when removing the mold.

Koransha Co., Ltd., has developed the "K-Process" to form near-net-shape ceramics in complicated configurations without such problems. We use a mixture of powder and liquid solidified as a mold instead of plaster. The solidified mold retains the designed shape and has the property of absorbing liquid. After molding ceramics slurry, the solidified mixture mold disintegrates at increased temperature. Near-net-shape green bodies remain without the problems.

We have achieved a sintered density in complicated shapes as high as the highest levels seen from conventional methods using a plaster mold, but with a smooth surface condition.

1. Introduction

At Koransha, an accumulation of the slip casting expertise obtained in years of manufacturing ceramic ware is used in fabricating fine ceramics. We have developed additives (dispersant, binder) for slip as well as our dispersing techniques. This has the following advantage: green density has been raised. Even sintering at atmospheric pressure enables the density of the sintered body to the maintained at levels higher than the theoretical density value of 99 percent. As a result, it has become possible to use the slip casting process in processing engineering ceramics. The technique is a mainstay in our processing of fine ceramics.

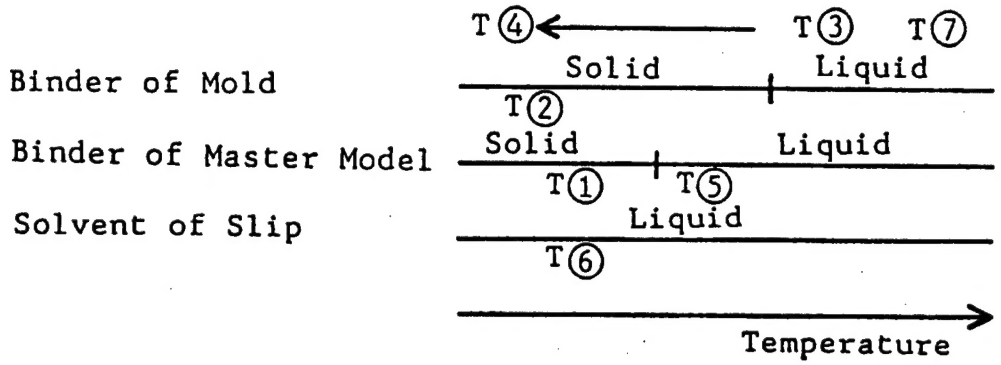

* T①,T② ..... follow the working temperature of the process in Figure 2 respectively.

Figure 1. States Change of Binders and Working Temperature in K-Process

In light of increased demand for complex shapes, such as reverse taper, and for high-dimensional accuracy in recent years, we have been developing new slip casting processes. This paper describes a new slip casting method (K process) and provides examples of the technique's applications.

2. New Slip Casting Process--Principle and Flow Chart of K Process

Drawbacks of slip casting using conventional plaster molds are that the mold must be divided into several parts when forming a complex shape, reducing operational efficiency to a great extent, and that the resulting green part often contains many deformations and cracks.

In the K process (Figures 1 and 2) a mixture of powder and liquid solidified is used as a mold instead of plaster. The solidified mold has water-absorbing properties. After the ceramic slurry is poured into the mold, heating makes the mold disintegrate, creating a complex green part to near-net shape.

When the mold, the binder for the master model, and the equilibrium temperature between the solid and liquid phases for the solvent of slip are selected (Figure 1) and the working temperatures for operations (1) through (7) are set, we are ready for the new slip casting (K process) described in Figure 2. Temperatures T(1) through T(7) in Figure 1 correspond to the temperatures for operations (1) through (7) in Figure 2.

The master model is formed at T(1) and the raw material powder for the mold is poured in at T(2). A binder with a solid-liquid equilibrium larger than that of the binder for the master model is poured into the powder at T(3), and the powder impregnated with the binder is refrigerated to the working temperature set for T(4) to form a mold. After a mold is formed, heat is applied to melt and drive off the master model, which generates a cavity. A ceramic slurry at T(6), dissolved in a solvent that remains liquid within the working temperature range, is poured into the cavity and left to accumulate. The mold is disintegrated at T(7), and the green body results.

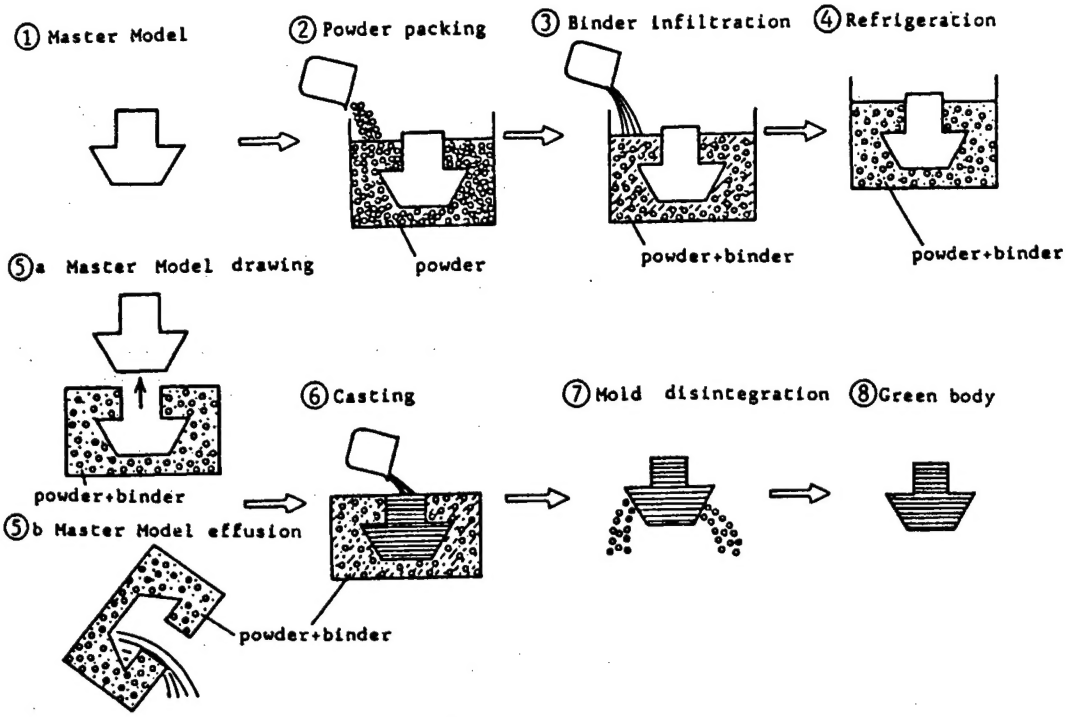

Figure 2. K Process

This sequence of process steps comprises the K process (patent pending). As for the process step (5)—letting the master model effuse—the mainstay is (5)b, but, depending on the shape, (5)a—drawing out the master model made of rubber—is used.

3. Example of Research--Water, Alcohol System

An example of materials used for the research and development of the K process is given in Table 1.

Table 1. Using Materials in This Report

Mold, master model	Polyethylene (average particle size: 20 μm)
Ceramic powder	Si_3N_4, Y_2O_3, Al_2O_3, deflocculent, binder
Binder of mold Master mold Solvent of slip	H_2O + C_2H_5OH

3.1 Process for Selection of Binder and Solvent for Slip and Working Temperature

A water plus ethyl alcohol system was used as the binder and solvent for slip for the mold and master model. The relationship between freezing temperatures and viscosities of the system were measured, and studies were done to examine

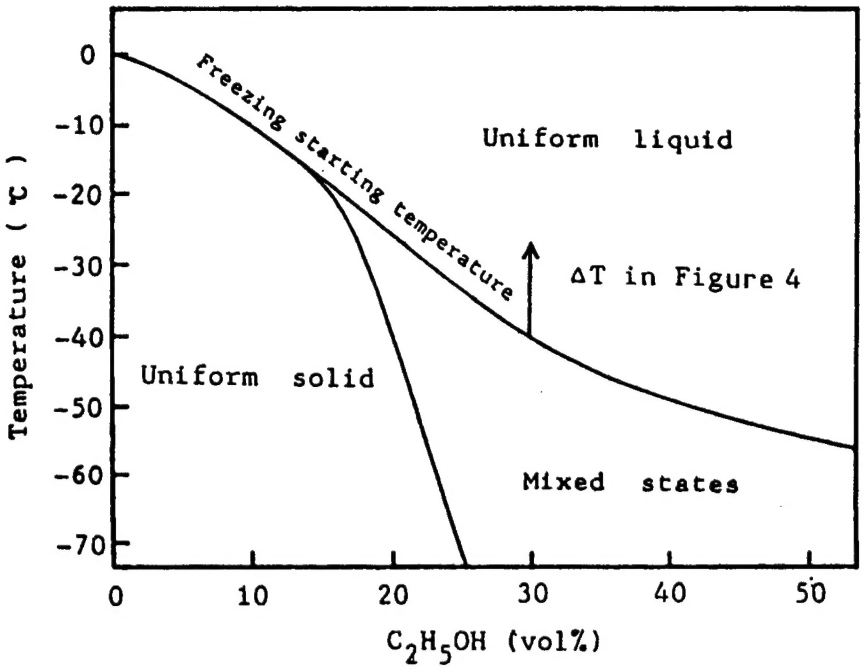

Figure 3. States of Binder at Low Temperature

the ratios of water and ethyl alcohol fractions that satisfied the conditions for the settings.

Figure 3 shows temperatures at which the water plus ethyl alcohol system begins to freeze. Depending on temperatures and composition, the system showed different states—uniform liquid, uniform solid, and an intermediate of the two. When the ethyl alcohol content was up to 10 percent or so by volume, the water plus ethyl alcohol system showed a uniform state of freezing, but when it increased to more than 20 volume percent, the system showed a nonuniform state of freezing, transforming itself into something like a sherbet. When the content was above 30 volume percent, the system could no longer be handled as a rigid body, even when kept at a temperature of −70°C. We used water only for the mold, water plus 15 percent ethyl alcohol by volume for the master model, and water plus 30 percent ethyl alcohol by volume for the solvent for slip.

Figure 4 shows the viscosity as a function of temperature for the water plus 30 volume percent ethyl alcohol solvent system and the solvent plus required powder, such as Si_3N_4 system. The difference between freezing and casting temperatures is represented by ΔT.

The solvent begins to freeze at −40°C. Using this temperature as the standard, ΔT in Figure 3 is plotted on the axis of abscissa in the graph, and viscosities of the solvent and slip are plotted on the axis or ordinate. At ΔT = 20°C, that is, −20°C, there is no effect of a solid phase, and the binder has a viscosity of about 6 cp. We added Si_3N_4 powder to the level where the solvent content (solvent/powder plus solvent) reached 50 percent. The results are shown by broken lines. With the addition of ceramic powder, the system's

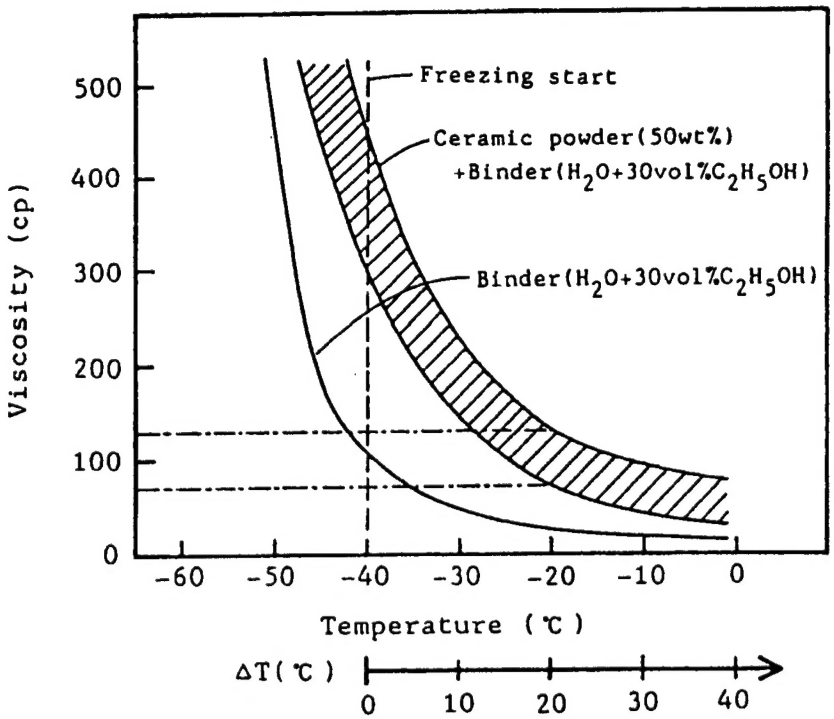

Figure 4. Viscosity of Binder and Slip

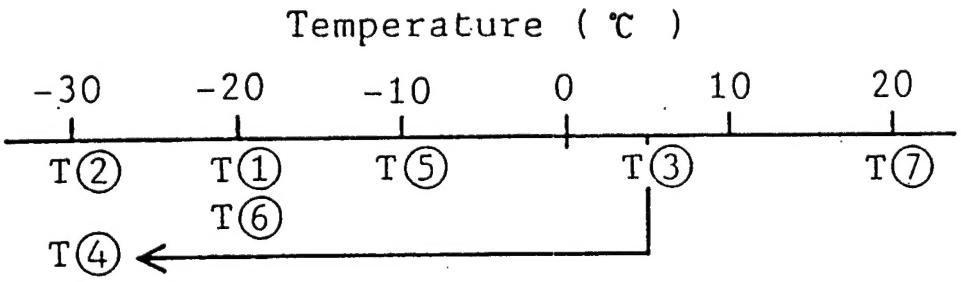

Binder of mold	H_2O
Binder of master model	H_2O+15vol%C_2H_5OH
Solvent of slip	H_2O+30vol%C_2H_5OH

* T①,T② ..... follow in Figures 1 & 2.

Figure 5. Working Temperature of K Process

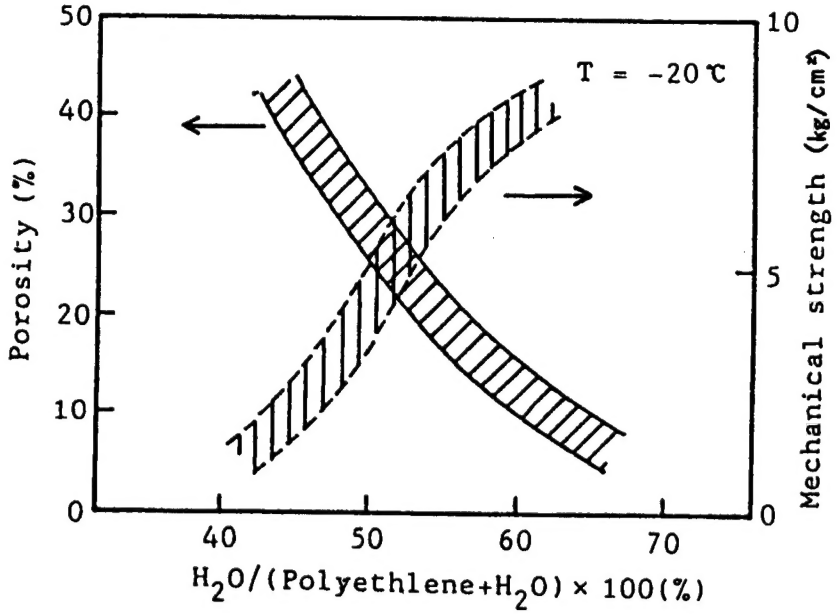

Figure 6. Porosity and Mechanical Strength of Mold

viscosity began to rise, reaching about 100 cp at the aforementioned temperature, which shows its availability for use as slip. After taking into account the effect of the solid phase and the ease of operation, we set the casting temperature at -20°C. Using this temperature as the standard, we determined the temperatures and water-ethyl alcohol ratios for each of the process steps given in Figure 2. The results are given in Figure 5.

3.2 Preparation of Master Model and Mold

The raw material for the master model was powder of polyethylene (PE). The binder was water plus 15 volume percent ethyl alcohol, and the ratio of PE and binder was 1:2 by weight.

As with the master model, the mold was formed using PE and water. To study the mold's capacity to absorb the slip solvent in the subsequent casting process, we measured the porosity of the mold and its mechanical strength at low temperature by changing the PE-water ratio to various levels. The results are given in Figure 6.

After taking into account the relationship between porosity and mechanical strength, we determined water content (water/water plus powder) at 55 percent. The mold's porosity at 20 percent was about one-half of a plaster mold. Its mechanical strength at 7 kg/cm was about one-half that of a plaster mold.

3.3 Conditions for Preparation of Slip

We measured viscosity at -20°C of the casting temperature set at 3.1 by adding solvent (water plus 30 volume percent alcohol) and further dispersant and binder (Figure 7) to the Si_3N_4 powder.

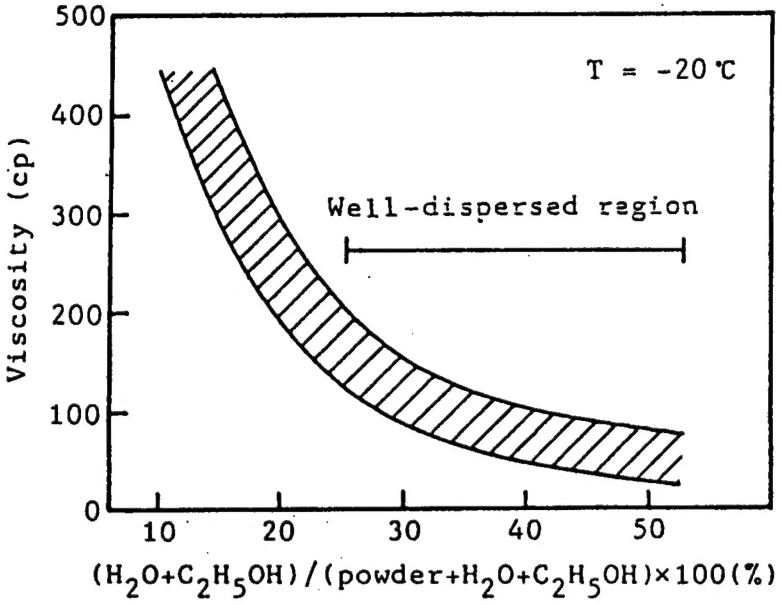

Figure 7. Viscosity of Slip

The powder dispersed well until the solvent content (solvent/powder plus solvent) reached 25~50 percent. After taking into account that our company's standard viscosity of slip for slip casting is 100 cp ± 30 cp, the ease of operation, and yields, we adopted the slip obtainable when the solvent content (solvent/powder plus solvent) was 35 percent.

4. Results of Actual Applications and Problems

The mold disintegrated exactly in the manner intended in the initial stage of the process' development (Photo 1), and a scar-free, complex-shaped green body of high-dimensional accuracy was obtained.

The green body was compared with a similar product based on a plaster mold (Table 2). Although the K process had an accumulative rate about one-fourth as large as that for the plaster process, the former was by no means inferior in other properties.

Table 2. Properties of Green and Sintered Si_3N_4 Materials

Item			Plaster mold	K process
Green body	Density	(g/cm^3)	1.80	1.80
	Accumulative rate	(mm/sec)	12	3
Sintered body	Density	(g/cm^3)	3.21	3.21
	Accumulative rate	(mm/sec)	100	100

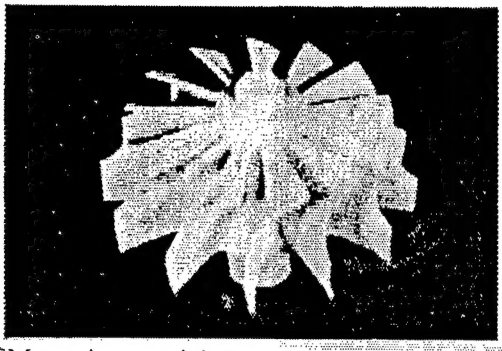

①Master Model

⑤Master Model effusion

②Powder packing

⑥Casting

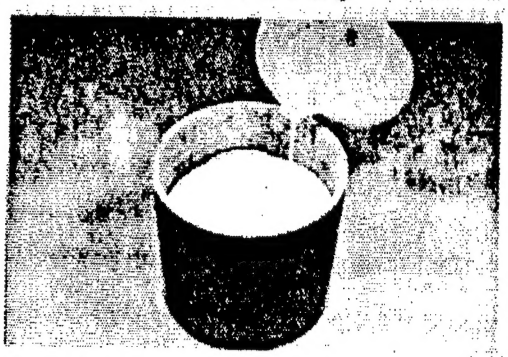

③Binder infiltration

⑦Mold disintegration

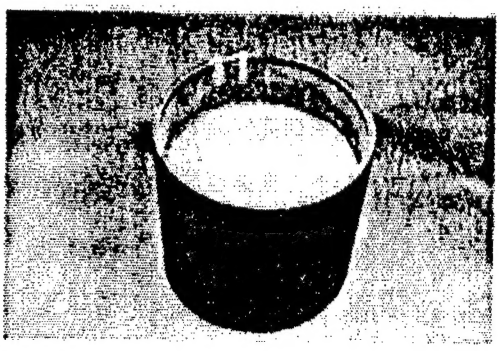

④Refrigeration

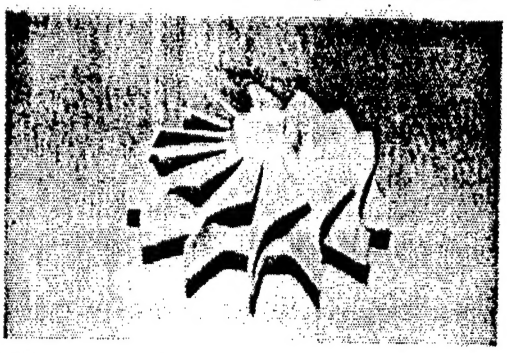

⑧Green body

Photo 1. K Process

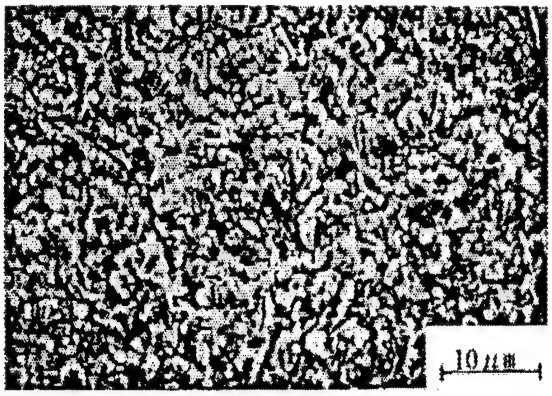

Photo 2. Sintered Si_3N_4 Materials in K Process

The sintered body formed in the K process had a composition similar to that formed in the plastic mold process. A scanning electron microscope (SEM) photograph of the sintered body is shown in Photo 2.

5. Conclusion

The K process enables green bodies to be obtained of an equal quality to those based on plaster molds. The K process, which features the ease of the master model effusion and natural disintegration of the mold, has the following advantages over the plaster mold process:

(1) Greens of complex shapes can be formed.
(2) The green can be easily released from the mold.
(3) The obtained greens are free from burrs or crack burrs.
(4) The mold materials can be recycled.
(5) The mold is free from abrasion; the resulting green has high-dimensional accuracy.

Problems with the K process are that working temperatures are below the freezing point and sophisticated temperature control is needed. The K process described in this report is in its early stages, using water and alcohol for the binder. We are now working on a new K process that can be executed at room temperature.

NK Process

1. Introduction

For forming ceramic parts of complex shapes, injection molding and slip casting are used. Injection molding featuring shorter processing time and high-dimensional accuracy is highly suited to volume production, but it has the following drawbacks:

(1) Because the material is injected at high pressure, the dies wear off rapidly. The high prices of dies make the technique unsuited for use in manufacturing a large variety of products in small quantities.

(2) The processing method cannot be used for manufacturing large-sized or thick products. Cracks appear in parts with a diameter in excess of 35 mm.

(3) Because thermoplastic resins are widely used as the binder, the process to drive off the resin requires application of heat of about 500°C for many hours, which increases cost.

Slip casting, on the other hand, uses plaster molds. The molds are cheap, and the process is suited for forming large-sized parts. Thus, the technique is suited for manufacturing a large variety of products in small quantities. It has the following drawbacks:

(1) Because the solvent must be absorbed by the plaster mold, a long time is needed before the ceramic slurry accumulates, which leads to lower productivity.

(2) The plaster mold wears off rapidly and generally has low-dimensional accuracy.

(3) In the case of thick parts, differences in density between the inside and outside arise.

We embarked on developing a new processing method, called the slip cast injection method, that incorporates advantages of the injection molding and slip casting methods. We are already studying the technique's application in ultrahard materials and metals.

2. NK Process

2.1 The NK process is an abbreviation of the new Koransha process. Using hardening resins for the binder, slip (slurry) is poured into a mold at atmospheric pressure, which hardens on its own, enabling the green part to be released from the mold in a shorter time. The process is similar to the process for curing cement.

Slip-casting techniques have advanced from the conventional method using a plaster mold, which has a history dating back to more than 100 years, to refrigeration casting (K process) announced a few years ago to the NK process, which allows the use of various kinds of molds (metal, plastic, and plaster) and enables various large and thick parts to be formed within five minutes.

In the NK process, the content of the resin binder accounts for only a few percent or less of the total volume, and it can be easily removed. The method also is suited to production of a large variety of parts in small quantities and volume production. At Koransha, a large part of the fine ceramics produced have been manufactured using the NK process.

2.2 Comparing Slip-Casting Method With NK Process

Table 1. Slip–Casting Method Vs. NK Process

Item	Slip casting process	NK process
Mold	Plaster, resin (water absorbing)	Metal, resin, plaster (no water–absorbing)
Green	Good uniformity, but porosity differences in thick parts	High uniformity
Core use	Not available	Available
Drawing	Occur depending on shape (large casting port)	No generation (small casting port)
Shrinkage	<	
Dimensional accuracy	About ± 3%	Below ± 1%
Characteristic (bending strength)	<	
Productivity	<	
Material loss	Small	Extremely small (calculable)

3. Manufacturing Process

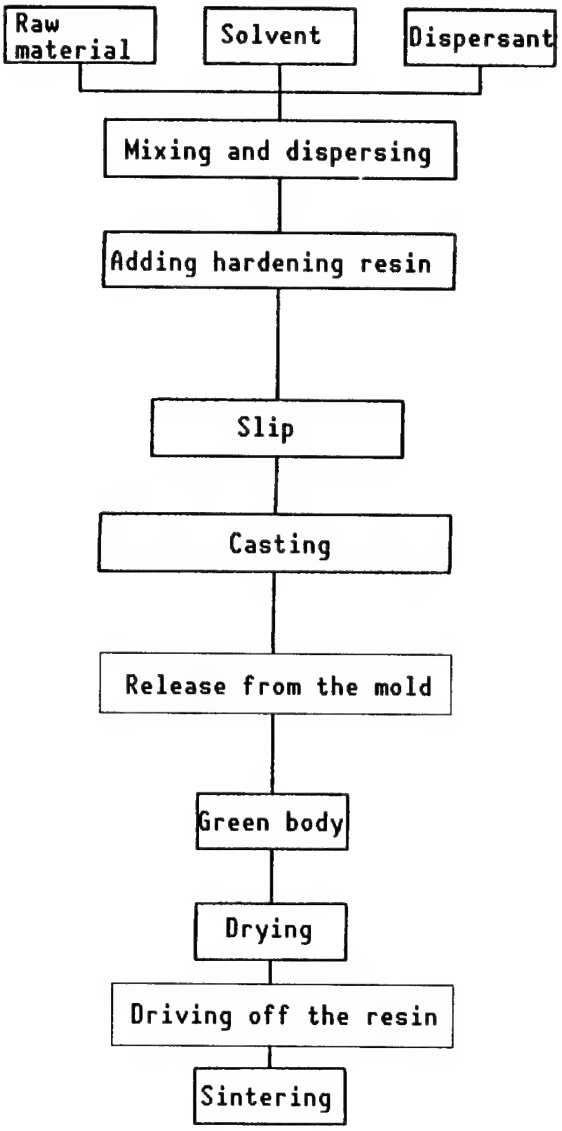

Figure 1. Manufacturing Process

• Sequence of processing steps

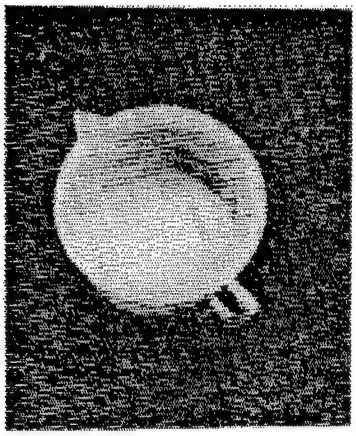

Slip

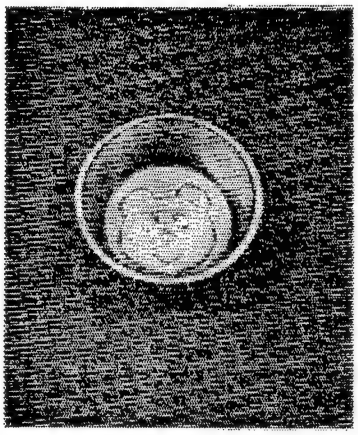

Die

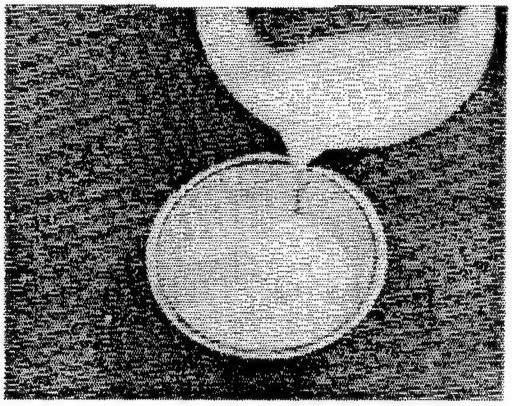

Pouring

Release from mold

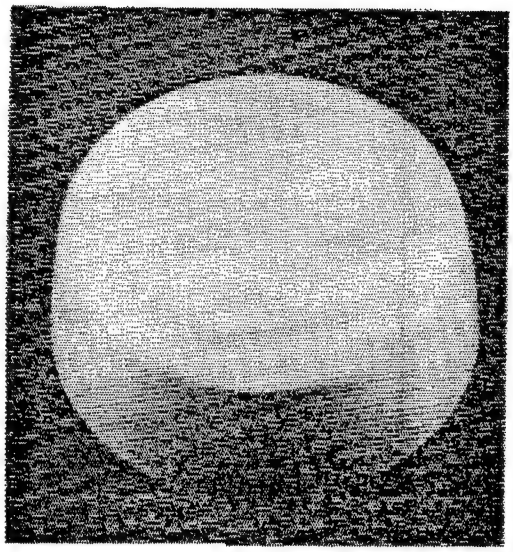

Green body

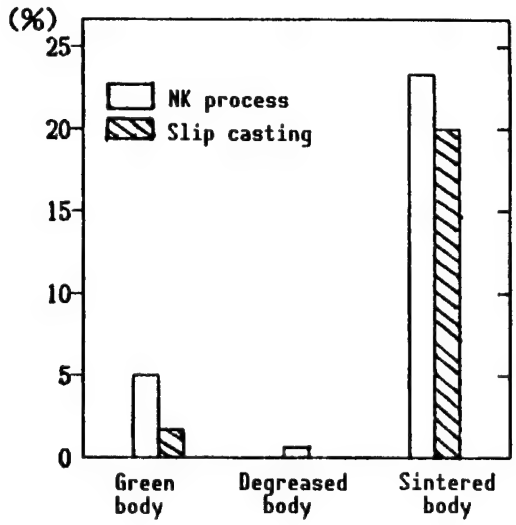

Figure 2.

4. Processing Additives

Binder	Hardening resins (phenol, acryl, urethane, urea, epoxy, PVA, etc.)
Solvent	Alcohols (methanol, ethanol, I.P.A.), water, aromatics (benzene, toluene, xylene)
Dispersant	C.M.C, polyacrylic ammonium salt, polyacrylic methyl, glycerine fatty acid ester

5. Manufacture of Fine Ceramics

5.1 PSZ (ZrO_2)

Powder PSZ: grain diameter 0.5 μm; relative surface area 7.5 m^2/g; Y_2O_3 0.3 mol percent.

This ceramic powder is added with 0.85 weight percent polycarboxylic ammonium dispersant. The mixture is then added to water so that it contains 21.5 weight percent water and is agitated in a ball mill for 12 hours for dispersion. The well-dispersed mixture is added to a 3.5 weight percent hardening resin, and the slip thus formed is poured into a mold. After being removed from the mold, the slip is dried at room temperature for 12 hours, followed by another drying process at 50°C for 12 hours. It is then heated to 600°C for driving off the resin and is sintered at 1,500°C.

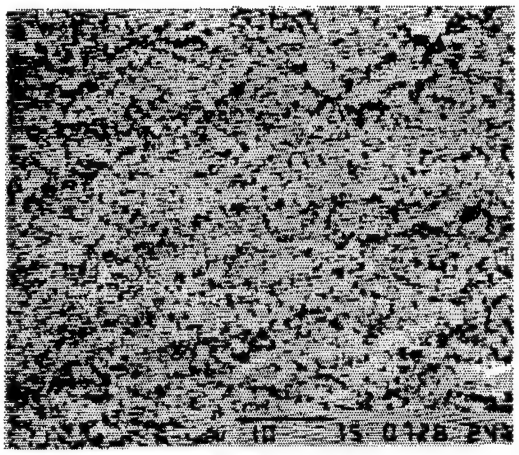

SEM Photo of Surface of Green Body

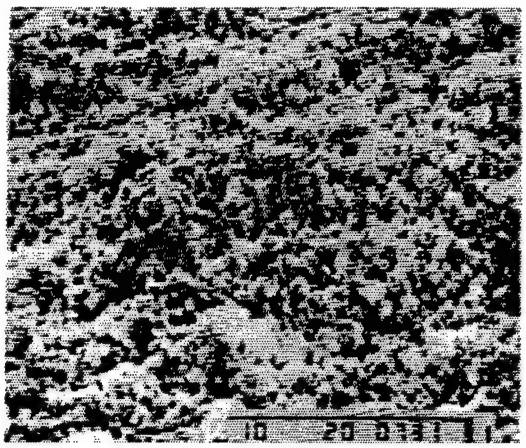

SEM Photo of Surface of Sintered Body

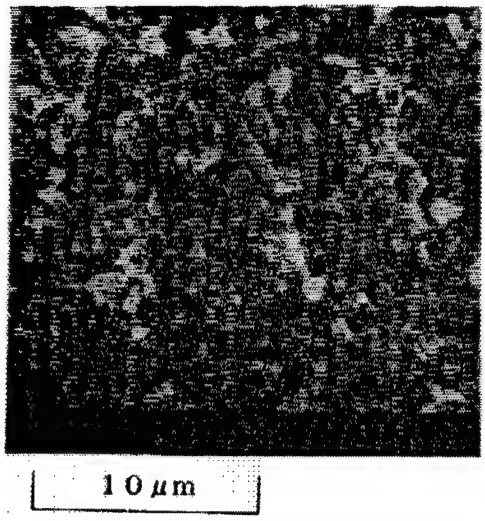

SEM Photo Surface of Sintered Body

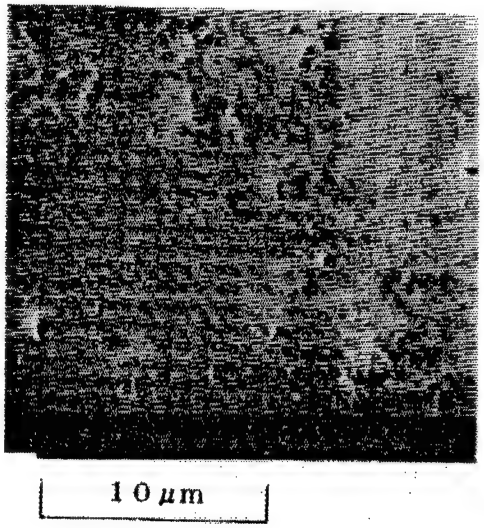

SEM Photo of Polished Surface of Sintered Body

- **Characteristics**

  - Bending strength (three-point bending): 131 kgf/mm^2
  - Density: 6.02
  - Shrinkage ratio: as shown in the graph (Figure 2), the total shrinkage from molding to sintering was 27.8 percent
  - Dimensional accuracy: ±0.9 percent

5.2 Si_3N_4

This ceramic was manufactured in roughly the same method as for PSZ (ZrO_2). Characteristic properties of E-10, a product manufactured by Ube Industries, Ltd., are:

- Bending strength (three-point bending): 110 kgf/mm^2
- Density: 3.22
- Shrinkage ratio: 25.1 percent (molding to sintered body)
- Dimensional accuracy: ±0.6 percent

6. Conclusion

• Characteristics of the NK process are:

(1) A variety of parts—thick, thin, or with complex shapes—can be obtained.
(2) It is adaptable to volume production and production of a variety of parts in small quantities.
(3) The use of dies enables high levels of surface accuracy and dimensional accuracy to be obtained.
(4) Enabling excellent material properties (bending strength, density).
(5) Degreasing can be done with ease.
(6) Green processing is available.

• Problems are:

(1) Depending on the type of powder, slip cannot be obtained.
(2) Care must be taken at the time of drying, depending on the type of solvent.
(3) There is also the problem of pot life.

7. Various Sintered Bodies

7.1 PSZ (ZrO_2)

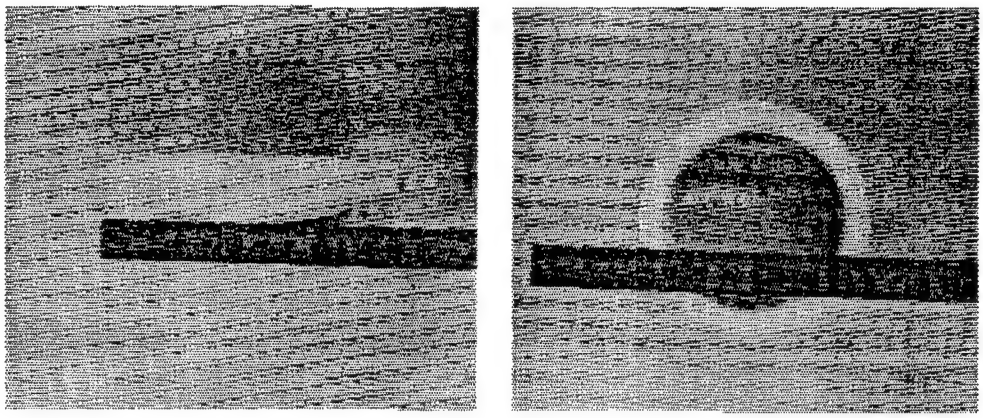

Columnar product (produced using a core)

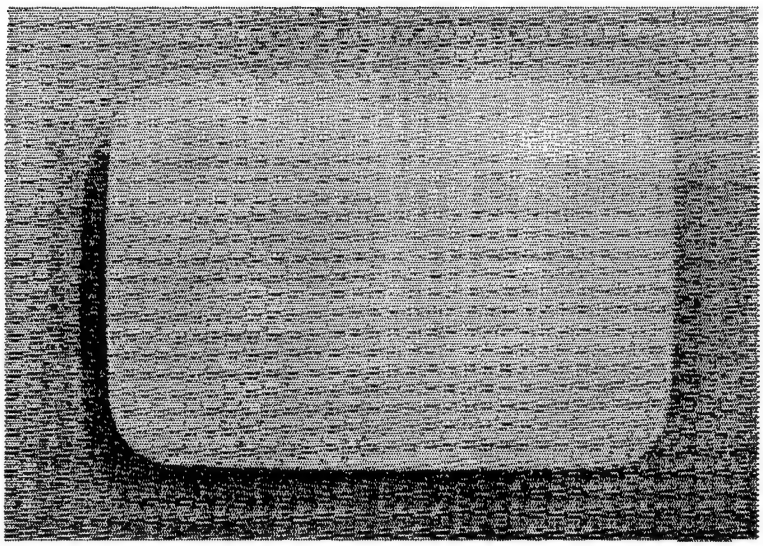

Lunchbox casting

PSZ (ZrO_2) Complex Shapes

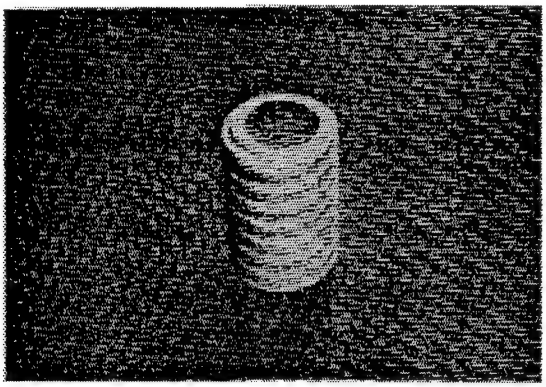

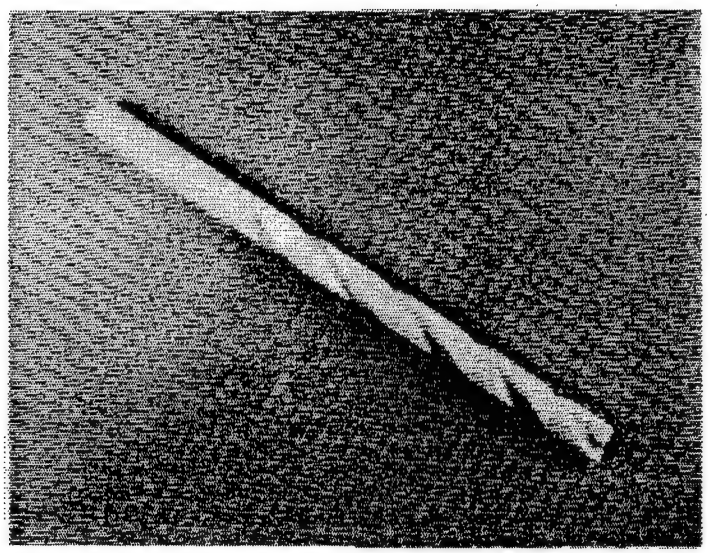

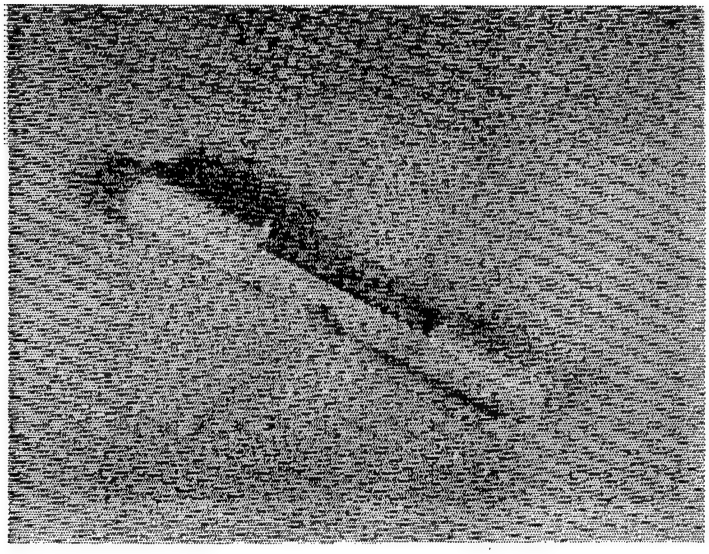

7.2 Si_3N_4

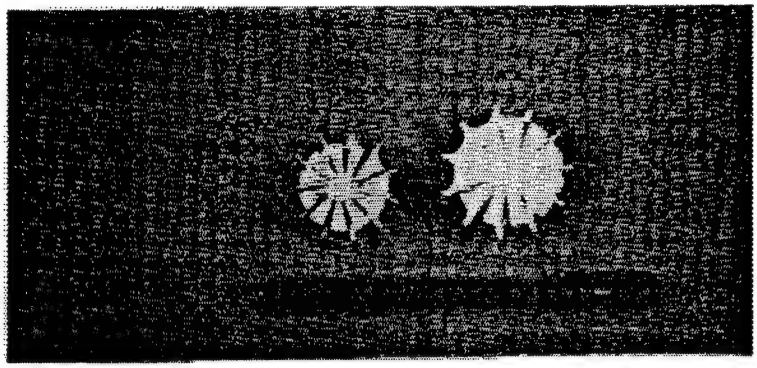

S i3 N4 rotor (left-sintered body; right-green after resin is driven off)

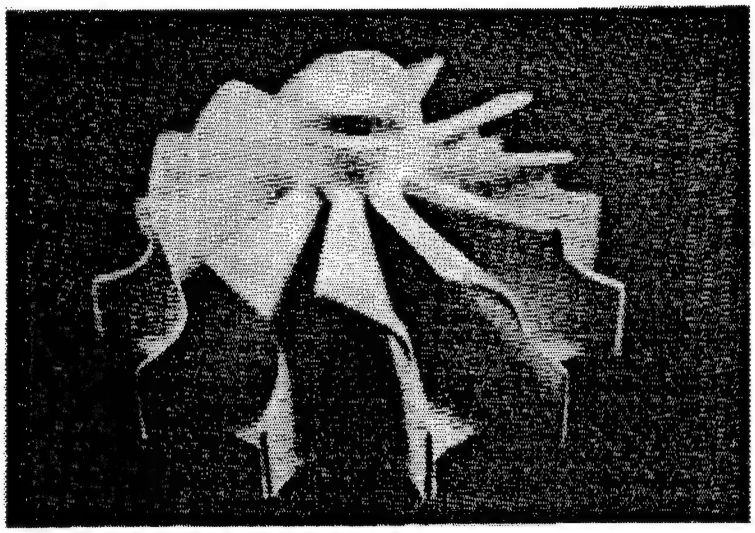

Green after resin is driven off

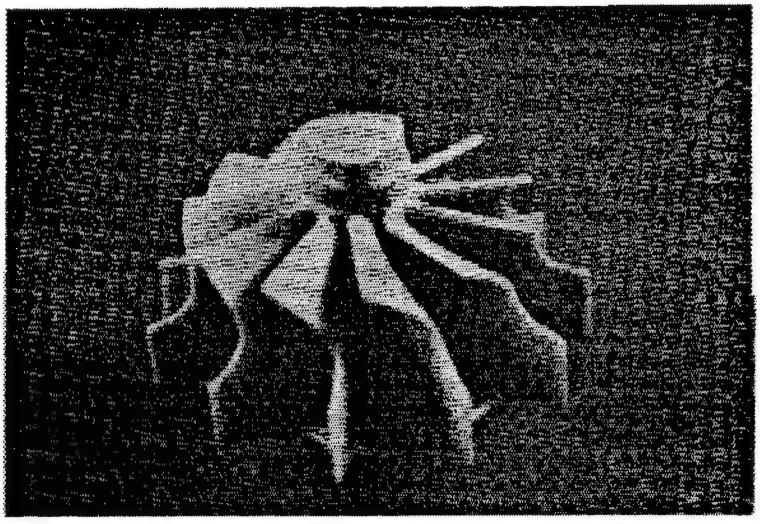

Sintered body

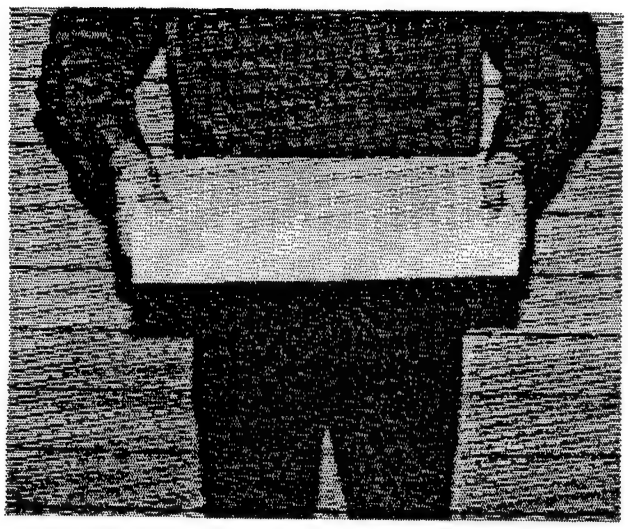

Si_3N_4 Large-Sized Thick Product

High-Speed Sintering of Ceramics

916C0033B Osaka DAI 18 KAI NYU SERAMIKKUSU SEMINA TEKISUTO in Japanese
2 Mar 91 pp 43-51

[Article by Kuniyoshi Nakagawa, Nakagawa Engineering Office]

[Text] **1. Sintering of Ceramics**

Sintering is an important process in the manufacture of ceramic parts. The process (Figure 1) consists of the following steps: disintegration and scattering of water and binder, disintegration and reaction of the raw material, and sintering. Temperature curves for each of these steps need to be kept moderate so that the processes will work on the part to be sintered uniformly through the length and breadth of it. The result is that sintering time tends to be long in theory as well as in experiment.

2. Approach to High-Speed Sintering

Eliminating factors requiring sintering for long hours is the key to realizing ceramic sintering at high speed. One method shortens the time needed for temperature raise by realizing a uniform distribution of temperature in the furnace. This approach can further be divided into a method involving improvements on the combustion system and heating method, and a method in which heat is blown in at high speed by designing the furnace in a way so that its cross section is large in breadth and low in height. The other method shortens the times needed for temperature raise and cooling by lowering the furnace's thermal capacity through the use of lightweight furnace materials and tool bricks.

3. Method Involving Improvements on Combustion System and Process

(1) Improvement on Burner

Changing the state of combustion (Figure 2), as in the Iso-Jet burner, from that in conventional burners enables the reach of the flame to be extended, resulting in uniform temperature distribution inside the furnace.

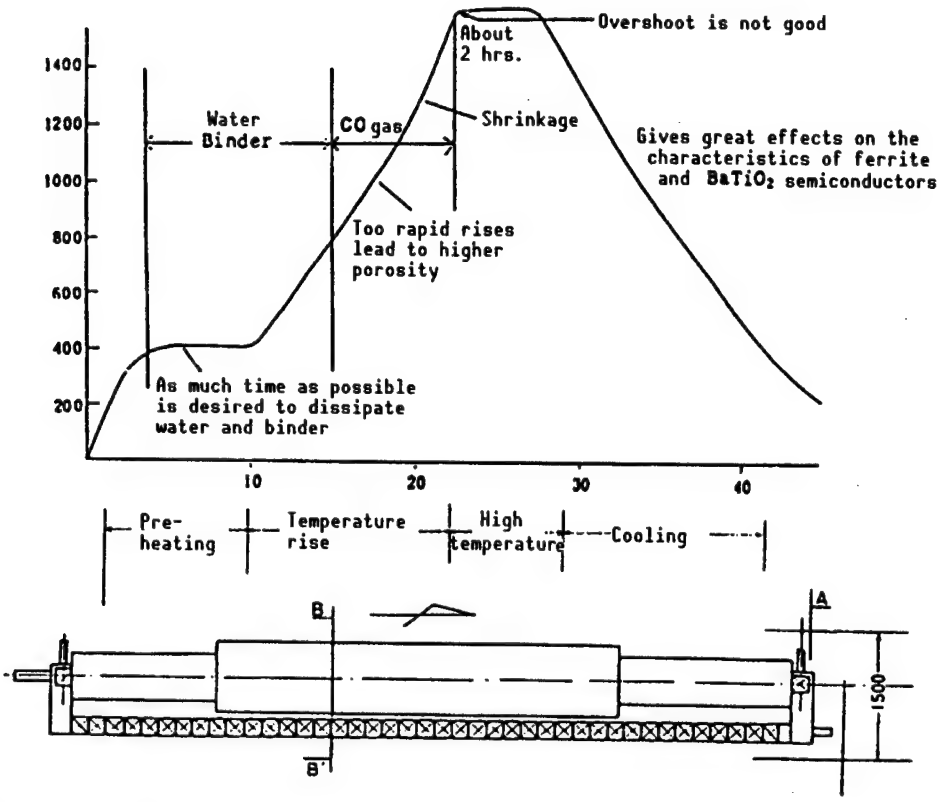

Figure 1. Example of Sintering Curve for Electronic Material

■ Temperature control in ISO JET® burner

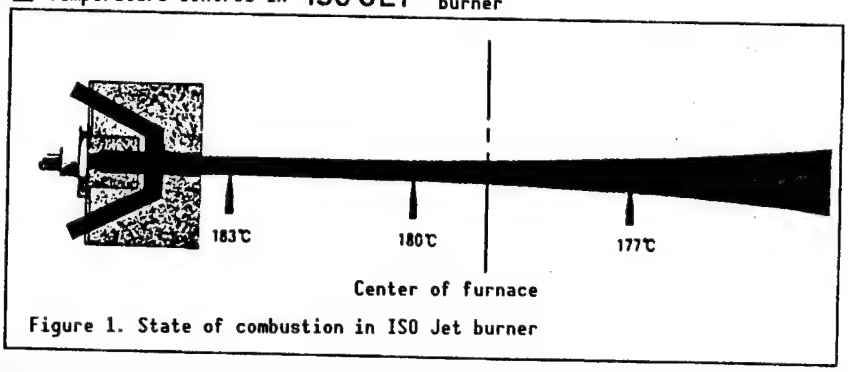

Figure 1. State of combustion in ISO Jet burner

■ Temperature control in conventional high-speed burner

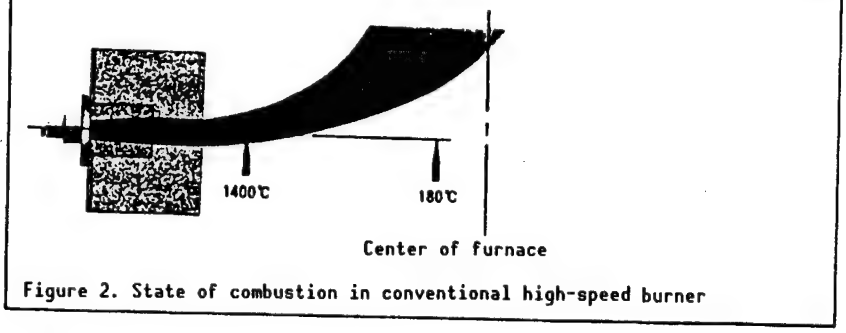

Figure 2. State of combustion in conventional high-speed burner

Figure 2. Temperature Control in Iso-Jet Burner

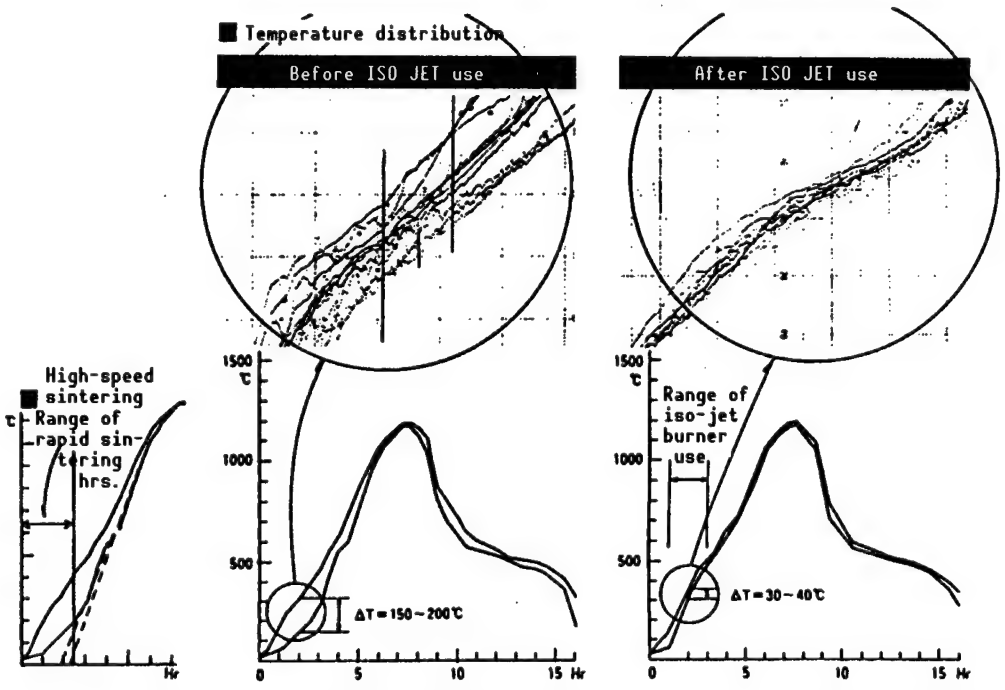

Figure 3. Temperature Distribution in Iso-Jet Burner

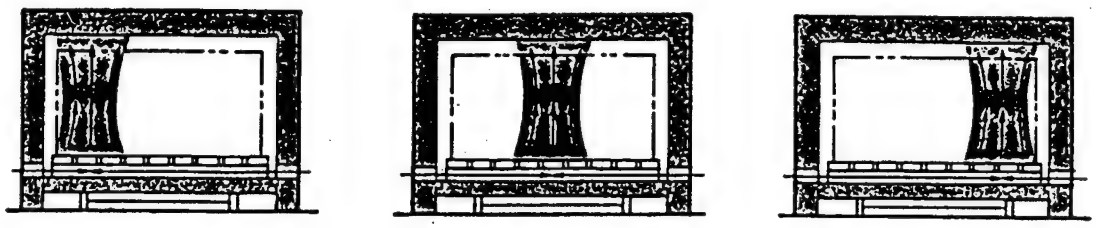

Figure 4. Direction of Iso-Jet Burners in Furnace

The result is that the time for temperature raise is shortened (Figure 3), making sintering at high speed possible.

(2) Improvement on Combustion System

As shown in Figure 4, letting two iso-jet burners placed opposite each other travel in the furnace's breadth direction at a certain cycle prevents the generation of cold spots on the door, walls, and floor of the furnace, a problem with conventional shuttle furnaces. This contributes to uniform temperature distribution inside the furnace, enabling high-speed sintering to be obtained (Figure 5).

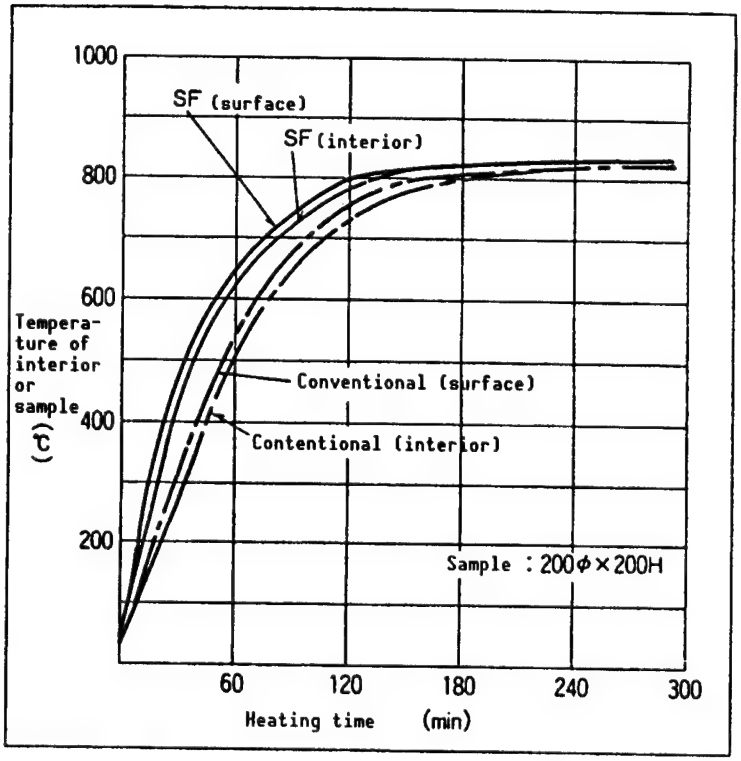

Figure 5. Results of Heating Speed Evaluation Test

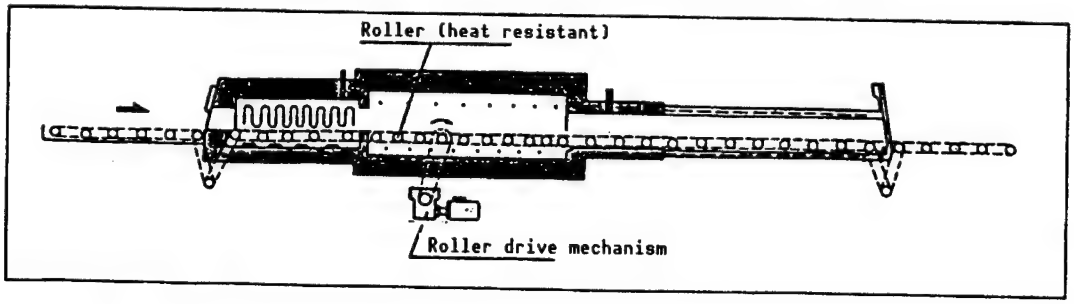

Figure 6. Roller-Hearth Kiln

4. Method Involving Roller-Hearth Kiln

(1) Roller-Hearth Kiln

A roller-hearth kiln (Figure 6) is a continuous hearth in which an object is placed directly or indirectly on a board, on a floor of ceramic rollers made of alumna, mullite, or silicon carbide. It travels by the action of the rotary motions of the rollers. Features of this furnace are:

1) Because the ceiling of the furnace is low compared to its height, temperature distribution inside the furnace is uniform.

2) Because of its roller drive mechanism, no tool bricks for sintering are needed. Even in cases when tool bricks for sintering are needed, thinner versions will do the job, reducing their thermal capacity and enabling high-speed sintering to be obtained.

(2) Insulating Material for Inner Lining

Using lightweight alumina boards for insulating liners of furnace increases the speed with which the furnace raises or cools its temperature. This enables the furnace to be operated as if it were a batch-type furnace.

Table 1. General Characteristics of Lightweight Insulating and Wool Materials

Kind	Item			
	Maximum service temperature (°C)	High specific gravity (kg/ℓ)	Bending strength	Thermal conductivity (kal/mh°C)
Boards				
Silica board	650	0.2	5.5	at 70°C 0.046
Super-board	1,000	0.2	6.0	at 350°C 0.072
Wool materials				
Iso-felt	1,000	0.11		at 400°C 0.075 at 800°C 0.16
Car wall felt	1,200	0.38		at 400°C 0.068 at 800°C 0.125
Car wall blanket	1,260	0.13		at 400°C 0.065 at 800°C 0.14
Car wall blanket	1,400	0.13		at 400°C 0.07 at 800°C 0.17
"Saphile" blanket	1,600	0.1		at 1,000°C 0.28 at 1,000°C 0.23 at 1,200°C 0.31 at 1,400°C 0.43

(3) Roller Materials

Table 2 lists rollers used in roller-hearth kilns. Which roller may be used is determined by the mode to which the roller is put to use and the temperature at which it is used.

Table 2. Rollers Used in Roller-Hearth Kilns (Materials and characteristics)

Material	Advantages	Disadvantages	Maximum service temperature	Uses
Stainless	●Withstand load	xHigh temperature use ΔBending	850°C	Ceramic ware (unglazed or dyed pottery)
Inconel (60%)	●Withstand load	ΔHigh temperature use ΔBending	1,150°C	Wall tiles
Mullite (63%)	●Thermal shock oDimensional accuracy	ΔWithstand load	1,100°C	Preheating zone: cooling zone
Mullite (76%)	oThermal shock oDimensional accuracy	ΔWithstand load	1,250°C	Tiles
Mullite (85%)	oHigh temperature use oDimensional accuracy	ΔWithstand load	1,300°C	External tiles Sanitary ceramic ware
Mullite (92%)	oHigh temperature use	ΔWithstand load	1,350°C	Ceramic ware Reducing sintering tiles
Mullite (100%)	●High temperature strength	ΔHigh cost ΔDimensional accuracy	1,500°C	Fine ceramics
Alumina	oHigh temperature strength	ΔDimensional accuracy xThermal shock	1,400°C	Fine ceramics
SiC	●High temperature strength	xHigh cost xDimensional accuracy	1,600°C	Fine ceramics
Compacted SiC	●High temperature strength	xHigh cost xDimensional accuracy	1,620°C	Alumina substrates

(4) Effects of Roller-Hearth Furnaces

The times needed for temperature raise, sintering, and cooling are short. This makes high-speed sintering possible and leads to higher productivity. An improved temperature distribution makes high-accuracy sintering possible.

When using a roller-hearth kiln, sintering time can be reduced to one-half to one-tenth that of conventional hearths--six to eight hours for condensers; two to three hours for chinaware; about one hour for tiles, raw pottery stone/feldspar porcelains; about 30 minutes for raw lime earthenware (gloss firing); and about six hours for ferrites (Table 3).

Table 3. Comparing Fuel Cost of Fellite Sintering RHK (M.T firms)

	Roller-hearth kiln	Pusher electric furnace (actual records)	Roller-hearth kiln
Furnace length	19.44 m	23.5 m	14.58 m
Scatter dimensions, weight	350 x 350 x 12t 3.2 kg	Sheath: 320 x 220 x 68H 3.5 kg Pellet plate: 350 x 350 x 30t 6.7 kg	350 x 350 x 12t 3.2 kg
Weight work workpieces loaded	ϕ25 x ϕ19 x 20H 30 g/piece 10-rows x 10-rows x 2 = 200 pieces/setter 6.0 kg/setter	ϕ25 x ϕ19 x 20H 30 g/piece 6-rows x 8-rows x 2 = 96 pieces/setter 2.0 kg/setter	ϕ25 x ϕ19 x 20H 30 g/piece 10-rows x 10-rows x 2 = 200 pieces/setter 6.0 kg/setter
Number of sintering rows	2 rows	Sheath: 3-level 2 rows	2 rows
Sintering hours	6 hours	20 hours	6 hours
Quantity of sintering	3,700 pieces/hr	2,707 pieces/hr	2,780 pieces/hr
Weight of sintering	111.0 kg/hr 80 tons/month	81.2 kg/hr 58 tons/month	83.4 kg/hr 60 tons/month

5. Method by the Use of Lightweight Tool Bricks

When blowing an object to be sintered into a furnace, the object is fed either by being placed on a board or by being stuffed into a canister, but the board or canister material tends to be heavy. One method of making tool bricks (Table 4) lighter, which reduces their thermal capacity, is to use high-strength materials such as recrystallized silicon carbide or silicon nitride combined with silicon carbide. The result is that the instrument bricks are formed thinner, and the total of the objects to be processed (the object to be sintered plus the instrument bricks) has a smaller thermal capacity, which makes high-speed sintering obtainable.

Table 4. Characteristics of Tool Bricks

Characteristics	Mullite	SiC–AlO laminate	Oxide-combined silicon carbide	Silicon nitride-combined silicon carbide	Recrystallized silicon carbide
Chemical components		Inside / Outside			
Al_2O_3	76%	70			
SiC		88	85	80	99
SiO_2	24	12 / 30	15	Si_3N_4 20	
Density	2.4	2.5	2.6	2.6	2.6
Bending strength (kg/cm)	150	150	260	400	600
Thermal expansion coefficient at 1,000°C	0.58		0.45	0.45	0.45
Thermal conductivity kcal/mhc			14.5	15.0	24.5

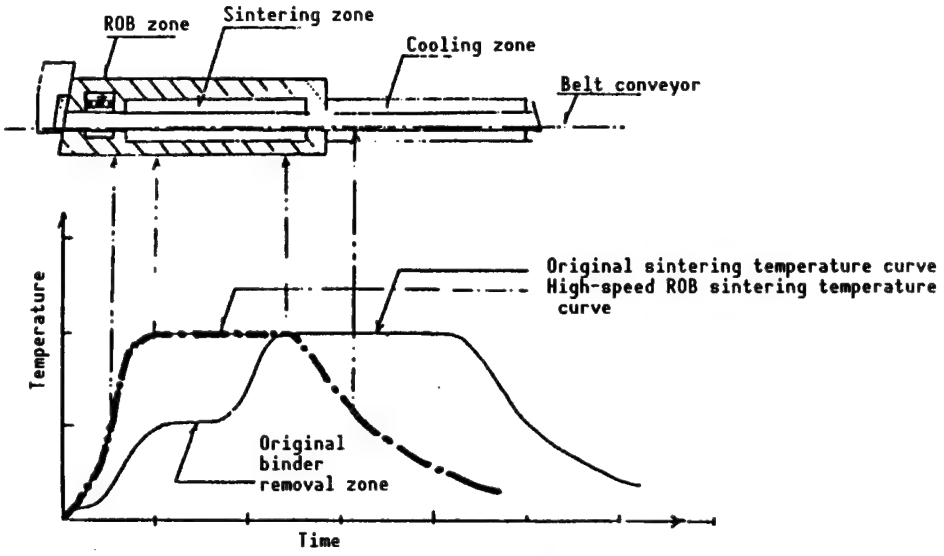

Figure 7. Example of Shortening the Process (With RBO) in a Resistance Furnace for Sintering

6. Method for Shortening Process

The energy utilization factor K can be expressed by the following equation:

$$k = \mu - L/N \cdot \alpha$$

where μ = efficiency
L = heat dissipation factor
N = rated heat supply
α = average load factor

To have a larger K, you must raise the efficiency, but raising N, the rated heat supply (electric power), results in a shorter processing time

As shown in Figure 7 (an example of thick-film hybrid sintering), turning the preheating section of the sintering furnace into a combustion furnace (RBO) enables the sintering process to be shortened, making it possible to sinter at high speed.

7. Conclusion

Among the expected effects of sintering at high speed are:

(1) The shorter sintering time contributes to higher sintering efficiency.

(2) The larger amount of sintering per unit time leads to a saving in space.

(3) The high speed with which the temperature inside the furnace can be changed enables the production of a large variety of products in small quantities in continuous furnaces like a roller-hearth kiln.

(4) The higher speeds with which temperature raise and cooling can be had enable the work cycle—loading into and/or off-loading from the furnace during daytime and sintering at night—to be established, contributing to manpower savings at night.

These advantages are expected to contribute to improved labor conditions, space savings, and enhanced sintering efficiency. For the technology to be exploited, shorter sintering times can be had only after improvements in raw materials and their mixing are obtained.

Functional Inorganic Thin Films by New Process

916C0033C Osaka DAI 18 KAI NYU SERAMIKKUSU SEMINA TEKISUTO in Japanese
2 Mar 91 pp 63-72

[Article by Takashi Hirao: "Functional Inorganic Thin Films by a New Process"]

[Text] **1. Introduction**

In recent years ion engineering technology has been drawing attention as a new process. Ion engineering technology is already being used in the manufacture of super-LSIs as an ion injection process and a sputtering process. The technology's application, however, is not limited to LSI manufacture. Ion engineering technology is finding applications in a broad range of activity, including development of new materials such as high-temperature superconducting materials and recording materials, giant microelectronics such as liquid crystal displays, and the development of solar cells, the so-called clean energy. This paper describes the basics and applications of ion engineering technology as a new process when it is used in the manufacture of functional, inorganic thin films for use in the above-mentioned devices.

Ion engineering technology has excellent features such as: fabrication and processing of thin films, which can be controlled at atomic or molecular levels; synthesis of materials in an equilibrium state by exploiting the ionic effect, which will enable their synthesis at low temperatures; and the technology, a nonequilibrium process, which may make it possible to synthesize materials not found in nature. The technology is finding increasing applications in a broad range of technical fields and industries.

2. Ion Engineering Technology

Ion engineering technology is defined as "the technology in which various kinds of materials are ionized in ultrahigh vacuums or reduced pressures. The ions thus generated are used for processing materials or for the synthesis or analysis of materials." The technology is broadly classified into the ion beam process and the plasma process. From a technical viewpoint, it is divided into ion injection, thin film fabrication, dry etching, and analysis (Figure 1). As a result of increasing growth, the technology's attributes have been used in various combinations, depending on the purpose. Combinations of ion

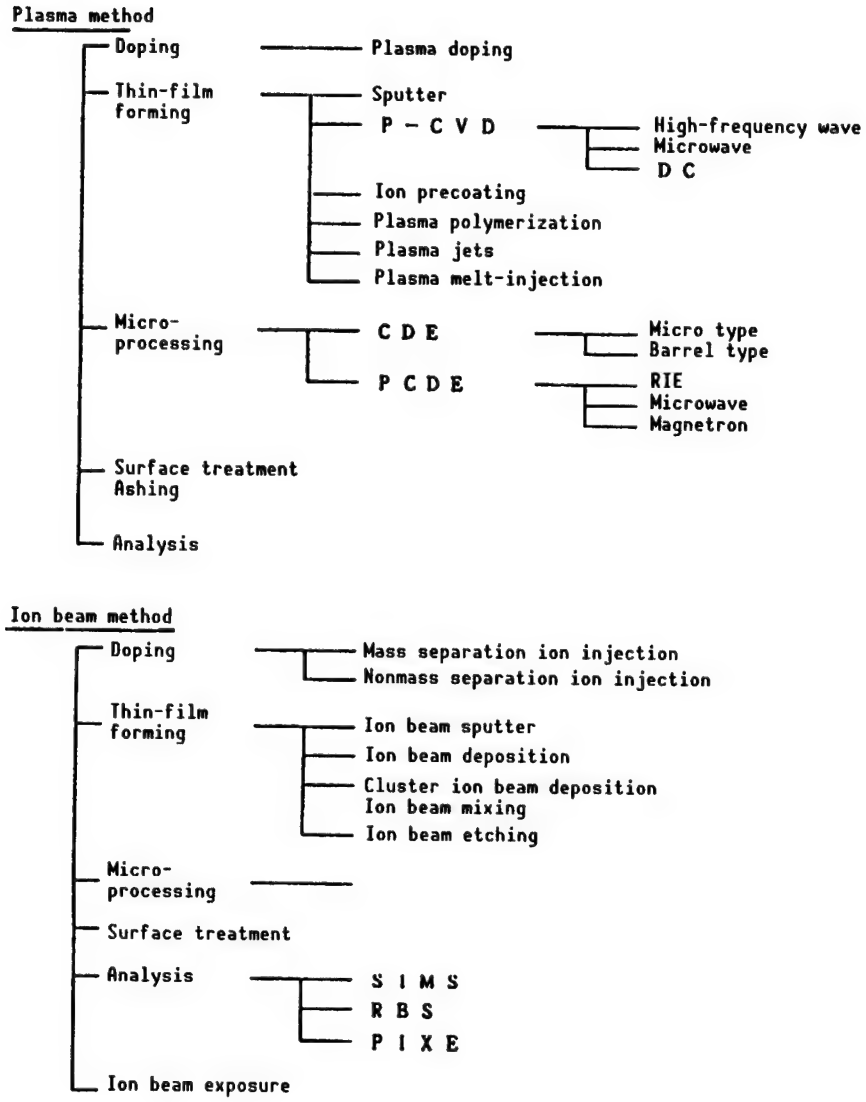

Figure 1. Classification of Ion Engineering Technology

beam plasma with deposition technology such as molecular beam epitaxy (MBE) have been used for R&D devices and material synthesis.

Ion engineering technology is a key technology in the R&D manufacture of various electronic devices, such as computers that support the advanced information society, super-LSIs, high-density and high-performance recording devices, and displays that are key devices in the highly important communications and video fields, solar cells, and high-temperature superconducting materials.

3. Super-LSIs

Much effort has been expended on the development of higher, faster, and more multifunction semiconductor integrated circuits based on silicon that form the key electronic devices in almost all industrial fields. As for the representative devices, dynamic random access memories (DRAMs), the development of a 64M-bit DRAM was first reported in 1990, and development of 256M and 1G-level DRAMs is anticipated.

Ion engineering technology is proving to be an indispensable technology in the manufacture of various devices, beginning with the 4M DRAM products. In the field of thin film formation, plasma tetraethoxide silane (TEOS):Si $(OC_2H_5)_4$ technology is used for forming interlevel insulating films (SiO_2), and magnetron sputtering technology is used for fabrication of wiring and electrodes of Al-Si-Cu. For the coating of protective film needed for raising the device reliability, the P-chemical vapor deposition (CVD) process is used to deposit a film of SiN_x.

4. Ferroelectrics (Ferroelectric memories)

Memories such as DRAMs and static random access memories (SRAMs) at present have an unrivaled position as super-LSIs, but thin film ferroelectric memories that take advantage of the polarization inversion characteristics of ferroelectric materials are gaining attention as a new device. These materials are ceramics of perovskite structures, of which lead zirconate titanate (PZT) is representative. Efforts have long been made to fabricate thin films of these materials requiring high substrate temperatures of as much as about 600°C and, because they are multielement compounds, it was difficult to control their composition. If ferroelectric materials are to be used as ferroelectric memories, the first requirement is for high-quality thin films of these materials to be fabricated in a method compatible with the semiconductor process. Forming temperature needs to be lowered, and deposition of thin film on the substrate interface needs to be strictly controlled from the initial stages of the process. Recently, many efforts have been made to fabricate thin films by using the sputtering method, the vacuum vapor deposition method, and the CVD method, but the establishment of heteroepitaxial technology based on a highly functional thin film forming method incorporating the ion engineering technique is becoming important.

5. Liquid Crystal Displays

Liquid crystal displays based on an active matrix drive mechanism are being widely used as thin, lightweight, and low-power consumption full-color displays. In an active matrix (Figure 2), a switch is incorporated in each pixel, and for each field (60 screens per second) pixels are apparently driven while retaining on/off data. The formula is advantageous in displaying multicolor, high-resolution, and higher gradation images. The formula is finding wide use in direct-viewing LCDs, such as the displays for small televisions, viewfinders, office automation equipment, and aircraft, as well as in large-screen projection TVs.

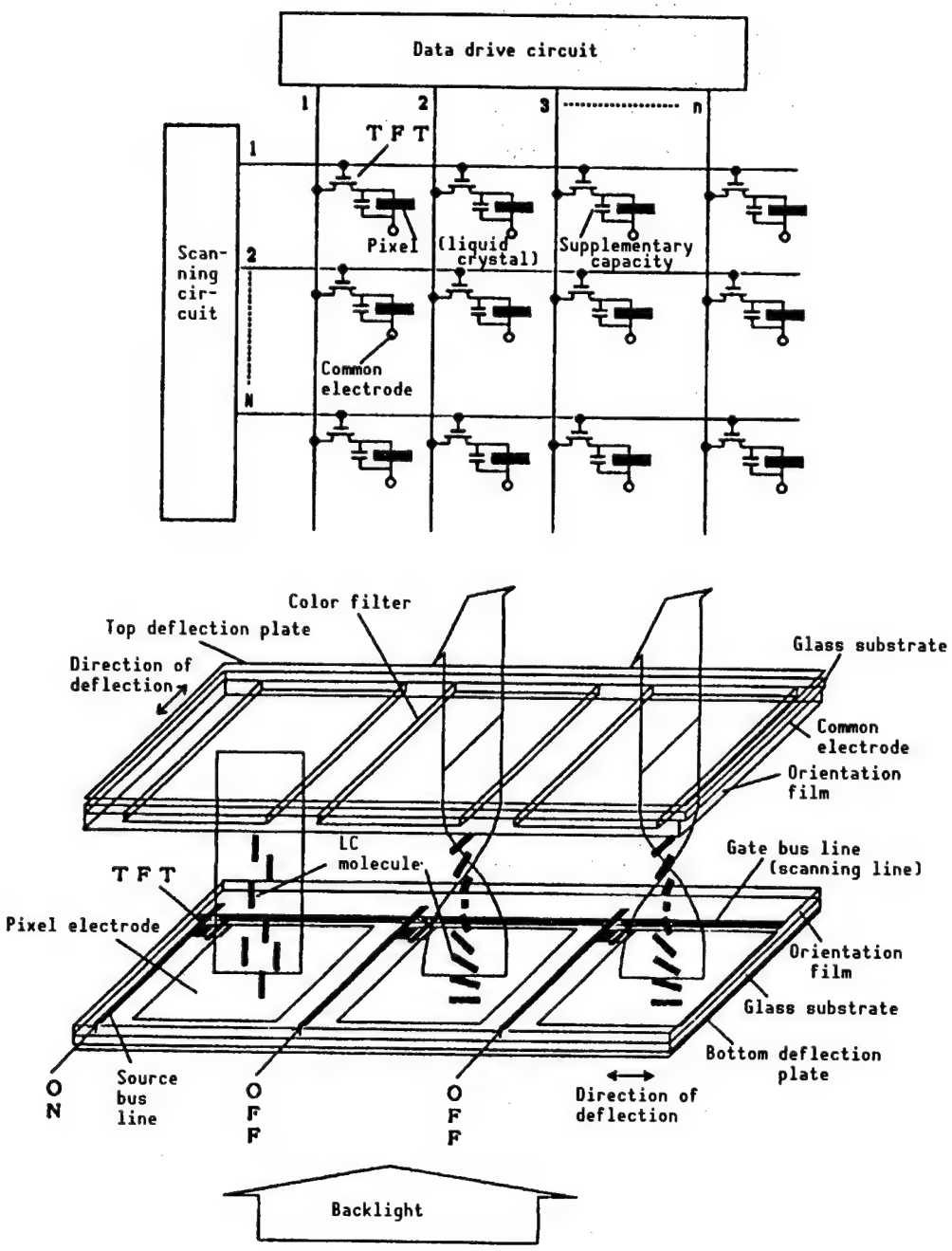

Figure 2. Conceptual Diagram and Cross Section of an Active Matrix LCD

In this formula, thin film transistors (TFTs) are mainly used as switching devices. Amorphous siliconhydride (a-Si:H) and polycrystalline silicon (poly-Si) are used as materials for thin-film transistors. Amorphous siliconhydride TFTs are widely used in all full-color LCDs, and for direct-viewing, prototypes of 15-inch panels have been manufactured. Poly-Si TFTs are used in viewfinders and projection-type LCDs.

LCDs rival 256K DRAMs in the number of switches, and their patterning linewidths equal those of 16K to 64K DRAMs. What makes LCDs stand out from LSIs is that these microscopic devices are formed on a large-area glass substrate of 5~14 inches square. Forming of a-Si:H films is done using the P-CVD process, but electrodes, metallizations for wiring, and transparent electrodes are formed using the sputtering process. In both processes the vertical both-side electrode discharge method is mainly used on production lines. For etching, the wet process using chemical solutions is being used at present, but studies are under way on the dry process, in preparation for the debut of high-density small products, such as projection LCDs and HDTVs. Research is being done on the large-area doping process as a replacement for the ion injection process and on growing larger area poly-Si TFTs at lower temperatures.

6. Solar Cells

Solar cells that convert the energy of solar light into electricity produce clean energy. The inexhaustible solar energy is gaining attention not only for environmental reasons but also as an alternative energy source to fossil fuels. For materials for solar cells, active research is being conducted on compound semiconductors such as polycrystalline Si and CdS/CdTe and amorphous thin films of a-Si and on conventional single crystals of Si and gallium arsenide (GaAs) in an effort to produce larger area and higher efficiency solar cells (Table 1). The P-CVD technology is used in the development of a-Si-based solar cells, and vapor deposition and sputtering technologies are used for the development of solar cells of compound semiconductor thin films.

Table 1. Trends in R&D of Solar Cells and Their Production

Material	Conversion efficiency (%)	Research institute	Cell area (cm^2)	1989 output (world, Japan)
Bulk				
Single crystal Si	24.2	New South Wales University		17.9MW, 2.7MW
	18.1			
Polycrystal Si	15.1	Sharp Corp.	100	10.8MW, 2.0MW
GaAs	23.9	Kyocera	225	
GaAs/GaSb	32.2	Mitsubishi Electric Corp.	1	
Thin films				
a-Si:H	12	Osaka University		13.1MW, 9.5MW
	10.05	Fuji Electric Co.	1200	
a-Si:H/$CuInSe_2$	15.6	Siemens	4	
CdS/CdTe	14.0	Microchemistry	1	
	8.1	Matsushita Batteries Co.	1200	
			1	
CdS/$CuInSe_2$	12.4	Boeing		
	9.2	Boeing	900	
CdS/Cu(In,Ga)Se_2	12.9	Boeing	1	
ZnO/CdS/$CuInSc_2$	14.1	ARCO-Solar	3.5	

7. Recording Materials (Photomagnetic disks)

Magnetic tapes, such as video and music tapes, and magnetic disks, such as floppy and hard disks and magnetic heads, are produced by sputter-depositing thin film of vertical magnetic recording materials of mainly the Co-Cr system. The rewritable, large-capacity, recording mediums, photomagnetic disks, are manufactured by forming by sputtering technology multilevel films of mainly TbFeCo magnetic films, dielectric films, and films of reflective materials. Common to all these recording materials is how to solve reliability problems arising from the scatter in the composition of the target alloys. It, along with problems associated with the introduction of specimens into the sputtering equipment and methods of transferring them, holds the key to their volume production.

8. Piezoelectric Materials (Piezoelectric infrared sensors)

Piezoelectric infrared sensors (Figure 3) are mainly used for measuring temperatures and for detecting invaders by a noncontact method. Compared with other infrared sensors, they have the following advantages: response speeds are fast, sensitivities are high, sensitivities are not wavelength dependent, and devices do not need to be refrigerated. The operating principle is to measure change in polarization brought about by change in temperature of the sensor caused by infrared light; that is, the voltage generated by the piezoelectric effect. Single crystals of ceramics such as (PbLa)TiO3, lead zirconate titanate (PZT), and $LiTaO_3$ are being widely used as point sensors.

Existing materials are short of meeting requirements demanded of high-density, one- or two-dimensional array sensors used for measuring temperature distribution in objects and for detecting positions of objects. Development of thin films oriented toward the axis of polarization is anticipated. For fabricating thin films, the widely used sputtering technology is making it possible to obtain $(PbLa)TiO_3$ thin films with excellent properties, but the technology has problems. High substrate temperatures (~600°C) are needed, and growth speeds are slow. Concrete efforts are about to take shape to grow at lower temperatures through ion irradiation and light-assist techniques, to improve crystallinity, and to increase growth speed through the CVD process.

9. New Diamond Materials

Although they are semiconductors with a broad forbidden band, new diamond materials (Table 2) such as diamond, SiC, and BN also feature high levels of mobility. This characteristic and their excellent heat- and environment-resistant properties give rise to their possible applications in electronic devices that operate at high temperatures and high speeds and in optical devices such as short wavelength lasers.

More attempts at manufacturing diamonds artificially are being made than before, and, at present, single crystal grains of up to 1 cm^2 have been produced. For diamonds to be widely used as device materials, they must first be fabricated into thin films. Technologies for making films of diamonds are processes in which gases are decomposed into ions or radicals for reactions

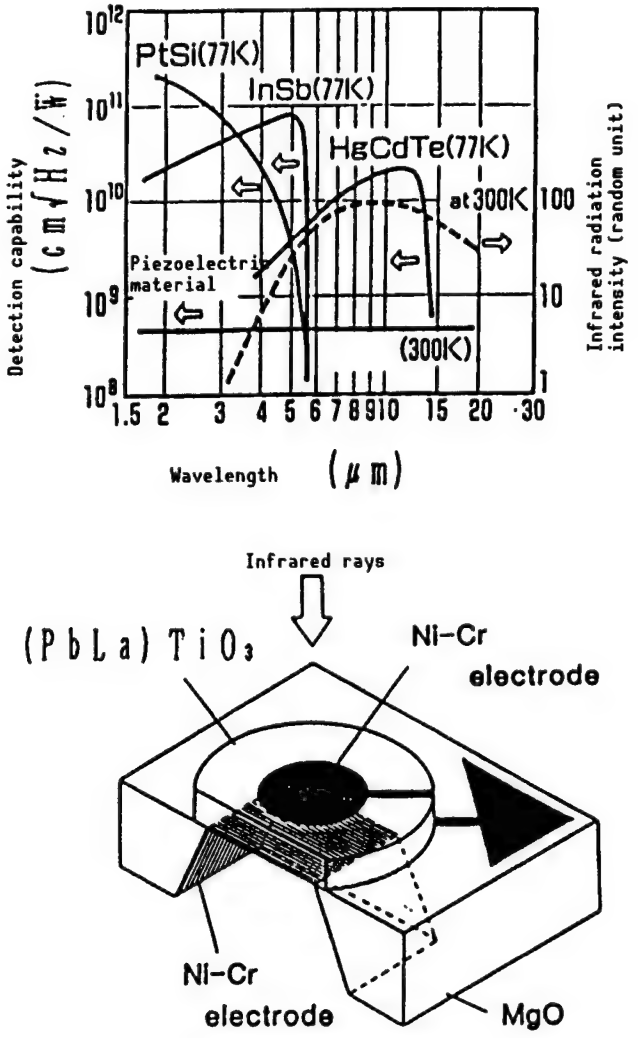

Figure 3. Comparison of Characteristics of Infrared Sensors of Various Materials and Composition of a Piezoelectric Sensor

(for example, the thermal filament method, the microwave P-CVD method, and the direct current P-CVD method). For film growth, a mixture of methane and hydrogen gas are decomposed and made to react under a pressure region of several ten Torr and are deposited on a substrate heated to 500~900°C. Thin films thus obtained, however, are polycrystalline films with grain diameters of several microns to several ten microns. As the technology stands now, only artificial diamond thin films with extremely uneven surfaces can be obtained.

If diamond thin films are to find practical use, the direction of activity will be toward development of heteroepitaxial technology and doping technology (especially n-type) that will enable planar diamond thin films to be obtained.

Table 2. Application Fields of New Diamond Materials

Properties		Applications	Application examples and effects		Tasks
Physical properties	Ultrahard	Tools	Grinding and cutting tools (grinding wheels, dressers, cutting tools, drills)	Ultrahigh precision processing, processing of hard-to-work materials	Large size, large area, high cohesion, high-speed film forming
	Abrasion resistance	Coating films	Protective coatings for optical and magnetic heads, magnetic tapes	High durability	Adhesion, uniformity, low-temperature film forming
	Sound conductivity	Acoustic products	Vibrators in speakers and microphones	Broad-band frequency, sound distort improvement	Adhesion, uniform film forming (quality & texture)
	Heat conductivity	Heat sinks	Semiconductor lasers and high-output microwave devices	Integrating devices into monolithic body	Forming thick films, forming large-area films
	Insulation	Passivation films	Insulating layers in devices and integrated circuits	Multilevel devices	Surface planarization, film growth at low temperature
Semiconductor properties	Wide-gap semiconductors	Devices operating at high temperatures	High-temperature sensors (thermistors), diodes and transistors operating at high temperature	High temperature operation, resistance to environment	Forming of metal electrodes, forming Si crystals, doping tech.
	High mobility	High-speed operation devices	High-speed operation transistors (bipolar, Schottky gate, MIS transistors)	High-speed operation	Device design, process technology, etching technology
	High-breakdown voltage	High-power devices	High-power transistors	High power	
	Light emitting	Short wavelength, light emitting devices	EL devices	Emitting of short wavelength light	Device design and process technology

Elucidating the mechanisms of generation of nuclei and film growth and exploiting the findings for development of technology for preparing substrates, deposition technology, and device fabrication technology will be future key tasks.

10. High-Temperature Superconducting Materials

If high-temperature superconductors are to find use in electronics, an essential precondition is establishment of a technology for making thin films of these materials. Superconducting materials of the La-based (transition temperatures: 30 K), Y-based (90 K), and Bi-based (120 K) systems so far have been discovered are all ceramics with high crystallization temperatures. It is necessary to develop processes that will enable thin films to be formed of

these materials at lower temperatures yet allow for precise controls of their crystallinity, composition, and oxygen content. Since the discovery of high-temperature superconductors, active research has been done on methods of forming thin films of these materials by using the sputtering process, the vacuum deposition process, and the CVD process. Technology has advanced to where thin films can be formed on single-crystal substrates of MgO heated to 600~800°C. To meet demands for control of thin films and materials synthesis at the levels of atomic layers, a sophisticated thin film forming technology that exploits the ion engineering technique is being used. Excellent results have so far been obtained with light, ion, and plasma-assist processes; the multidimensional vapor deposition, reactive vapor deposition, and laser application processes.

11. Conclusion

As electronic devices advance, ion engineering technology will gain added importance as a new process in R&D and the manufacture of inorganic functional materials. In light of such needs, efforts have recently been made to elevate the sophistication of the technology as well as to integrate the technology with some other technology. Advances in ion engineering technology are expected to contribute greatly to the growth of electronic devices and further growth of the whole industry.

References

1. Carrano, J., et al., IEDM '89, 1989, p 255.
2. Lechner, B.J., et al., IEEE INT. SOLID-STATE CIRCUITS CONF. DIG., 1969, p 52.
3. Shibusawa, M., et al., SID '89 DIG., 1989, p 230.
4. Kobayashi, I., et al., Ibid., p. 114.
5. Ichikawa, K., et al., Euro Display '90, 1990, p 370.
6. Yoshida, A., et al., JPN. J. APPL. PHYS., Vol 30, 1991, p L67.
7. Kawachi, G., et al., Ibid., Vol 29, 1990, p L2370.
8. Matsumoto, S., et al., J. MAT. SCI., Vol 17, 1982, p 3106.
9. Kawarada, H., et al., JPN. J. APPL. PHYS., Vol 26, 1987, p L1032.
10. Suzuki, K., et al., APPL. PHYS. LETT., Vol 50, 1987, p 728.
11. Bednorz, J.G. and Muller, K.A., Z. PHYS., Vol B64, 1986, p 189.
12. Adachi, H., et al., JPN. J. APPL. PHYS., Vol 27, 1988, p L1883.

Fine Powder by Spray Pyrolysis, Sintering Characteristics

916C0033D Osaka DAI 18 KAI NYU SERAMIKKUSU SEMINA TEKISUTO in Japanese
2 Mar 91 pp 73-81

[Article by Nozomu Otsuga and Kazuhiro Nonaka, Tokyo Institute of Technology: "Preparation of Fine Powders by Spray Pyrolysis and Their Sintering Characteristics"]

[Text] **1. Introduction**

Compared with other materials, ceramics have many excellent properties, and great expectation is placed on them as next-generation materials. Almost all ceramics are produced by using powder as the raw material and sintering it. Because properties of the raw material powder have, in many cases, direct impact on properties of the product, the raw material powder is very important. In general, powders featuring ease of sintering, uniform quality, and low costs are demanded.

Many fine powder synthesizing methods have been studied. The spray pyrolysis method, among others, is generally best suited to synthesis of fine powders featuring high sintering ease and uniformity. The technique works best when synthesizing a multielement fine powder. With a proper selection of the raw material, density of the starting solution, and the spray method, the technology allows powders to be sintered at relatively low costs.

2. Principles and Features of Spray Pyrolysis Process

The spray pyrolysis process is a method for preparing a powder from a liquid phase. In the spray pyrolysis process (Figures 1 and 2), a solution containing the raw material elements are blown into a high-temperature atmosphere as microscopic droplets. Solvent evaporation (combustion), precipitation of the raw material chemical species, and pyrolysis occur within several seconds, enabling the fine powder of choice to be had. The materials used for spray pyrolysis include inorganic salts soluble in water or alcohol, such as nitrates, sulfates, and chlorides, as well as salts of organic acid, or alkoxide.

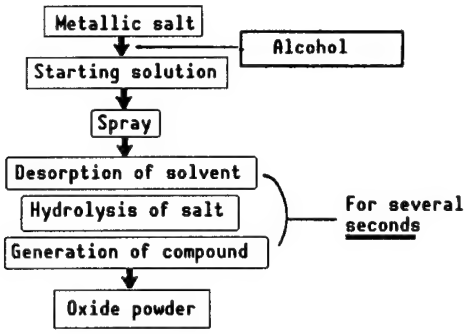

Figure 1. Principles of Spray Hydrolysis Process

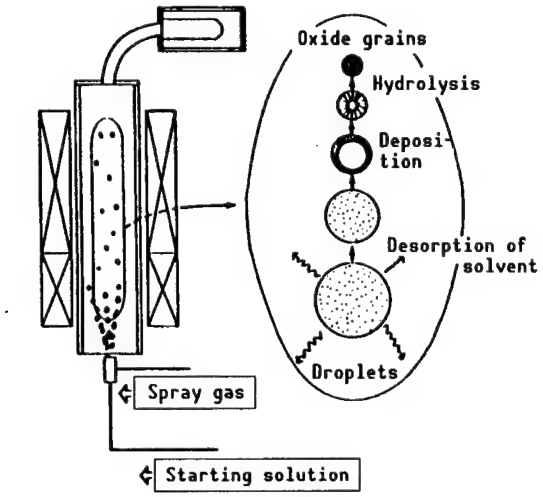

Figure 2. Process of Spray Hydrolysis

Features of the spray pyrolysis process are:

(1) The powder synthesis from solution to final product can be accomplished in a single process.
(2) The loop of process that needs to be controlled is extremely short.
(3) Each droplet from the sprayed solution functions as an independent reaction system.
(4) Processing time is very short.
(5) Equipment is relatively simple.
(6) Continuous synthesis is possible.
(7) The process can be easily scaled up.

The spray pyrolysis process has many advantages not found in other synthesis methods, and the technique enables multielement fine powders featuring fine and uniform grain sizes to be obtained.

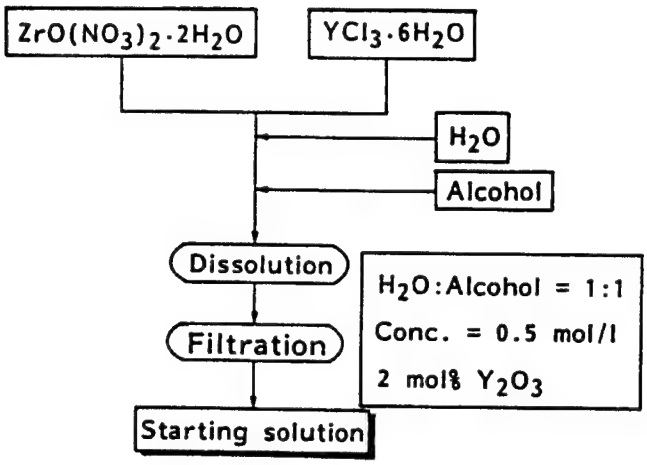

Figure 3. Preparation of Y-ZrO_2 Starting Solution

3. Synthesis and Sintering of Yttrium Partially Stabilized Zirconia (Y-ZrO_2)

Y-ZrO_2 ceramics are known for high strength and high tenacity. As for the raw materials for these ceramics, powders that can be easily sintered yet are highly uniform in composition are needed. Figure 3 shows the sequence of the steps for preparing a starting solution. The raw material 2mol%Y_2O_3-ZrO_2 solution was prepared by dissolving zirconyl nitrate and yttrium chloride in a mixed solution of water and alcohol.

Figure 4 shows the spray pyrolysis equipment and two-fluid spray used. The raw material solution is sprayed, together with compressed air, as microscopic droplets by the two-fluid spray. The sizes of the droplets can be controlled by adjusting the ratio of the amount of compressed air supply to the amount of solution supply.

Figure 5 shows changes in the morphology of grains with changing amounts of air flow for a 2mol%$Y_2O_3ZrO_2$ synthesized powder. With increasing amounts of air flow, grain sizes diminished. Thus, the sizes of the grains were proportional to the sizes of the original droplets.

Table 1 gives the results of analysis of the synthesized powder's elements by electron probe microanalyzer (EPMA). For the composition of the solution, 2mol%Y_2O_3, the analysis values are all within ±15 percent. Y_2O_3 is dispersed roughly uniformly.

Figure 6 shows changes in the sintering curve corresponding to densities of the starting solution for the synthesized powder. The lower the density of the starting solution from which the powder was synthesized, the lower the temperature at which sintering started. However, powders made from high-density solutions could be densified up to 99 percent of the theoretical density when sintered at 1,400°C, registering bending strengths of about 100 kg/mm^2.

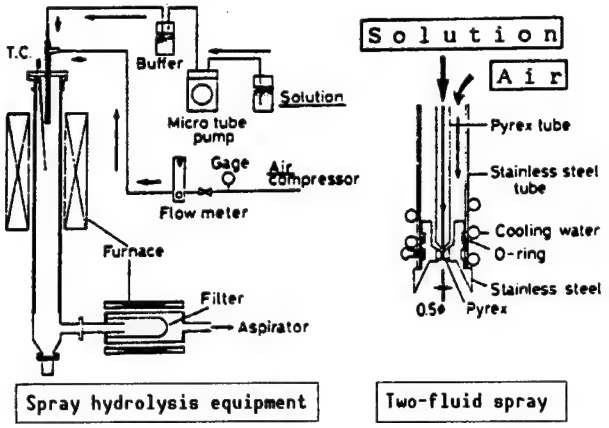

Figure 4. Spray Hydrolysis Equipment and Spray(er)

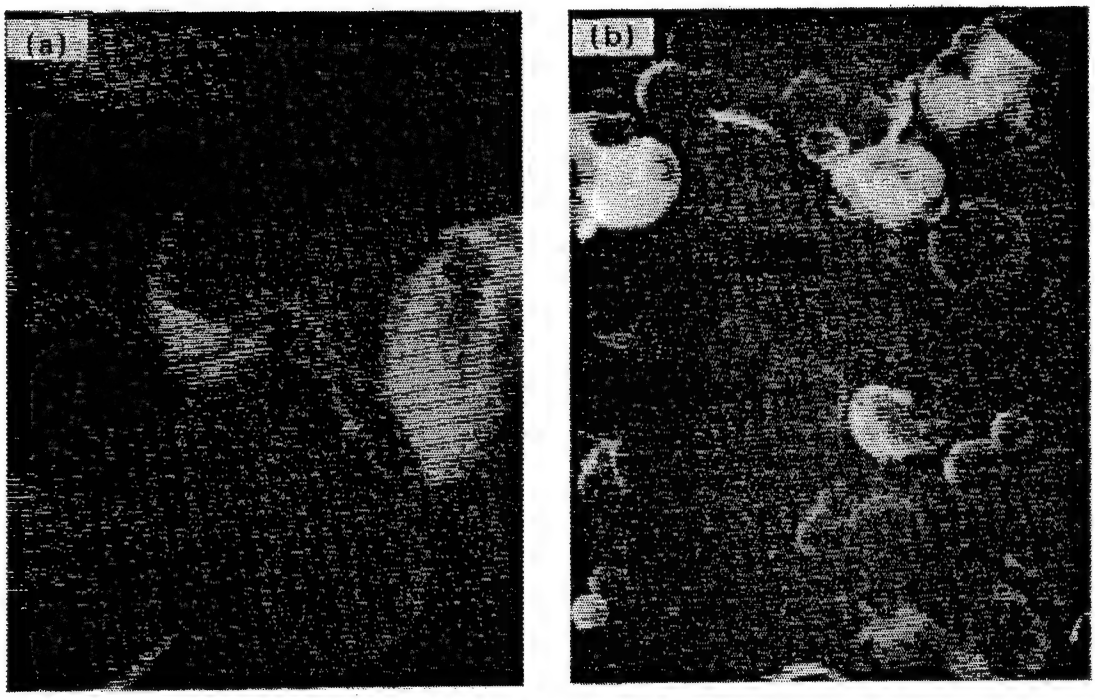

Figure 5. Effect of Air Flow on Morphological Changes of Grains of 2mol%Y_2O_3–ZrO_2 Synthesized Powder

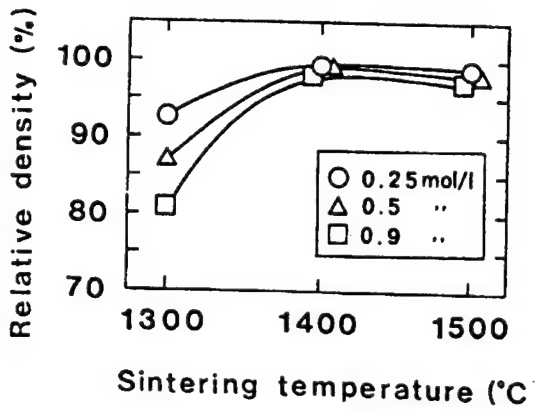

Figure 6. Sintering Curves for Synthesized Powders Prepared Using Different Densities of Starting Solution

Table 1. Results of Analysis of Synthesized Powder's Elements by EPMA

Particle number	Mol%Y_2O_3	Particle size (μm)
1	2.07	3
2	2.33	1
3	2.03	1
4	1.97	5
5	2.07	1
6	1.76	2
7	1.69	1
8	1.88	5

4. Synthesis and Sintering of Zirconia Dispersed Alumina (ZTA)

Alumina ceramics are the most widely used ceramics of all fine ceramics. Alumina that has zirconia grains dispersed in it to form an alumina-zirconia complex has greatly enhanced strength and tenacity. To obtain a ZTA product with excellent mechanical properties, the first priority is to produce a compact, fine-structured sintered body by inhibiting the growth of alumina grains and making sure that microscopic zirconia grains are uniformly dispersed in the matrix of alumina. Figure 7 shows the process for preparing a raw material solution for ZTA. We used aluminum nitrate for the alumina source and zirconyl nitrate for the zirconia source.

Figure 8 shows changes with heat for an Al_2O_3-15wt%ZrO_2 synthesized powder. The synthesized powder had large relative surface areas from 30~70m^2/g and was of an amorphous state, but heating the powder led the microscopic tetragonal zirconia to disperse between α-alumina grains, giving it a crystalline structure.

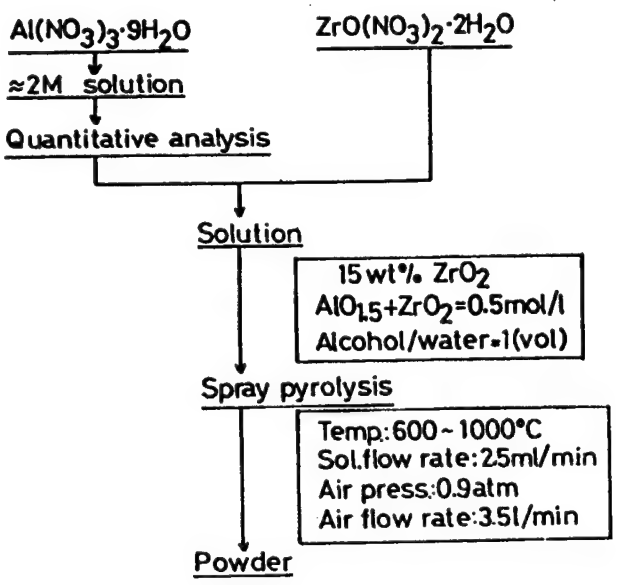

Figure 7. Preparation of ZTA Raw Material Solution

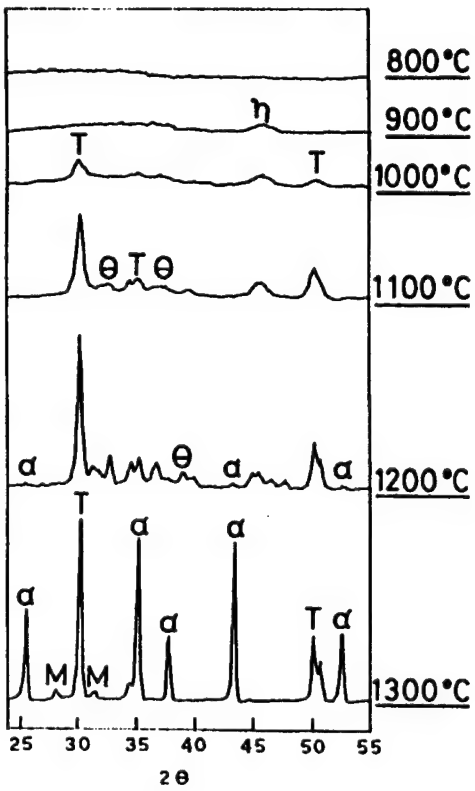

Figure 8. Changes in Al_2O_3–15wt%ZrO_2 Powder With Heat

Figure 9 shows changes in the size of the crystallites, caused by heating tetragonal zirconia contained in the synthesized powder. For comparison, the figure also contains the results of a similar study of a powder prepared by the conventional oxide mixing method. The specimen prepared by the spray pyrolysis process has crystallites of tetragonal zirconia that are much smaller in size than those of the specimen prepared by the oxide mixing method.

Figure 10 shows the relationship between the ratio of the tetragonal zirconia contained in the synthesized powder and heating temperature. Those zirconia grains contained in the powder that was obtained by the spray pyrolysis process did not, it was discovered, turn monoclinic even if heated at high temperatures and then cooled, and most of them remained tetragonal. Sintering of the powder showed that it began to be compacted at 1,600°C, a relatively lower temperature, producing a microscopic structure of composite that had submicron zirconia grains dispersed in the grain boundaries and inside the alumina grains.

Figure 11 shows the relationship between the sintered body's bending strength and fracture toughness and the zirconia content. Bending strength reached its highest point when the zirconia content was 20 percent in weight, obtaining about 1.7 times as high a strength as that of a specimen of alumina alone.

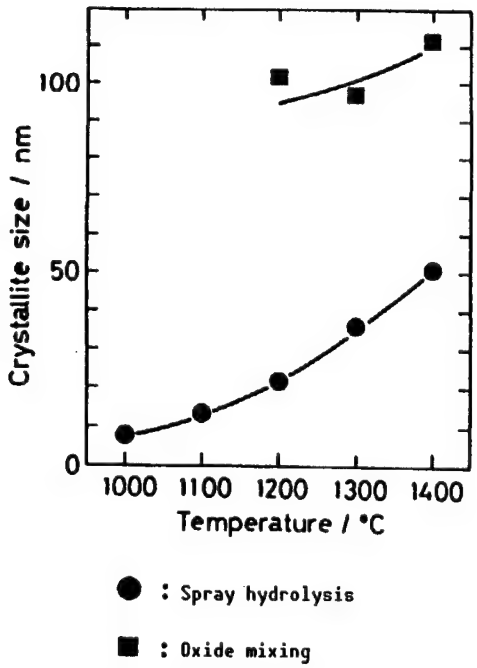

Figure 9. Changes in Size of Crystallites of Tetragonal Zirconia With Heat

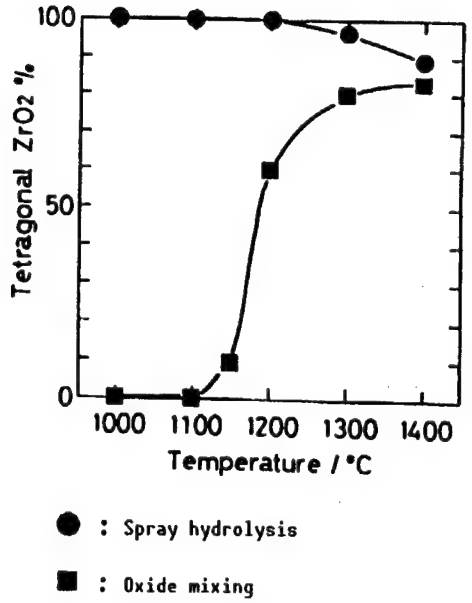

Figure 10. Changes in the Ratio of Tetragonal Zirconia With Heat

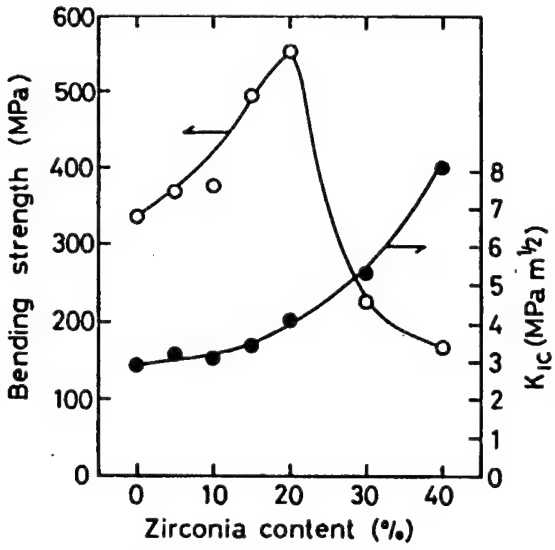

Figure 11. Relationship Between Sintered Body's Bending Strength and Fracture Toughness and Zirconia Content

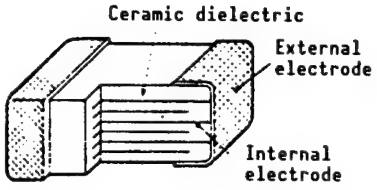

Figure 12. Internal Structure of Multi-level Ceramic Condenser (MLC)

Fracture toughness, on the other hand, kept increasing with increasing alumina content.

The spray pyrolysis process enables compound systems of ceramic materials that are easy to sinter yet have a fine and uniform dispersion of ingredients to be obtained.

5. Synthesis and Sintering of Barium Titanate

One of the important applications of barium titanate is its use in multilevel ceramic condensers (MLC). Ceramic dielectrics and internal electrodes are stacked in layers (Figure 12). An MLC is small in size but has large capacitance. Recent tasks with MLCs are lower costs, smaller sizes, and larger capacities. Studies have been made on the use of base metals for the internal electrodes and on the use of thinner dielectric layers (<10 μm). A powder that has both ease of sintering and uniform quality has been demanded as the raw material.

Drawing on the strengths of the spray pyrolysis process, i.e., the ease with which it enables the composition to be controlled and the ease with which it enables trace amounts of elements to be dispersed uniformly, we trial manufactured sintered bodies of ferroelectric barium titanate that can be sintered at low temperature.

Figure 13 shows the procedures for preparation of the starting solution. For materials, we used barium nitrate and titanium isopropoxide. In some experiments, a solution of copper nitrate was added to use copper oxide as the sintering aid.

Figure 14 shows X-ray diffraction patterns of the synthesized powders and of synthesized powders calcined under various conditions. Single phases of barium titanate were obtained after preliminary sintering at 620°C for an hour.

Figure 15 shows the results of analysis of grain distribution for synthesized powder and grain distribution for the same synthesized powder that was pulverized in a vibration mill. Relatively simple pulverization resulted obtaining a very sharp grain distribution curve.

For comparison, Figure 16 shows the sintering curve for synthesized powder, along with the sintering curve for a powder prepared using the conventional solid-phase reaction method.

Figure 17 shows changes in the degree of sintering when the ratio of barium and titanium in the composition is changed. In the figure the sintering temperatures needed for the sintering density to reach 90 percent of the theoretical density are given. The synthesized powder showed an improvement in the degree of sintering when the content of barium in the composition was on the higher side of the norm. The best result was obtained when the content of barium was 3 mol percent above its stoichiometric composition.

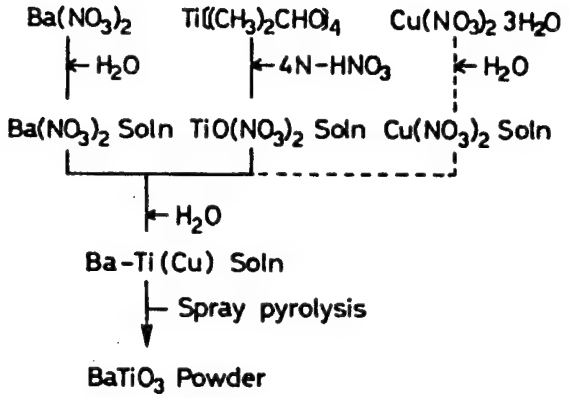

Figure 13. Preparation of Barium Titanate Raw Material Solution

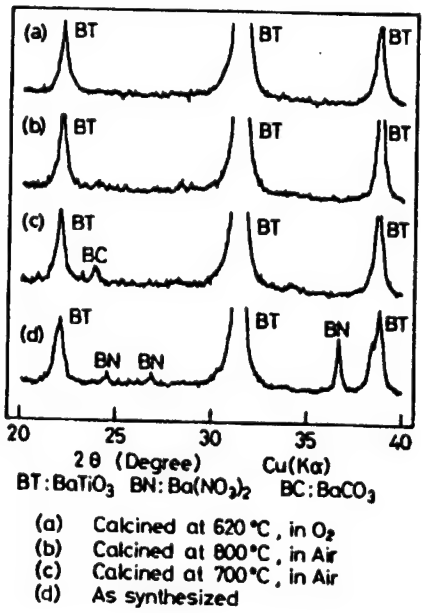

Figure 14. X-Ray Diffraction Patterns of Synthesized Powders of Barium Titanate and of Synthesized Powders of Barium Titanate Calcined

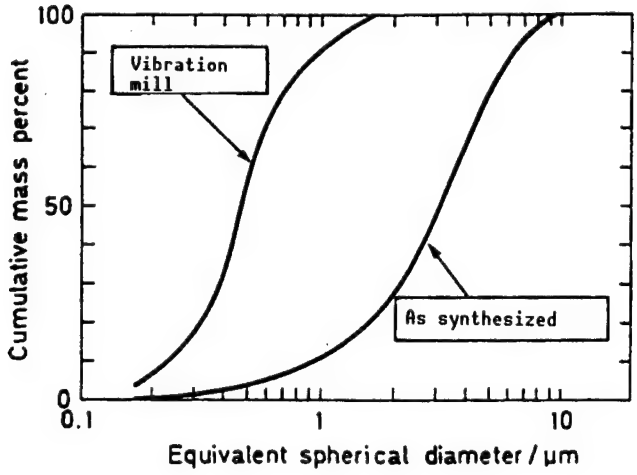

Figure 15. Results of an Analysis of Grain Distribution in Barium Titanate Powders

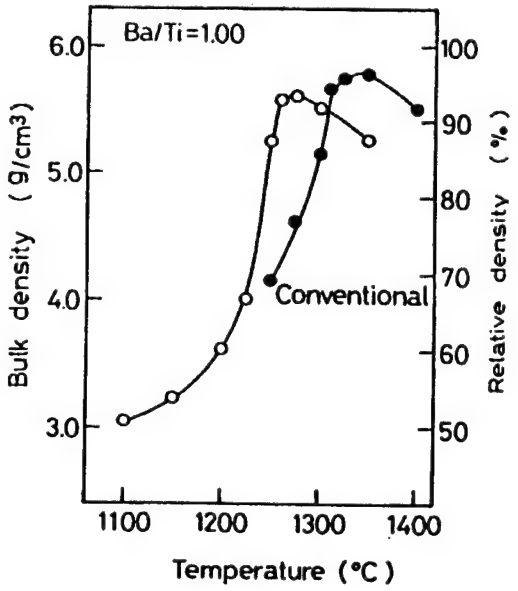

Figure 16. Sintering Curves for Synthesized Powders of Barium Titanate

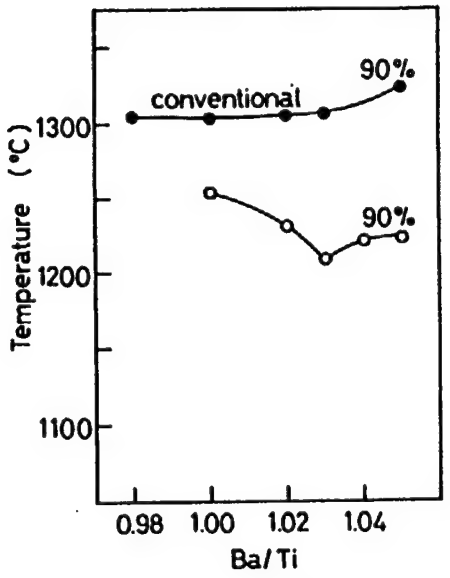

Figure 17. Relationship Between Degree of Sintering and Barium/Titanium Composition Ratio for Synthesized Powders

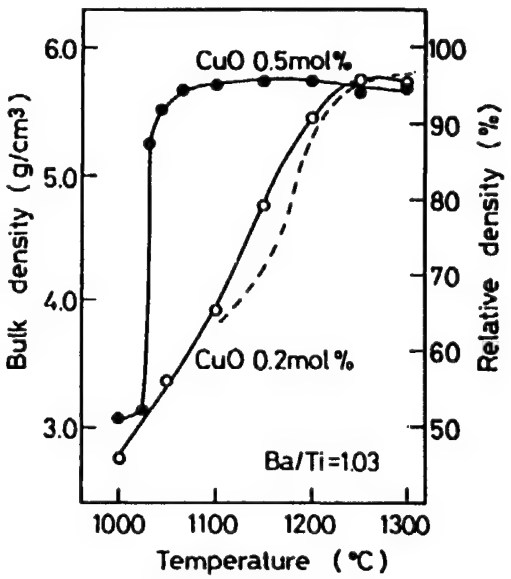

Figure 18. Low-Temperature Sintering of Barium Titanate Synthesized Powders by Addition of Copper Oxide (a 3 mol percent excess of barium)

Figure 18 shows sintering curves for powders (Ba/Ti - 1, 03) that were added with 0~1 mol percent of copper oxide. As with the powder containing no copper oxide, the powders added with up to 0.3 mol percent of copper oxide showed moderately increasing densities with increasing sintering temperatures. However, when the content of copper oxide was above 0.4 mol percent,the densities rose sharply in the sintering temperature range of 1,025~1,075°C. The synthesized powder added with 0.5 mol percent of copper oxide achieved a degree of sintering equal to about 95 percent of the theoretical density.

The degree of sintering of barium titanate is greatly affected by the ratio of barium and titanium in the composition, and barium titanate of an appropriate composition can be sintered at a reduced temperature. It has also been known that adding trace amounts of an additive enables the sintering temperature to be lowered to a great extent. In reality, the raw materials for MLC contain many other elements, in addition to barium titanate, so great care is required to realize a homogeneous quality of these diverse elements. We believe the advantages of the spray pyrolysis process will become more apparent, the larger the number of elements that go into the raw material powder.

Synthesis of Functional Materials by Sol-Gel Method

916C0033E Osaka DAI 18 KAI NYU SERAMIKKUSU SEMINA TEKISUTO in Japanese
2 Mar 91 pp 83-93

[Article by Toshinobu Yoko and Sumio Sakubana, Chemical Institute of Kyoto University: "Low-Temperature Synthesis of Functional Materials by Sol-Gel Method:]

[Text] **1. Introduction**

In recent years the sol-gel process has been gaining attention from both the materials science and engineering perspective as a technology that enables functional, inorganic materials to be synthesized at low temperature. In the sol-gel process, the starting material is metal alkoxide (M(OR)n, R:alkyl group), metallic salts, and metal acetylacetonate dissolved in an organic solvent. The solution is hydrolyzed and reacted for condensation polymerization which produces a sol of oxide fine particles suspended in the solvent. If the hydrolysis occurs rapidly, a deposition of ultrafine particles occurs. If a filamentary polymer is generated in the sol, it will be possible to spin gel fibers. If a sol containing a three-dimensionally grown polymer is gelled, the result will be a hard-to-crack bulk gel. Gel coating films can be obtained from these sols containing polymers of intermediate levels of polymerization. The various gels can be converted into glass or ceramics at temperatures 400~1,000°C lower than those normally required for their manufacture. With the sol-gel method, it is possible to directly manufacture a product of a desired shape by controlling the condensation polymerization reaction. When the low-temperature synthesis feature of the sol-gel process is taken into account, the technology may be used for the manufacture of materials for use as matrixes for functional materials (both organic and inorganic). Materials by the sol-gel process are expected to find applications in a broad range of fields as composite materials. The following are expected of the sol-gel process:

(1) Some materials can be manufactured only by the sol-gel process.
(2) Highly functional materials can be synthesized.
(3) High throughput is expected.

This paper presents an outline of the sol-gel process, the current status of applications of the technology in the development of highly functional ceramic materials, and its future. It will not, however, dwell on the synthesis of raw material fine powders.

2. An Outline of the Sol-Gel Process

2.1 Sol-Gel Reaction

For starting materials, metal halides, metal oxyhalides, and metallic organic compounds are used. Metal alkoxides are most widely used because 1) a high-purity raw material can be obtained, 2) there is no need for removing nonvolatile elements like halides, and 3) it is easy to control the hydrolysis and condensation for polymerization processes. In metal alkoxides, the speed with which the hydrolysis reaction progresses can be controlled to some extent by changing the type of alkoxyl group. For example, the longer the alkyl groups and the higher the level of branching, the greater the stability of hydrolysis because of stereoscopic impedance. When this nature is exploited, the problem that occurs when preparing compound oxides, that is, the effect of a difference in speeds with which different kinds of metal alkoxides are hydrolyzed, can be solved to some extent. Theoretically, the hydrolysis reaction and the condensation polymerization reaction are expressed as:

$$M(OR)_n + nH_2O \xrightarrow{hydrolysis} M(OH)_n + nROH \quad (1)$$

$$M(OH)_n \xrightarrow{condensation\ polymerization} MO_{n/2} + n/2H_2O \quad (2)$$

In general, metal alkoxides lack affinity with water. If they are to be mixed uniformly, it is necessary to have a solvent common to them all. Adding water directly to highly reactive metal alkoxides leads to partial hydrolysis, causing them to precipitate. To prevent the occurrence of this phenomenon, in most cases both the metal alkoxides and water are diluted with a common solvent such as alcohol. The actual reactions take a much more complex shape than is expected from the above formulas.

To tell a conclusion, if the quantity of water is small relative to the quantity of alkoxides when using an acid catalyst, the particles of oxides formed in the sol are of the filament type. If the water quantity is large, three-dimensionally grown particles are formed. If an alkaline catalyst is used in place of an acid catalyst, three-dimensionally grown particles are obtained at all times.

2.2 Direct Synthesis of Bulk Gels

Preparing rod-like gels with a diameter above 10 mm or gel plates of sizes above 10 cm x 10 cm in area and 5~20 mm in thickness is difficult because they are vulnerable to cracks and splits during drying. To solve the problem, the seven methods listed in Table 1 have been proposed for silica gels.

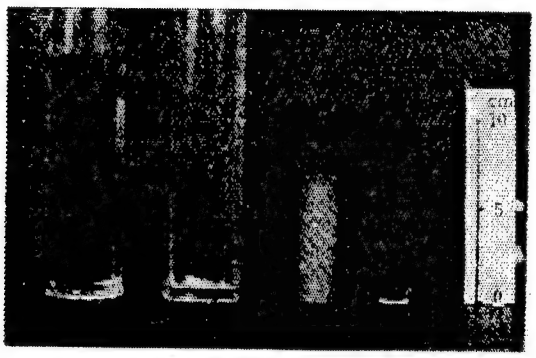

Figure 1. Synthesis of Silica Glass Bulk Using DCCA

Table 1. Various Methods for Synthesizing Silica Gels

Method	Remark	Investigators
(a) Supercritical drying	No capillary force works.	Zarzycki
(b) Hydrolysis and poly-condensation at neutral or weakly basic condition	Formation of large particles resulting in smaller capillary force.	Yamane, Susa
(c) Use of silica fine powder as starting material	Large particles make the capillary force small.	Rabinovich, Scherer
(d) Mixing of silica fine powder	Large particles make the capillary force small.	Toki
(e) Use of solvent with higher boiling point and lower surface tension than water	Low surface tension of the solvent at the final stage of drying.	Hench, Adachi, Sakka
(f) Use of tetramethoxy silane solution of high HCl content	Formation of large particles resulting in small capillary force	Kozuka, Sakka
(g) Spinodal decomposition	Formation of interconnective pores	Nakanishi, Soga

A principle common to all these methods is to suppress the capillary force working on the silica gel as much as possible. In practice, the methods proposed are supercritical drying, large-diameter pores, and retention of a solvent with a surface tension smaller than that of water through the last stage of drying. Figure 1 shows an example of a silica glass rod prepared by using a drying constraint and control agent (DCCA) called dimethylformamide.

Figure 2. SiO_2 Glass Fiber Synthesized by Heat Treating Gel Fiber at 1,073 K

Ceramics are usually manufactured by sintering formed bodies of powders. The use of a fine powder of less than 0.1 μm leads to the formation of secondary particles, and attempts have been made at forming ceramic products directly from the gel by bypassing the troublesome powder process. A mixture of $Si(OC_2H_5)$ and $Al(O\text{-}secC_4H_9)_3$ was hydrolyzed using an HCl or an NH_3 catalyst to obtain gels. The gels thus obtained were derived and sintered at 1,500°C for three hours. The gel obtained with the use of NH_3 catalyst produced a highly compact sintered body with a relative density of 97.6 percent. Compared with the sintered body, a product which was obtained by compacting a powder of the same alkoxide starting material into a green and by sintering the green at 1,500°C, the direct synthesis method simplifies the process to a great extent yet results in a compact sintered body at relatively low temperatures.

2.3 Synthesis of Fibers

Fibers can be spun directly from spinnable sols. However, not all sols render themselves to fiber spinning. Spinnable sols need to have a viscosity of more than 10 poises and have filamentary polymers inside themselves. The morphology of a polymer can be controlled by adjusting the amount of water needed for hydrolysis. For silica sols, a spinnable sol can be prepared by adjusting the ratio of the amount of water to that of alkoxide to the 1.5~5 range and by using an acid as the catalyst. Heating the gel fibers spun from these sols at 800°C enables them to be turned into SiO_2 glass fiber. Figure 2 shows an industrially manufactured SiO_2 glass fiber.

Table 2 gives ceramic fibers of Al_2O_3, ZrO_2, TiO_2, and $BaTiO_3$ that can be manufactured only the sol-gel process.

2.4 Coating Films

For coating, sols that have their water content adjusted so that they will have polymers more grown than filamentary polymers grow internally and that have their levels of dilution with solvent increased to prevent partial hydrolysis are suited. The composition of sols for coating is highly dependent on the kind of oxide, and an appropriate composition needs to be found for a

Table 2. Examples of Glass and Ceramic Fibers

Fibers (system)	Characteristics	Investigator
Silica glass (SiO_2)	Insulating	Kamiya, Sakka Asahi Glass Co.
Alumina (Al_2O_3)	Insulating	Sumitomo
Silica–alumina (SiO_2–Al_2O_3)	Insulating	3M
Titania (TiO_2)	Insulating	Kamiya, Yoko
Stabilized zirconia (ZrO_2:CaO)	Insulating	Kamiya, Yoko
Barium titanate ($BaTiO_3$)	Ferroelectric	Yoko, Kamiya
Lead titanate ($PbTiO_3$)	Ferroelectrc	Kamiya
Lithium niobate ($LiNbO_3$)	Dielectric	Hirano
Titanium nitride (TiN)	Electronconducting	Kamiya, Yoko
β–alumina (Na_2O–Al_2O_3)	Ion–conducting	Sakka
Superconducting ($YBa_2Cu_3O_{7-x}$, Bi–Pb–Ca–Sr–Cu–O systems)	Superconducting	Sakka

given oxide. The stability of coating solutions, that is, their life, is very important from practical use perspective. This can be realized by chemically modifying metal alkoxides with a chelating agent such as β–diketones and amines.

Among the methods for obtaining deposition of a coating film on the substrate are the spray method in which a sol is sprayed, the spinner method in which a sol is dripped onto a rotating substrate and is dispersed by the action of the centrifugal force, the dip coating method in which a substrate is dipped into a sol and is pulled up, and the screen printing method. These processes have various features and should be used where their advantages can be put to the greatest use.

The objectives of coating film can be broadly divided into modifying the surface of a substrate and protecting it from damage and exploiting the functional capabilities of the thin film itself. As shown in Table 3, the functional capabilities are further subdivided into optical, electromagnetic, chemical and mechanical protective, and catalytic capabilities. Some optical capabilities are already being put to practical use in the form of reflection, antireflection, and selective reflection film, but a large majority are still in the development or planning stages. Various capabilities of these coating films are briefly described in Table 3.

A. Optical Films

Optical films are one of the most important applications of coating films produced by the sol–gel method. Called "Sol–Gel Optics," this field has recently been seeing a great growth.

Table 3. Application Examples of Coating Films by Sol-Gel Process

Function/ applications	Uses	Composition
A. Optical		
Coloring, absorption of light	Infrared ray shielding, coloring of light-shielding glass	TiO_2–SiO_2 SiO_2–R_mO_n (R = Cr, Mn, Co, Ni, Cu) Fe_2O_3, Cr_2O_3, CoO
Inference film	Coloring	TiO_2
Reflecting film	Heat shielding	ITO, FeO, VO_2–SiO_2
Antireflection film	Nuclear fusion, display	SiO_2, TiO_2–SiO_2
Selective reflection film	HUD windshield	TiO_2–SiO_2 (2000A)
Patterning	Optical disk	SiO_2–TiO_2, B_2O_3
Phosphor doping	Pigment laser, solar cell	SiO_2, Al_2O_3 + organic pigments
Organic-inorganic complexes	PHB, nonlinear optical materials	SiO_2, Al_2O_3 + CdS, organic materials
Refractive index distribution	Waveguide	$PbTi_4O_9$, $LiNbO_3$ SiO_2–TiO_2, Ta_2O_5
B. Electromagnetic		
Ferroelectric film	Capacitor, IC memory, optical shutter	$BaTiO_3$, Pb (Ti,Zr) O_3 $KTaO_3$, PMN, PFN, SBN
Piezoelectric film	SAW device	$LiNbO_3$, $Li_2B_4O_7$
Electron conductor film	Transparent electrode	In_2O_3–SnO_2 CdO–SnO_2
	Antistatic application	V_2O_5
Thin films of superconductors		YBCO, BSCCO
Films of ion-conductors	Solid electrolytes for batteries	β–Al_2O_3, Li_2O–SiO_2 "nashikon," $LiAlSi_nO_m$
EC film	Display element	WO_3, V_2O_5, TiO_2–CeO_2
Films of magnetic bodies	Magnetic and magneto-optical recording	$NiFe_2O_4$, Fe_3O_4, YIG boro-silicate glass Fe_2O_3
C. Chemical-mechanical protection		
Protective film for glasses, copper plates, and semi-conductors	Preventing alkalines from diffusing,	SiO_2
	Corrosion and heat resistance	ZrO_2–SiO_2, ZrO_2
	Passivation	GeO_2–SiO_2, Si–O–N
	Increase in strength	SiO_2
D. Catalytic		
Semiconductor electrode, catalytic carrier film	Optical, electrical dialysis of water, catalyst	TiO_2, $SrTiO_3$ Al_2O_3:Pt SiO_2, TiO_2, Al_2O_3

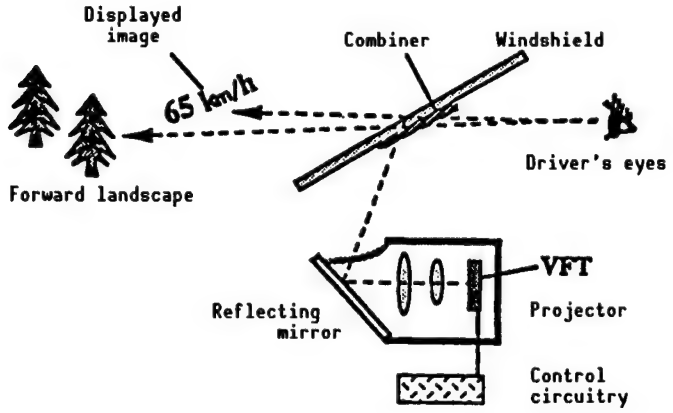

Figure 3. Optics for Heads-Up Display (HUD)

A characteristic of the sol-gel method is the generation of a liquid stage called sol at room temperature, a technique that enables the liquid-state sol to be doped with various elements. Nitrate or acetate transition elements are added to an SiO_2 sol, and the mixture is stirred for a uniform solution. Applying the product to a window glass turns the window into tainted glass. The upper limits of oxide densities, where films of a uniform quality could be obtained, were 10 mol percent for Cr_2O_3, 20 mol percent for Mn_2O_3, 45 mol percent for Fe_2O_3, 45 mol percent for CoO, 55 mol percent for NiO, and 45 mol percent for CuO. The transmissivities of 0.2~0.5 μm-thick coating films of the respective densities at 555 nm were 81 percent for Cr, 68 percent for Mn, 63 percent for Fe, about 0 percent for Co, 59 percent for Ni, and 95 percent for Cu. Despite the thinness of the films, strong absorption (coloring was observed.

TiO_2 material has a large index of refraction, so even "skinny" films generate an interference color of a beautiful tone. Consequently, film color differs subtly from film thickness to film thickness, and the transmitted light and the reflected light produce different colors, making the two colors supplementary. Films of TiO_2-SiO_2 glass are used as reflection, antireflection, and selective reflection films. As shown in Figure 3, selective reflection films are incorporated in vehicles as heads-up displays (HUDs). At present. HUDs are used only for presenting vehicle speed, but, in the future, they are expected to grow into intelligent displays, presenting navigation-related data such as road maps and other information.

Examples of applications where features of the sol-gel process, such as low-temperature synthesis and mixing at molecular levels, are exploited to a high degree are considered to be the gel or glass complexes doped with functional organic materials or inorganic materials. Thin films of SiO_2 or Al_2O_3 doped with rhodamine 6G, for example, have been confirmed to be capable of laser oscillation. An attempt was made to exploit laser oscillation for production of nondirectional solar cells. Attempts are underway to fabricate thin films of gels doped with organic materials that display the hole-burning effect or fabricate organic or nonorganic materials that display two- or three-dimensional nonlinear optical effects.

Attempts are also under way to fabricate glass thin film read-only memory (ROM) disks, in which a die (stamper) is pressed against a gel while it is still soft for patterning. The gel is then sintered. Far superior to existing plastic disks in terms of durability, glass thin film disks may find widespread use in the future.

A few reports have been published on successful trials of such composites for use as optical waveguides.

B. Electrical and Magnetic Capabilities

Applications of the sol-gel process in electronics are expected to increase greatly. As shown in the table, various functional thin films have been trial manufactured, such as films of dielectrics, piezoelectrics, electron conductors, superconductors, ion conductors, EC ("electrochromism"), and magnetic substances.

Compound oxides, led by perovskite compounds, are widely used for oxide thin films for use in electronics. Thin films of crystals, like glasses, prepared by the sol-gel process are transparent. This feature is extremely important in that it enables electronics and magnetic materials to be used as optoelectronic and magnetooptical materials, respectively.

When a $BaTiO_3$ film prepared from a sol--the sol was obtained by mixing well isopropoxides of Ba and Ti, adding acetic acid to the mixture, as a catalyst, and letting the mixture hydrolyze--was subjected to heat treatment at 500°C. It remained amorphous but at 600°C, it had a precipitation of the $BaTiO_3$ phase. Despite the fact that the heat treatment occurred in air, the formation of $BaCO_3$ was not observed, nor was there precipitation of any other crystal phases. This indicates that mixing the Ba and Ti atoms while they were in a liquid state enabled them to be mixed uniformly at the atomic level.

Besides ITO, Cd_2SnO_4 is known as the material for transparent electrodes. Films made by the high-frequency sputtering or spray method have precipitation of CdO, SnO_2, $CdSnO_3$ in addition to Cd_2SnO_4, which causes their electrical properties to degrade. Films prepared by impregnation in the sol-gel process enables single-phase film of Cd_2SnO_4 to be obtained at lower temperatures because a complex compound in the sol and stoichiometry is maintained:

$$2Cd(OAC)_2 + Sn(O\text{-}nBu)_4 \rightarrow \{Cd_2(OAC)_4 \cdot Sn(O\text{-}nBu)_4\}$$

$$\xrightarrow{H_2O} Cd_2SnO_4 + 4AcOH + 4nBuOH \qquad (3)$$

Films of ferrodielectric materials are gaining attention for use as large-capacity capacitors, and nonvolatile IC memories. Transparent films are expected to find use in superhigh-speed shutters and photography materials by drawing on their Kerr effect. Attempts have been made to synthesize PZT, $Pb(Fe_{1/2}Nb_{1/2})O_3$(PFN), $Pb(Mg_{1/3}Nb_{2/3})O_3$(PMN), and $Sr_{1-x}Ba_xNb_2O_6$(SBN).

Piezoelectric thin films oriented to any specific directions are very important as the materials for SAW devices.

Attempts have also been made to synthesize ferrite thin films, which are Fery magnetic materials. The obtained Fe_3O_4 thin films reportedly possess an antimagnetic force larger than that of their bulk material. Synthesis of the representative magnetooptical material, garnet ferrite, has also been attempted.

EC films are regarded promising as displays, and the sol-gel process is most appropriate for the manufacture of large-sized EC films. EC films of WO_3, V_2O_3, TiO_2-CeO_2 have been manufactured with this in mind. It has also been reported that V_2O_5 films prepared by the sol-gel process have high electrical conductivities, equal to those of crystals.

C. Chemical and Mechanical Protection Capabilities

Coating films are highly effective in raising the substrates's resistance to oxidation and chemicals. These are occasionally used as the diffusion barrier between the substrate and coating film (especially against alkali). Attempts have been made for heat treating SiO_2 coating films in ammonia and using them as Si-O-N passivation films. Ordinary soda lime glasses beginning with SiO_2 glass, as well as the representative glass fiber, E glass, have exceedingly lower resistance to alkali. Coating the surfaces of E glass fibers with ZrO_2 film, for example, will enable alkali resistance of those fibers to be increased. It has also been reported that applying a coating of SiO_2 on the scratched surface of an SiO_2 glass rod improves mechanical strength. The increased strength is thought to have come from the fact that the scars on the glass rod's surface were filled by the coating.

D. Coating Films as Catalysts

TiO_2 coating films, prepared from a sol obtained by hydrolyzing titanium isopropoxide, were shown to have higher energy conversion efficiency than single crystal TiO_2 when used as electrodes for photoelectric-chemical reactions. The higher efficiency is thought to have been caused by the numerous pores on the surface of the films.

Alkoxide of Si is added with an ethylene glycol solution containing nitrates of Ni, Fe, and Co and is hydrolyzed into a gel. The gel is reduced by hydrogen to have precipitations of Fe, Ni, and Co and the alloys inside the silica medium. The result is an excellent catalytic material with metallic particles dispersed inside it. These metallic particles have extremely small particle diameter distribution, a great help in elucidating the mechanism of catalytic action.

3. Synthesis of Advanced Materials by Sol-Gel Process

3.1 Advanced Materials With Gradient and Composite Microstructures

Advantages of the sol-gel process in the synthesis of advanced materials are:

(1) The application of the sol-gel process enables the properties of materials to be greatly improved.
(2) The materials can be synthesized only with the sol-gel process.

Because of the differences in microstructures, the sol-gel process enables:

(1) Materials with a uniform microstructure of composition (including porous materials).
(2) Materials with a gradient microstructure or composition.
(3) Materials with a composite microstructure or composition to be produced.

Some examples of synthesized materials are given in Table 4. The table contains mostly examples of bulk materials, but the same classification can be made for thin films, fibers, and fine powders.

Table 4. Synthesis of High-Performance Functional Material by Sol-Gel Process

Microstructure of product/ Example	Incorporation of second component	Application
Uniform microstructure		
Preform of optical fiber		Optical fiber
Mullite ceramics		Dense ceramics
Alumina sheet		Substrate of IC
Mica glass-ceramics		Machinable ceramics
Porous silica		Filtration, purification
Gradient composition		
Graded index lenses	Cations extracted from gel	Image formation
Asymmetric ultra-fine filter	Introduction of sol into calcinated Al_2O_3	Filtration, purification
Composite micro-structure		
Glass containing Cd(S,Se) crystals	Diffusion of ions into gel	Nonlinear optical glass
Organic-inorganic composite	Reaction of the compounds in solution introduction into porous gel	Hard contact lens Sealing Lightweight optical materials Nonlinear optical glass
Functional organic molecules-containing material	Gelation of solution	Laser, PHB materials
Multilayer TiO_2-SiO_2 coating film	Repeated coating	Reflecting, anti-reflecting

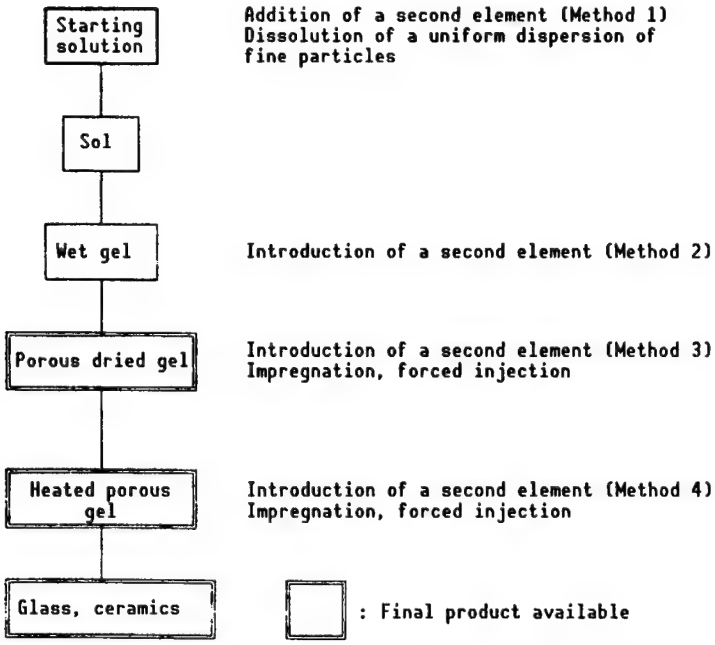

Figure 4. Synthesis of Functional Composites and Gradient Materials by Sol-Gel Process

In the initial stage of the research on the sol-gel process, the emphasis in research was overwhelmingly directed at uniform microstructure, but research is shifting to gradient and composite microstructures. To synthesize materials with a gradient or composite microstructure by the sol-gel process, a second element needs to be added or removed at one of the process stages.

With the second, third, and fourth methods (Figure 4), the second element is introduced into a wet gel, a porous dried gel, and a porous heating gel, respectively, by diffusion or injection. When the second element is introduced or when the second element is removed, controlling the diffusion enables a material with a gradient microstructure or a gradient composition to be obtained.

3.2 Examples of Applications

3.2.1 GRIN Lenses

A few attempts have been made to use the sol-gel process to produce a GRIN rod lens of which the index of refraction diminishes radially from its center toward its radius vector. Compared with the ion exchange process using molten salts, the technique enables GRIN lenses four to five times as large to be obtained.

A rod-like wet gel of SiO_2-GeO_2 (SiO_2-TiO_2) is produced by hydrolysis or condensation polymerization of the two-element system of $Si(OCH_3)_4$-$Ge(OC_2H_5)_4$ ($Si(OCH_3)_4$-$Ti(OC_4H_9)_4$). This gel is dipped into a neutral or weak acid solution to let Ge(Ti) liquate out partially (method 2). This technique is called the destuffing. Drying and sintering the gel of the Ge(Ti) with a density gradient

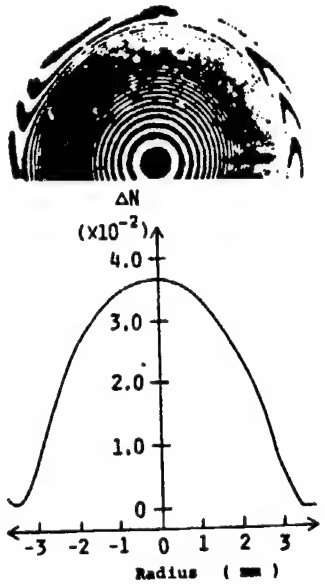

Figure 5. Light Interference Pattern and Distribution of Refractive Indexes for GRIN Lens

enables a GRIN lens to be obtained. In another technique, a porous gel is dipped into a water solution containing Pb to allow the Pb to be uniformly introduced into the pores (staffing). To give it a back index of refraction, the gel is dipped into a KNO_3 water solution to allow the Pb to be liquated out partially (method 2).

The interference pattern and the index of refraction distribution of a cross section of the GRIN lens thus obtained are shown in Figure 5.

3.2.2 Nonsymmetrical Ultrafine Filters

Ceramics are best suited as the raw materials for filters that need to withstand high temperatures and high pressures and have high levels of stability against microorganisms and chemical agents. Coet, et al., produced a nonsymmetrical ultrafine filter using the sol-gel process. The inside of a 2-mm thick alumina tube with pores 10 μm in size was coated with a 40 μm thick alumina coating containing 0.8 μm pores. This was further overlayed with a 15 μm coating film containing 0.2 μm diameter pores. The filter with a nonsymmetrical structure thus obtained satisfies the above-mentioned conditions and guarantees fast filtration speeds.

3.2.3 Glasses Containing Functional Microcrystals and Their Thin Films

Glasses containing superconducting ultrafine particles (10 μm) as the nonlinear optical material of high three-dimensional nonlinear susceptibility are gaining attention. Much research has been conducted on $CdS_{1-x}Se_x$ as the semiconductor because the material has been used in filter glasses. However, the material easily disintegrates or evaporates at high temperature. When large amounts are included as dopant, it fails to melt, thereby making it

impossible to produce glasses of a uniform quality. The amount that can be added as dopant is 0.5~1 weight percent at best. With the sol-gel process the starting material takes a liquid state at room temperature, and this enables large amounts of superconducting elements to be doped. The lower temperatures at which heat treatment can be applied also allows the process a potential to synthesize excellent nonlinear optical materials. Two methods are being tried: one in which Cd, S, and Se sources are introduced into the starting material (method 1), and the other in which a dried gel containing Cd is heat treated in an H_2S or H_2Se atmosphere (method 3). Active research is under way.

3.2.4 Organic-Inorganic Composites

Synthesizing inorganic-organic composites without the use of the sol-gel process is extremely difficult. With the sol-gel process, there are two methods of synthesizing such composites. With the starting solution, organic and inorganic materials are mixed at the same time (method 1), and with a porous gelled body or a vitreous body, organic materials are impregnated (method 3).

Using "epoxy silane," "methacryl oxysilane," and titanium alkoxide as the starting material, Schmidt, et al., synthesized an organic polymer gel containing either -Si-O- bonds or -Ti-O- bonds (method 1). The gel featuring high strength, flexibility, wettability, and high oxygen penetrability has been commercialized in the form of contact lenses. Using similar methods, research is being conducted on the synthesis of patterning materials, transparent barrier films, sealing agents, lithium ion conductors, and nonlinear optical materials.

Optical composite materials featuring light weight, transparency, and high mechanical strength have been synthesized by letting porous gels impregnated with molten PMMA, for example (method 3). In a fourth method, composite materials for optics have been synthesized, in which a gel is heated to about 600°C to produce a somewhat transparent glass. The remaining pores are impregnated with functional organic materials such as pigments (method 4).

3.2.5 Composite Materials Containing Organic Materials of Molecular Dispersion Function

Optical transparent alumina or silica gels containing a uniform dispersion of molecules or functional organic materials, such as phosphor, pigment laser, hole burning (PHB), and nonlinear optics materials, are gaining attention as high-function, nonlinear optics materials. Particles of these functional organic materials easily get associated with one another in a solution. If such an association has taken place, it is impossible to obtain the intended functionality. Therefore, it is necessary to confine the particles of these organic materials as they are in a matrix. This is feasible only with method 1.

The hole-burning effect has now been observed in silica gels doped with DAQ and in alumina thin films doped with DNQ. Laser oscillation has also been

confirmed in alumina thin films doped with rhodamine 6G. Research is actively under way on synthesis of gels for nonlinear optics.

4. Conclusion

The sol-gel process has been used in the synthesis of various shapes of functional materials, such as bulk, thin film, and fiber, from such materials as ceramics, glass, and their composites. As for the functionality of the sol-gel derived products, they are finding use in a wide variety of applications, such as optics, electronics, magnetic, and mechanical and chemical fields. Some functional materials, such as organic-inorganic composites, can be synthesized only by the use of the sol-gel process. Others can be synthesized by other means. Even with the latter class of materials, the sol-gel process may become applicable if the technique's characteristics are proved beneficial in their synthesis. Applications of the sol-gel process will no doubt increase in the future.

References

1. Sakuhana, S., "Science of the Sol-Gel Process; Low-Temperature Synthesis of Functional Glasses and Ceramics," Agune Shofusha Publishing Co., 1988.

2. Sakuhana, S., et al., JOURNAL OF The JAPAN INSTITUTE OF METALS, Vol 27, 1988, pp 775-783.

3. "Sol-Gel, Science and Technology," ed. by M.A. Aegerter, et al., WORLD SCIENTIFIC, 1989.

4. J. NON-CRYSTAL. SOLIDS, Vol 121, 1990.

5. Proceedings of the International Society for Optical Engineering, "Sol-Gel Optics," ed. by J.D. Mackenzie and D.R. Ulrich, Vol 1328, 1990.

6. Sakka, S. and Yoko, T., "Sol-Gel Derived Films and Applications," in "Chemistry, Spectroscopy, and Applications of Sol-Gel Glasses," ed. by C.K. Jorgensen and R. Reisfeld, Springer-Verlag, in press.

Mechanical Alloying

916C0033F Osaka DAI 18 KAI NYU SERAMIKKUSU SEMINA TEKISUTO in Japanese
2 Mar 91 pp 95-100

[Article by Hideo Shingu, Metal Science and Technology, Faculty of Engineering, Kyoto University]

[Text] **1. Introduction**

Mechanical alloying (MA) is a method of producing an alloy without going through the melting and forging process, in which metals while in their solid phase state are mixed and kneaded together, or it may be called a technique of dispersing the second phase into the matrix phase. A technology developed by Benjamin of the Inco Corporation in the United States in early 1970, the basic process of and the structures available with the technology are described in detail in the article written by the developer in 1976. The MA technology is also described in detail in "The Metals Handbook." Mechanical alloying of light metals is described in detail in the latest paper by Froces. Beginning with this journal, several papers on MA have already been published in Japan. In recent years MA research has been actively undertaken worldwide, triggered by the discovery that some MA-derived alloys displayed amorphous properties. Amorphization has been discovered in alloys with aluminum as their major element. Much research has been done on the formation of nonequilibrium alloy phases and of ultrafine structures, in addition to the formation of amorphous structures. International conferences on MA have been held several times in the United States and Europe, and an international symposium on MA is slated to be held in Kyoto in May of next year.

In this paper, the basic technology of MA, of which much has already been written, is omitted. The author's views on the principles of the MA process and thermodynamics of the nonequilibrium phase formation, based on the results of experiments, are introduced.

2. Principles of Mechanical Alloying Process

The dispersion of fine particles through the repetition of cold pressure compaction and destruction (formation of dispersoids), is a basic of the MA process. The basic principle is applicable to all kinds of processes,

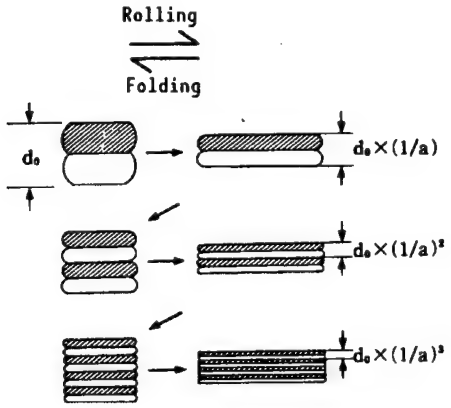

Figure 1. Principles of the Process for Ultrafine Mixing of Different Kinds of Elements by Mechanical Alloying

In a repetition of mechanical folding and rolling action, if the draft per action is (1/a), a repetition of the action by n times enables the original size d_0 to be reduced to $d(n) = d_0(1/a)^n$. When a = 3, n = 10, the approximate distance between the different kinds of elements is about $d_0 \times 10^{-5}$.

including mechanical alloying using a ball mill of mechanical alloying techniques using attrition or vibration mills. The repetition of compaction and destruction may be modeled as that of rolling and folding. Forging of a Japanese sword, rice-cake making, or the manufacturing process of crumbs for pies share the common basic principle with mechanical alloying.

Figure 1 shows a series of rollings and foldings. Suppose that the draft from the first rolling is one-third. If the rolling and folding is repeated 10 times, we get a value of $(1/3)^{10} = 10^{-5}$, that is, the thickness is reduced to about one-hundred thousandth that of the two starting materials, producing an extremely fine two-layer laminate. This may be called a process for the formation of an artificial lattice by mechanical means. It explains why mechanical alloying enables many materials to be formed into nanolevel microstructures.

Questions have been raised about whether the process as described in Figure 1 really takes place in MA techniques using various high-energy mills. It has also been observed that the energies of the impact of the balls in the ball mill may not lead to an instantaneous melt and freeze phenomenon. Figure 2 shows an experiment in repeated rolling. In the experiment, a mixture of the original powders was staffed into a stainless steel pipe, 18 mm in inside diameter and 19 mm in outside diameter, and the stainless pipe was pressed to about a 10 mm thickness. The flattened pipe was cold rolled down to 0.5 mm while taking care so that the temperature rise caused by the rolling would be constrained as much as possible. The sample powder was taken out by peeling of the stainless steel, to be refilled in another stainless steel pipe of the same size, and rolling was repeated. Because the refill of the powder was done in random directions, the experiment conditions were, to be exact, not the same as those given in Figure 1, but a repetition of cold rolling many times over at low temperatures enabled us to observe changes in the structure.

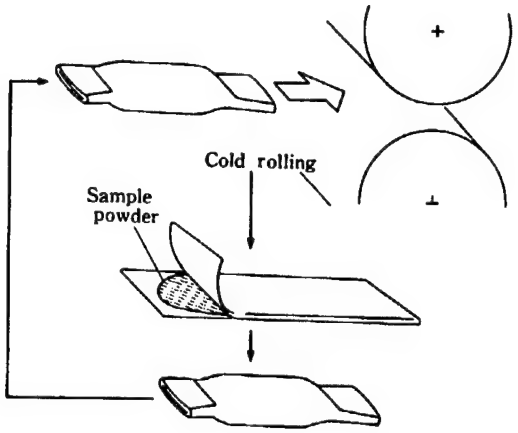

Figure 2. Explanation of Mechanical Alloying Experiment by Repeated Rolling
A mixed powder staffed in a stainless steel pipe is rolled, the sample powder is taken out and is staffed again in a pipe of the same size as that of the original pipe, and rolling is repeated.

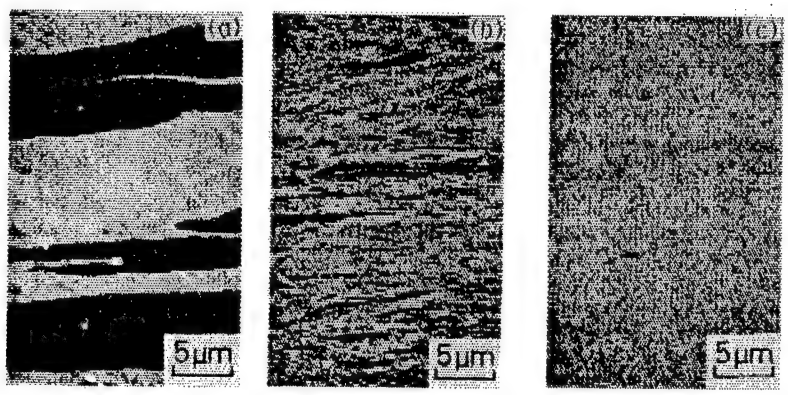

Figure 3. SEM Observations of Mechanical Alloying Process in Repeated Rolling of Ag and Fe Powders
(a) After first rolling; (b) After five rollings; (c) After 200 rollings. Black spots are Ag.

Figure 3 is a scanning electron microscope (SEM) observation of the process by which the structure of an Ag-Fe system is turned into a microstructure after repeated rolling. Ag and Fe do not mix with one another, even when they are in a liquid-phase state. A microstructure of an Ag-Fe system cannot be obtained with the forging technique.

Figure 4 is a transmission electron microscope (TEM) photograph of a Cu-Fe system subjected to a repetition of similar rolling, together with an MA structure obtained using a ball mill.

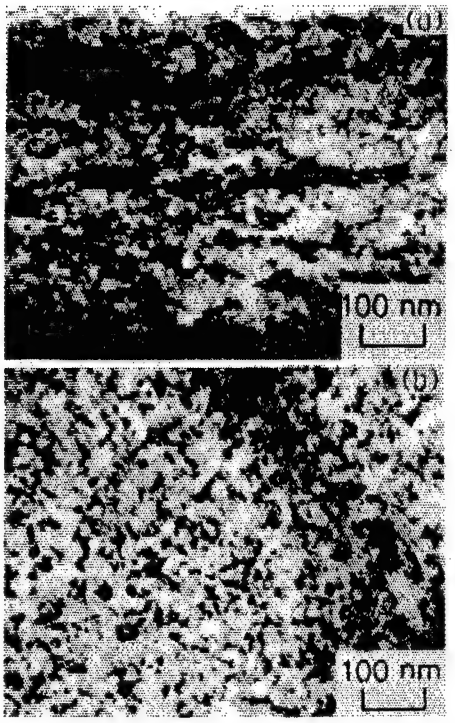

Figure 4. TEM Photograph of Cu-Fe System
(a) shows the structure that was obtained by subjecting a Cu-Fe mixed powder to a repetition of rolling 30 times;
(b) is a TEM image of the structure of the same mixed powder subjected to a treatment in a ball mill for 200 hours.

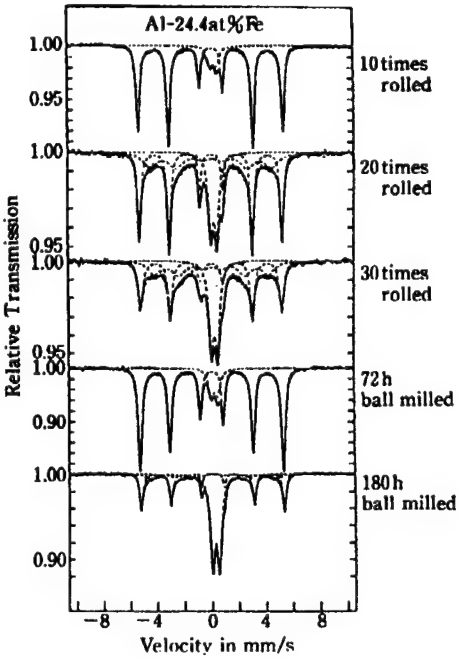

Figure 5. Comparison of Two Alloys of Mixed Powder With an Al-24.4 Atomic Percent Fe
One was produced in a repeated rolling process, and the other was produced by milling in a mill. The nonmagnetic peaks in the Mossbauer spectrum for Fe^{57} correspond to the formation of amorphous phases. In both MA processes, amorphous phases are formed from the initial stages of mechanical alloying.

As can be seen from these examples, the basic principle of MA process is a repetition of rolling. Figure 5 shows a comparison of microscopic structural changes, measured by changes in the Mossbauer spectrum, in an Al-Fe system for the repeated rolling and ball mill techniques. The peaks in the absorption of nonmagnetic iron at the center of the graphs for both the repeated rolling and ball mill methods show the slow incorporation of Fe into the amorphous phase from the initial stages of mechanical alloying.

In mills in actual use, the MA processes, the basic principle of which is repeated rolling, are thought to progress, with the friction and slip between particles contributing to kneading of the alloying elements into a microstructure. Recent tribology research has confirmed that when the surface of a pure copper was scrubbed with a steel for friction, there was observed on the surface of the copper a formation of a layer of an alloy of copper and iron

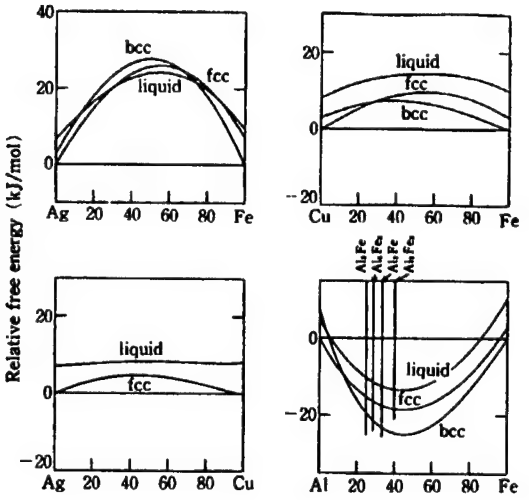

Figure 6. Relative Value of Free Energy at 500 K for Various Phases in Ag–Fe, Cu–Fe, Ag–Cu, and Al–Fe Alloys The diagrams are plotted using mixtures of the powders for the elements as the standard line.

the order of submicrons in thickness. It has also been confirmed that the crystal grains inside the layer had dimensions on the order of nanometers.

3. Thermodynamics for the Formation of Nonequilibrium Phases by MA

Nonequilibrium phases formed by mechanical alloying include:

(1) ultrafine crystal grains (nanostructures);
(2) supersaturated solid solutes;
(3) metastable crystal phases; and
(4) amorphous phases.

The technique of cooling liquids at superfast speeds is seeking to duplicate phases. In the superfast cooling of liquids, the basic principle by which a nonequilibrium phase could be produced was to freeze rapidly the stable-phase high-temperature liquid phase to bring about an excess cooling of the liquid, that is, to cause the hierarchy of free energies to reverse. What relations are there among the mixture of the element powders of the starting materials, the nonequilibrium phase, and the free energy of the stabilized phase in mechanical alloying?

Figure 6 shows the free energy compositions for various phases at 500 K in Ag–Fe, Cu–Fe, Ag–Cu, and Al–Fe systems. These diagrams are plotted using the free energies of the pure elements at 500 K in their stable crystal phases as the standards. The horizontal line linking the original points in each diagram shows the value of the free energy of the mixture of the powders of the two elements.

Figure 7 shows the state-of-equilibrium diagrams for these systems.

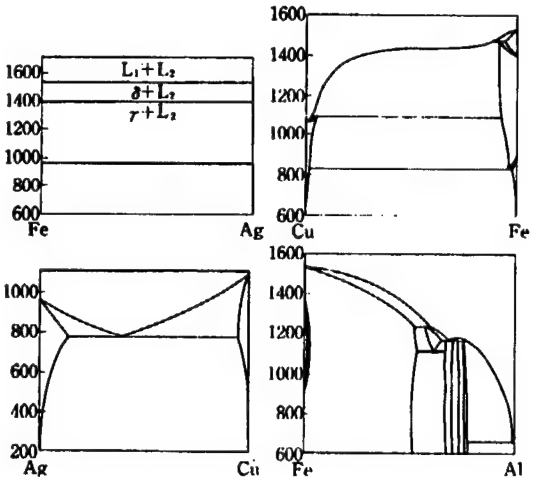

Figure 7. Equilibrium-State Diagrams for Alloy Systems Shown in Figure 6

In Figure 6, let us consider the hierarchy of free energy. In the Al-Fe system, the mixture of powders of the elements has the highest hierarchy except in the compositional areas closer to the Al and Fe ends. That is, the mixture of the powders has a free energy higher than that of the supercooled liquid. Bringing Al-Fe to melt and cooling the melt to the temperature of 500 K is not an easy task, but kneading Al and Fe powders and keeping the mixture's temperature at 500 K is a simple operation. With MA, depending on materials, kneading enables the starting materials in an exceedingly high energy state to be gradually changed into nonequilibrium phases with a lower free energy hierarchy. In an Al-Fe system, mechanical alloying leads to the generation of an amorphous phase. In Figure 6, the phenomenon can be thought of as the mixed powder of Al and Fe metastably "dissolving" by mechanical alloying and the melt supercooling to turn into a liquid.

What will result when mechanical alloying takes place in systems in which the free energy value of the mixed powder is lower in hierarchy than those in other phases? Of the systems shown in Figure 6, the free energy value of the Ag-Fe mixture has the largest positive value. The system's equilibrium state diagram shown in Figure 7 is that of a phase-segregation type, a state in which those elements will not mix even in their liquid phase. Subjecting the system to mechanical alloying turns it into a well-mixed microstructure (Figure 3). Both Ag and Fe dissolve into each other as solid solutions, but their amounts are not large. In Cu-Fe systems, in which the value of free energy of mixing is much lower, Fe is incorporated into Cu of fcc on the Cu side, and Cu is incorporated into Fe of bcc on the Fe side, both as solid solutions. In Ag-Cu systems in which the mixture has a positive but small free energy value, MA has been confirmed to lead to formation of an oversaturated solid solution throughout the entire composition in experiments. Figure 8 gives the results of measurements of the lattice parameters of the forced solution obtained by mechanical alloying. They agree well with the results of the lattice parameter of an alloy obtained in an experiment involving freezing of a liquid at ultrafast speeds, given in the figure for comparison.

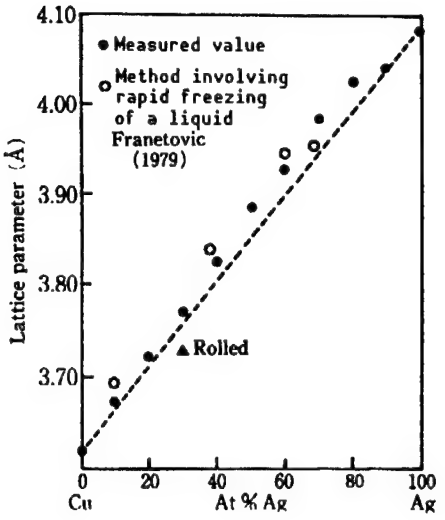

Figure 8. Relationship Between Lattice Parameters of Ag–Cu Alloy Obtained by Mechanical Alloying and Its Alloy Compositions
For comparison, similar relations are also shown for an alloy obtained in a rapid freezing of a liquid method.

From the deviations of the positive values from Vegard's Law, we can qualitatively explain that the free energy of the mixture is positive, that is, Ag and Cu are elements that slightly repel one another. P. Duwez tested the rapid freezing of a liquid method using an Ag–Cu system, and the intersections (T_0 curve) between free energies of the supercooled liquid and those of the oversaturated solid solution alloy are not too far apart, which is why the alloy tends to have a 100–percent solid solution in rapid freezing. The fact that the same tendency is observed in mechanical alloying, an operation that completely differs from rapid freezing, suggests that thermodynamic conditions have a large influence on the formation of nonequilibrium phases.

The fact that oversaturated solid solution alloys can be formed by mechanical alloying even in systems in which the free energy of the mixture is positive reveals that the energy state has risen over that for the mixed powder, the starting material. The accumulation of energy (enthalpy) by mechanical alloying can be measured using the differential scanning calorimetry (DSC) technique. Figure 9 shows results of measurement of Ag–Cu. Even in the pure metals, Ag and Cu, calories are accumulated by mechanical alloying, and the degrees of accumulation are much higher for their alloy. The values are seen to be above the free energy values of the mixed powder for the oversaturated solid solution alloy.

This energy may be considered as an accumulation of interfacial energy in the grain boundaries between microscopic crystal grains. In alloy systems in which the free energy values of liquids frozen excessively are smaller than the accumulated energy values, even those systems that have the free energy of the mixture showing a positive value may be formed amorphously by mechanical alloying.

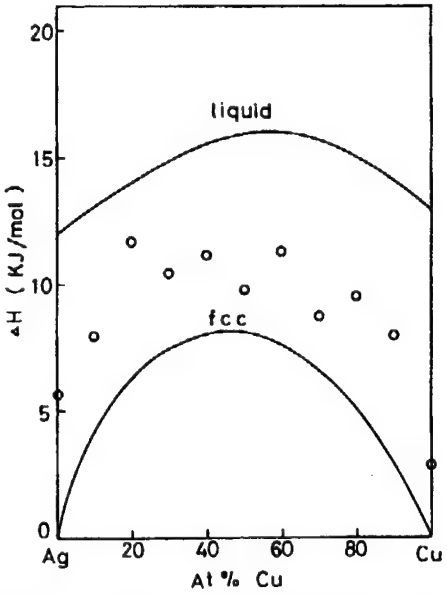

Figure 9. Values of Energy Accumulated in Ag–Cu, Measured by a Scanning Calorimeter (DSC)

Table 1. Nonequilibrium Structures in Various Alloys Obtained by Repeated Rolling or Ball Milling

Alloys studied	Metastable phases observed		Enthalpy of mixing in liquid state
	Repeated rolling	Ball milling	(kJ/mol)
$Ag_{50}Fe_{50}$	Almost no SS	Partial SS	20.3
$Cu_{70}Fe_{30}$	Partial SS	SS	7.3
$Ag_{30}Cu_{70}$	Partial SS	SS	3.3
$Al_{67}Fe_{33}$	Partial SS plus Am.	Am.	−18.8

SS = Oversaturated solid solution
Am = Amorphous phase

Table 1 summarizes the chemical properties of the four classes of alloy systems obtained by mechanical alloying. In the experiment, amorphous phases were obtained only in those alloy systems that had negative free energy values of mixtures, that is, the class of Al–Fe alloys that showed a strong tendency to form intermetallic compounds. The formation of amorphous phases was also observed in the class of Al–Ti alloys produced by mechanical alloying. For Al–Ni alloy systems, mechanical alloying tended to give them amorphous phases, but long hours of mechanical alloying led to the formation of an equilibrium phase of NiAl. In Al–Ni alloys, the enthalpy for the formation of a compound was exceedingly large, about 50 kJ/mol in the case of $Al_{50}Ni_{50}$ composition, and the energy difference (phase transformation motive power) between the mixed

powder and the intermetallic compound was large. These may explain the tendency to form compounds rather than amorphous phases. In Al–Cu alloys in which the free energy values of mixing were negative but were not so large, mechanical alloying of a greater part of the Al side of the composition led to the formation of neither an amorphous phase nor an Al_2Cu phase. The stable phase and only a Cu–rich compound called metastable Al_4Cu_9 was formed. The reason is not yet known, but it may be that in Al–Cu alloys, atoms have a large mobility even at room temperature. Hence, even if the composition has once turned amorphous, it may soon change phase to become a compound. In fact, measurements of an MA powder immediately after mechanical alloying and after a passage of a few days during which it was kept at room temperature produced different lattice parameters. What phase will be generated is determined by the driving force for phase metamorphosis and kinetic factors such as the ease with which the nuclei for the phase are formed and the velocity of the growth. Forecasting is very difficult.

4. Solid Forming of MA Powder

Regardless of the MA technique involved, all nonequilibrium materials obtained by mechanical alloying take a powdery form. To measure their physical properties or exploit them as materials for some products, they have to be formed into solids. In the initial stages of the development of the MA technique by Inco Corporation, the objective was to manufacture Ni–based superalloys. The basic principle was this: An MA powder is hot extruded, and heat–treating the extrusion, while keeping the oxide dispersion at the state as it was at the start of MA, enables the crystal grains to be recrystallized in large enough sizes. However, it has been proven in experiments that formed materials obtained by extruding or hot pressing in vacuum aluminum alloys prepared by mechanical alloying have much difficulty in increasing their crystal grain sizes even when heated to a temperature of about 400°C. Experiments will be conducted on development of materials with excellent properties by solidifying and fabricating MA powders into formed shapes so that their nonequilibrium structures remain intact.

Reportedly, mechanical alloying of TiAl alloys, followed by hot pressing in vacuum, enables the microscopic crystal grains of the MA powder to be kept intact to some extent, suggesting the possibility for superelasticity of microscopic grains. In this context, the use of hot pressing in vacuum and hot isostatic pressing (HIP) techniques for solid forming of MA powders will increase. As an alternative, a pressure–forming process called the pseudo–HIP method (a method for solidifying and forming MA powder under conditions of pressurizing, heating, and vacuum), in which a solid pressure medium such as sand is used, has been devised (Figure 10). In addition to safety, the use of sand as a pressure medium has the following advantages: heating or pressurizing can be easily applied and the spaces between sand grains can be evacuated.

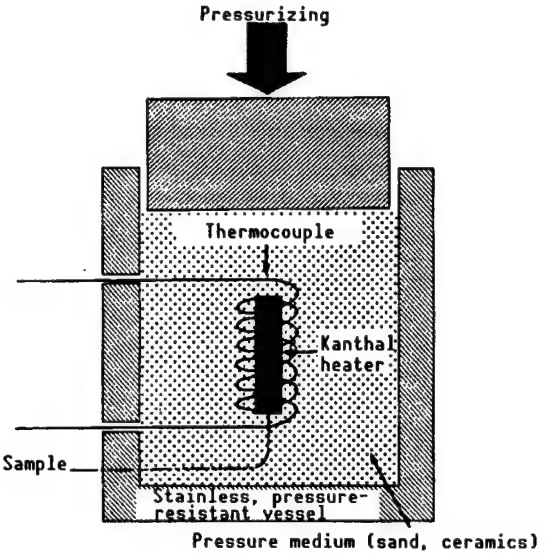

Figure 10. Example of Pseudo-HIP Process

5. Conclusion

The MA process will enable the production of the type of nonequilibrium materials now available with rapid cooling and solidification techniques. Because no liquids are used in the process, we do not have to worry about crucibles for melting or ambients or about the difference in melting points, oxidation, or evaporation. Mechanical alloying has been proven capable of creating nonequilibrium states (for example, the capacity to form amorphous structures, degrees of oversaturation in alloys, degrees of finesse of crystal grains) that are on a par with or superior to those obtained with rapid solidification techniques. Aluminum, in particular, has properties best suited to its use as the basic material for the formation of nonequilibrium alloys by mechanical alloying, such as plastic transitions, resistance to oxidation, and the ease of shaping after mechanical alloying.

References

1. Benjamin, J.S., "Mechanical Alloying," SCIENTIFIC AMERICAN, Vol 234 No 5, 1976, p 40.

2. "Metals Handbook," ASM, Vol 7, 1984, pp 56-70, 722-727.

3. Sundaresan, R. and Froes, F.H., "Mechanical Alloying of Light Metals," NEW MATERIALS BY MECHANICAL ALLOYING TECHNIQUES, Ed. E. Arzt and L. Schultz, DGM, 1989, p 243.

4. Horiuchi, R., et al., "Mechanical Alloying of Aluminum and Fiber-Reinforced Alloys," LIGHT METALS, No 32, 1982, p 688.

5. Text for the 30th Symposium of the Japan Institute of Light Metals, "Recent Powder Metallurgy Technology for Aluminum Alloys," 1987.

6. A minifeature article in the JOURNAL OF THE JAPAN INSTITUTE OF METALS, "Recent Trends in Research on Mechanical Alloying," Vol 27 No 10, 1988.

7. Shingu, H., "The Formation of Amorphous Alloys by Mechanical Alloying," CHEMISTRY, Vol 43 No 11, 1988, p 760.

8. "Solid State Amorphizing Transformation," Ed., R.B. Schwarz and W.L. Johnson, Elsevier Lausanne, 1988.

9. "Solid State Powder Processing," Ed. A.H. Clauer and J.J. deBarbadillo, TMS, 1990.

10. International Symposium on Amorphization by Solid State Reaction, held at Grenoble, France, February 1990.

11. ASM International Conference on Structural Applications of Mechanical Alloying, held at Myrtle Beach, S.C., U.S.A., March 1990.

12. Shingu, P.H.,

13. Shingu, P.H., et al., "Nanometer Order Crystalline Structures of Al-Fe Alloys Produced by Mechanical Alloying," Suppl. Trans. JIM, Vol 29, 1988, p 3.

14. Rigney, D.A., "Sliding Wear of Metals," ANN. REV. MAT. SCI, Vol 18, 1988, p 141.

15. Inoue, N., Ishihara, K.N., and Shingu, P.H., "Nonequilibrium Phases of Al-Ti Alloys Formed by Mechanical Alloying and RF Sputtering," Proceedings First International SAMPE, 1989, p 13.

16. Shingu, H., et al., "Mechanical Alloying of Al-Cu Systems," Preprint for presentation at the 1990 Spring Meeting of the Japan Institute of metals, p 372.

17. Ibid., "Mechanical Alloying and Formation of Al-Fe Alloys," LIGHT METALS, No 38, 1988, p 165.

18. Sugimoto, H., Ameyama, K., Inada, T., and Tokizane, M., "The Structure and Mechanical Properties of TiAl Compact Produced by Hot Pressing of Mechanically Alloyed Powder,"

19. Shingu, H., The test for a Japan Institute of Metals seminar, "Intermetallic Compounds," 1990, p 61.

20. Shingu, H., et al., "Reaction Synthesis of Intermetallic Compounds by (Pseudo)-HIP Technology and Their Forming to Near-Net Shape," POWDER AND POWDER METALLURGY, No 37, 1990, p 78.

Design of Ceramics by Computer Graphics

916C0033G Osaka DAI 18 KAI NYU SERAMIKKUSU SEMINA TEKISUTO in Japanese
2 Mar 91 pp 101-110

[Article by Akira Miyamoto, Faculty of Engineering, Kyoto University: "Design of Functional Ceramics by Computer Graphics"]

[Text] **1. Introduction**

Since the development of the ENIAC computer in 1946 by Morkly and (Exhert), the world's first, helped by advances in vacuum tube, diode, integrated circuit (IC), large-scale integration (LSI), and super-LSI technology, computers have come to be used at rapid speeds in a variety of fields including science, technology, and arts. In the chemical field, computers have had a great impact on the ways in which research and development is promoted by making it possible to use such techniques and systems as quantum chemistry calculations; simulation systems like molecular dynamics (MD) method, Monte Carlo (MC) method, and molecular mechanics (MM); artificial intelligence systems; database systems; and computer graphics (CG).

Computer graphics demand high levels of computer functions but the technique is user-friendly for people engaged in the front line of materials development. This paper describes applications of computer graphics in the development of inorganic functional materials such as vanadium oxide catalysts used in cleaning nitrogen oxides or in selective oxidation of hydrocarbons, zeolites for high-performance absorption and desorption, magnetic materials for magnetic tapes, high-temperature superconducting thin films, and gold catalysts for use in the cleaning of carbon monoxides.

2. V_2O_5/TiO_2 Ultrathin-Layer Catalysts

The element V_2O_5, which plays an important role as a catalyst in the reaction for purification of nitrogen oxides (NO_x) and in the selective oxidation reaction of hydrocarbons, is rarely used but is used fixated and dispersed in oxides such as TiO_2, Al_2O_3, SiO_2, and ZrO_2. The performance of a catalyst is greatly dependent on the kind of carrier oxide, but TiO_2 carriers show excellent properties in most reactions. To elucidate the effect of the TiO_2 carrier, studies have been done using a variety of equipment.

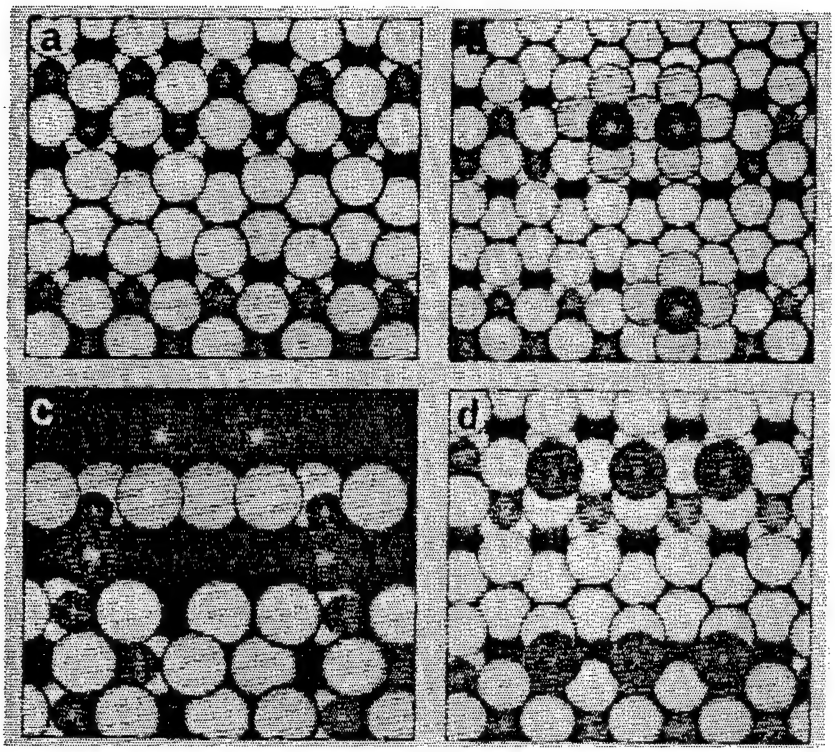

Figure 1. On TiO_2 (Anatase) (010) Plane (a) VO_5, (b) V_2O_9, Unit, and (c) and (d), Bonds of V_2O_5 Clusters

According to the results of research by the rectangular pulse method, the (010) plane of V_2O_5 is selectively exposed to the surface in the case of V_2O_5/TiO_2. Epitaxial growth of V_2O_5 as such is not observed in any other carriers such as Al_2O_3, ZrO_2, and SiO_2.

The crystal structure of V_2O_5 consists of quadrangular pyramid units of VO_5 bound together in a zigzag chain. Crystallographic research on conformity between various crystal planes of the carrier oxides and these VO_5 units or (010) planes, which was conducted using computer graphics is described. In TiO_2 (anatase), six oxygen ions are arranged around a Ti ion, but on the (010) plane, four oxygen ions exist around a Ti ion on the same plane (Figure 1(a)), making it possible for them to bind with the four oxygen ions on the bottom surface of a VO_5 quadrangular pyramid unit. The bond distances and bond angles are small, meaning a VO_5 unit has a crystallographical conformity to the (010) plane of TiO_2 (anatase) (Figure 1(b)). Similarly, a good fit exists for a V_2O_5 cluster containing a large number of VO_5 units (Figure 1(c),(d)), enabling epitaxial growth on the (010) plane of V_2O_5.

3. High-Temperature Superconducting Oxide Thin Films

Since the discovery of high-temperature superconductors by Bednorz and Muller, active research has been done on high-temperature superconductors worldwide. However, these superconductors have problems: how to develop bulk oxides whose crystals feature high critical temperatures (T_c) and high critical current

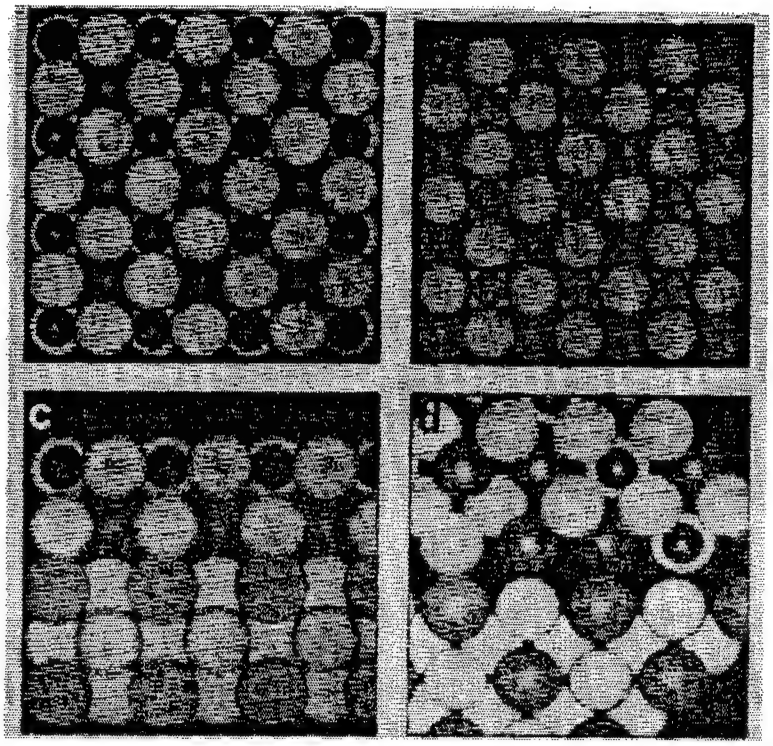

Figure 2. Computer Graphics Images of Epitaxial Junctions of La_2CuO_4 on $SrTiO_3$ Substrates
(a) La_2CuO_4 (001) plane
(b) $SrTiO_3$ (100) plane
(c) La_2CuO_4 (001) plane on $SrTiO_3$ (100) plane
(d) La_2CuO_4 (103) plane on $SrTiO_3$ (110) plane

density (J_c) and how to fabricate thin films of these bulk oxides so they will find use in a new class of superconducting devices. As for superconducting materials, the development of the La-Ba-Cu-O system (40 K class) was followed by development of the Ba-Y-Cu-O (90 K class), Bi-Sr-Ca-Cu-O (120 K class), and Ti-Ba-Ca-Cu-O (130 K class) systems. As the substrate materials for these systems, studies are being done on $SrTiO_3$, MgO, ZrO_2, SiO_2, TiO_2, CaF_2, Al_2O_3, and Ag. $SrTiO_3$, MgO, and ZrO_2, among others, are gaining attention. This paper discusses the interaction between substrate and oxide in high-temperature thin films, using the epitaxial growth of La_2CuO_4 on $SrTiO_3$ as an example.

Of various crystal planes of La_2CuO_4, a CG image of the (001) plane is the most important of all in the realization of a superconducting phenomenon (Figure 2(a)). Given in Figure 2(b) is a computer image of the (100) plane of $SrTiO_3$, a material with excellent features for use as substrates for thin films of high-temperature superconductors. Four oxygen ions are arranged around a Ti one on the planar plane and one is positioned below it, for a total of five oxygen ions. This arrangement resembles well the arrangement of ions around a Cu ion in La_2CuO_4. Ionic radii of Cu and Ti and of La and Sr are very close. Figure 2(c) gives a cross section of the junction of the (001) plane of La_2CuO_4 to the (100) plane of $SrTiO_3$. Atomic arrangements of the two oxides at the

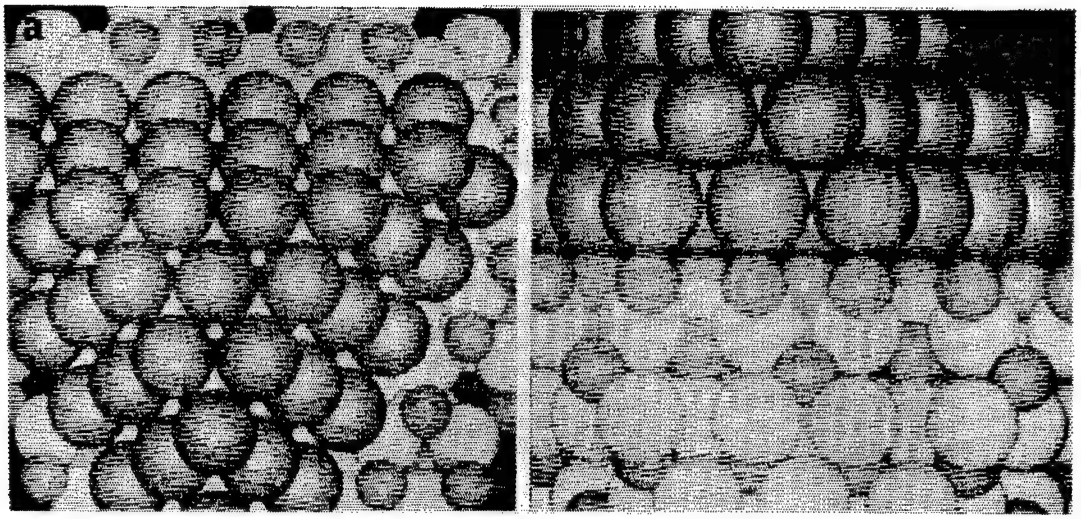

Figure 3. CG Images of Junctions at Interface Between Co_3O_4 (111) Plane and Au (111) Plane

interface are in good agreement. Furthermore, oxygen anions of $SrTiO_3$ are located close to cations of La_2CuO_4 at the interface, and oxygen anions of $SrTiO_3$ are positioned in the vicinities of oxygen anions of La_2CuO_4, showing that the heterojunction of the two oxides is expected from the perspective of energy. This explains the results of experiments in epitaxial growth of the La_2CuO_4 (001) plane on the (100) plane of the $SrTiO_3$ substrate. Looking at the computer graphic images of the La_2CuO_4 (103) plane on the (110) plane of $SrTiO_3$ and the atomic arrangements of the two oxides at the interface, the cation and anion distributions well explain the results of experiments in epitaxial growth of the (103) plane of La_2CuO_4 on the (110) plane of $SrTiO_3$. Using similar methods, junctions of $Ba_2YCu_3O_{7-x}$ of MgO on $SrTiO_3$ substrates and of La_2CuO_4 or $Ba_2YCu_3O_{7-x}$ on ZrO_2 substrates are being investigated.

4. Junctions at the Metal-Carrier Interface in Gold Catalysts

Gold, the most stable of all precious metals, is lacking in activity when used as a catalyst. Haruta, et al., have shown that the use of a coprecipitation method enables ultrafine grains of gold with grain diameters of less than 10 nm to be fixated into a metal oxide. Au/α–Fe_2O_3, Au/Co_3O_4, and Au/NiO, among others, showed especially high levels of activity in low–temperature oxidation of carbon monoxide. Observations by a high–resolution electron microscope revealed the junctions of the (111) plane of the Au on the (110) plane of α–Fe_2O_3, the (111) plane of Au on the (111) plane Co_3O_2, and the (111) plane of Au on the (111) plane of NiO. Figure 3 shows computer images of junctions at the interface between the (111) plane of Co_3O_4 and the (111) plane of Au. Figure 3(a) shows the junction surface as seen from the direction of the (111) plane of Co_3O_4. Figure 3(b) shows a cross section of a junction surface. Arrangements of Co ions and oxygen ions at the interface resemble closely that of Au, and all Co ions have Au atoms positioned above. Figure 3 is an example of a case in which Co ions are exposed to the surface, but a similar phenomenon is seen even when oxygen ions are exposed. The (111) plane of NiO

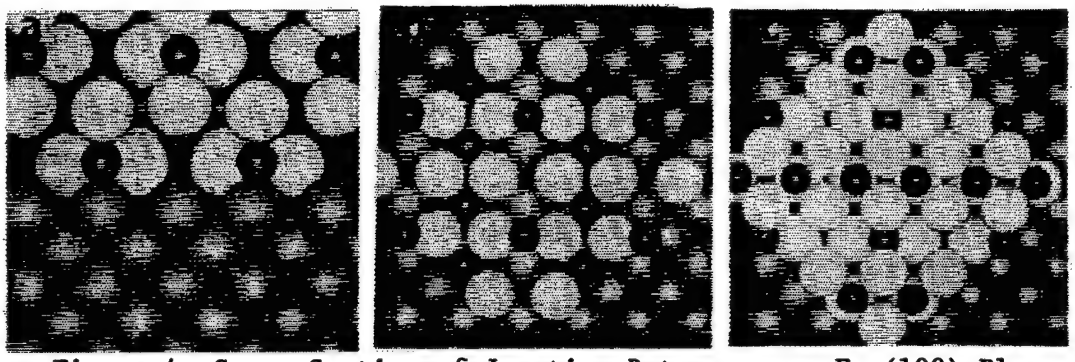

Figure 4. Cross Section of Junction Between an α–Fe (100) Plane and an Fe_2O_3 Plane (a), a Monatomic Layer of Fe_2O_3 on α–Fe (100) Plane (b), and a Two-Atomic Layer Fe_2O_3 (c)

and the (111) plane of Au also have been shown to have a conformity of atomic arrangement.

5. Oxidation Protective Films of Metal Magnetic Bodies

Fine-grain metallic iron (metal) has about two times as much magnetization as cobalt epitaxial iron oxide. Its coercive force can be simply controlled to 1,000~1,500 Oe. For these reasons, the metal is beginning to find use as the magnetic recording material for high-density recording. Two methods are available for the manufacture of the metal's powder: one involves reduction of iron hydroxide, and the other involves evaporation of metal in an inert gas. Metal tape using the metal powder as its magnetic recording medium has a problem with increasing corrosion: it suffers from decreasing output power, and the tape needs to be provided with an anticorrosion treatment. Kishimoto, et al., have shown that oxidizing the film gradually at temperatures of 40~80°C in an oxygen–nitrogen mixed gas ambient enables a fine-grain protective film of Fe_3O_4 to be formed on the surface of the needle-like α–Fe.

Figure 4 shows computer images of the interface of a junction between the (100) plane of an α–Fe crystal and the (100) plane of Fe_3O_4. As seen in the figure, Fe atoms on the (100) plane of α–Fe show good conformity with Fe ions or oxygen ions on the (100) plane of Fe_3O_4. Although a single atomic layer of Fe–O is unable to coat the entire Fe surface (Figure 4(b)), if the oxide layer is properly formed a coating about two layers of atoms thick can protect the Fe.

6. Molecular-Sieve Properties of Zeolite

Molecules which are smaller than the pores of zeolites are adsorbed but molecules larger than those pores are not adsorbed. This is the molecular-sieve character of zeolites. However, if separation is to be had at much higher levels, an understanding of the possibility of diffusion into the pores is not enough. An understanding at the molecular level of what effects the porous structure of zeolites and the structure of the molecules to be adsorbed will have on the adsorbing properties of the zeolites is important.

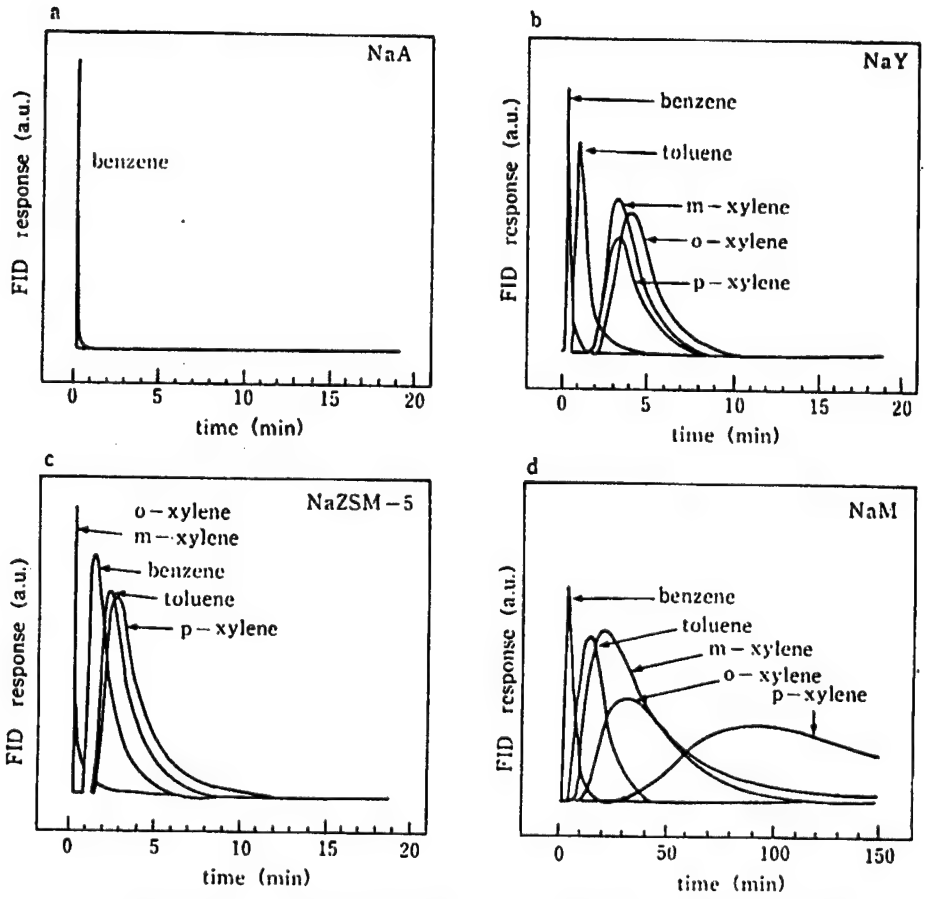

Figure 5. Chromatograms of Aromatic Hydrocarbons Adsorbed n Zeolites (300°C)

Examples of studies conducted using computer graphics on the characteristics of zeolites with different porous structures to adsorb para-aromatics are introduced.

Figure 5 gives chromatograms of aromatic hydrocarbons adsorbed on NaA, NaY, NaZSM-5, and NaM. The adsorbing characteristics differ greatly, depending on the shapes of the molecules to be adsorbed and the kinds of the zeolites used.

Figure 6 shows computer images of the aromatic hydrocarbons adsorbed on different zeolites. For NaA zeolite (Figures 5(a) and 6(a)), the collision radii of benzene rings are much larger than those of the 8-oxygen-atom rings of the A-type zeolite. Consequently, benzene is not adsorbed into NaA. In NaY (Figure 5(b)), all molecules are adsorbed and adsorption increases with benzene toluene < xylene (in that order). There are, however, not many differences in the level of adsorption among the three isomers of xylene because the Y type's oxygen-12 rings are sufficiently larger than the o-xylene and m-xylene (Figure 6(b)). Furthermore, the lack of three-dimensional obstacles on the walls of the pores enables all the molecules to be adsorbed.

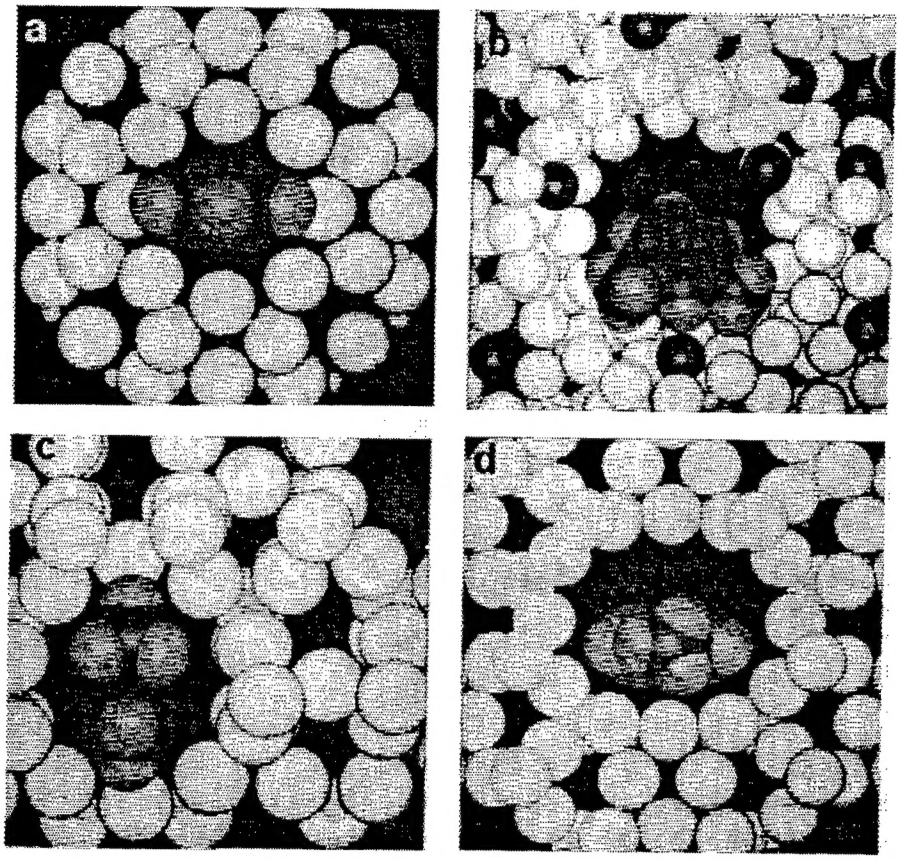

Figure 6. Computer Graphic Images of Aromatic Hydrocarbons Adsorbed Inside Zeolite Pores

In NaZSM-5 having 10-oxygen-atom rings (Figures 5(c), 6(c)), benzene, toluene, and p-xylene are adsorbed but o-xylene and m-xylene are scarcely adsorbed. Adsorption is much larger in NaM (Figures 5(d), 6(d)) than in NaY and NaZSM-5. As with NaY having the same 12-atom rings, NaM tends to adsorb molecules having larger numbers of methyl groups more readily than others, but of all xylene monomers, p-xylene is adsorbed most readily. As shown in Figure 6(d), NaM has oval pores, and the curvatures of the ellipsoids and the Van der Waals curvatures of benzene molecules are in good conformity. For toluene and p-xylene, it is believed the same good conformity occurs when they are adsorbed with the directions of their molecular axes in the same direction as those of the one-dimensional pores of NaM. The adsorption increases eases in the number of methyl groups. These circumstances agree well with experiment results.

7. Multiple Functions of Solid Catalysts

Cooperative catalytic functions by multifunctional groups existing on the surfaces of solids, such as the acid-base site cooperative catalytic action, are important concepts in the design of high-activity, high-selectivity catalysts. Ito, et al., have suggested that side-chain alkylation reactions of toluene by methanol are caused by the cooperative acid-base catalytic action.

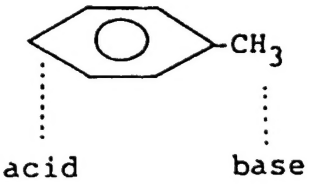

Figure 7. Acid-Base Pair Site

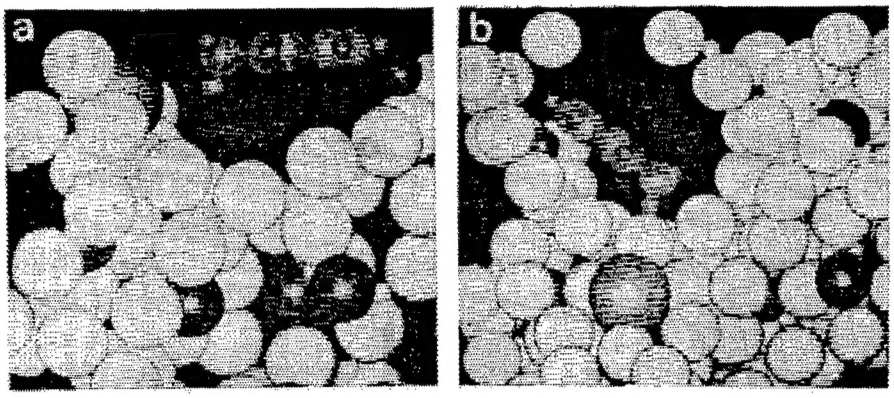

Figure 8. Computer Graphic Images of Toluene Adsorbed on RbLiNaY (a) and RbLiNaX (b)

That is, the existence of an acid-base pair site (Figure 7) is important for cooperative reaction, in which the toluene's methyl radicals interact with base sites. At the same time, the benzene rings interact with acid sites in a concerted manner.

We examine the probability of the formation of an acid-base pair site in various zeolites using computer graphics technology. Figure 8 shows computer images of toluene adsorbed on Rb, Li ion exchange Y-type zeolite (RbLiNaY), and Rb, Li ion exchange X-type zeolite (RbLiNaX). Base sites are formed on oxygen anions positioned adjacent to Rb cations, but in these zeolites Li ions are positioned close to basic oxygen anions. Consequently, in these zeolites cooperative interactions between acid sites and basic sites are thought to take place more easily than in other zeolites, including ZSM-5. This agrees well with experiment results in which the side-chain alkyl reactions of toluene by methanol and X- and Y-type zeolites have much higher levels of activation than ZSM-5 or "moldenite." A closer examination of Figure 8 reveals that on the RbLiNaY catalyst, methyl radicals cannot achieve a good fit to basic oxygen anions even if benzene rings have managed to get themselves adsorbed by Li cations because of the distances between Li cations and basic oxygen anions. On the RbLiNaX catalyst (Figure 8(b)), the formation of pair sites in which molecules of toluene interact simultaneously with acid sites and basic sites becomes possible. This agrees well with experiment results in which X-type zeolites display much higher levels of activation than Y-type zeolites.

8. Visualization of Dynamic Structures and Properties: Simulation of the molecular dynamics of the process for fixation of ultrafine metallic particles on a metal oxide carrier

The molecular dynamics (MD) method elucidates the structure and properties of composites by solving the equations of motion of atoms or particles that constitute matter. The technique has been used in unraveling the structures and physical properties of a large variety of materials, ranging from simple liquids to water, molten salts, inorganic crystals, glass, and proteins. We have investigated the structures and functions of a large variety of materials using computer graphics. In the process, we have come to see a need for treating structures of materials dynamically. As a first step to research into catalysts and surface functional materials using MD and computer graphics, we attempted to simulate the process by which ultrafine grains of gold are fixated on the (100) plane of MgO.

MD calculations were conducted using the molecular dynamics program for inorganic crystals, XDORTO. Motions of atoms were calculated using the Verlet method under a periodic boundary condition. The electrostatic interactions were calculated using the Ewald method. Temperature and pressure controls used the forced scaling method. Setting Δt for a step at $2.5\sim10^{-5}$, we conducted calculations for several thousand to ten thousands of steps under various temperature and pressure conditions. Dynamic movements of each of the atoms were visualized using computer graphics. For interatomic potentials, we considered two-body interactions, each consisting of the electrostatic potential, the neighbor-repulsion potential, and the Morse potential. The parameters were determined so that bulk crystal structures of MgO or gold would be realized.

Figure 9(a) shows the results of an MD simulation of the (100) plane (600 K) of MgO. Formation of a surface gives rise to a problem of what change the lattice constant on the surface and the relative positions of Mg and O ions will undergo relative to their values inside the bulk, but changes are small on the MgO (100) plane, as shown in the figure. The results agree well with the results of experiments obtained by reflected high-energy electron diffraction (RHEED). We also conducted MD calculations of clusters of atoms of gold with varying numbers of atoms. Figure 9(b) shows a computer image of a three-dimensional cluster of Au_{32}, obtained after 2,500-step calculations at 6,000 K. From the figure, we can see that the thermal motion of the surface atoms changed the three-dimensional structure with a large surface energy into a smaller spherical cluster.

We conducted MD calculations of systems that had gold clusters with different numbers of atoms positioned near the (100) plane of MgO. Calculation results of a system with an Au_{32} cluster are shown in Figure 9. While carrying on with its own thermal motion, the Au_{32} cluster as a whole approaches the surface of MgO gradually (Figure 9(c)) and, after 6,200 steps (Figure 9(d)), is fixated into the MgO as a semispherical Au_{32} cluster.

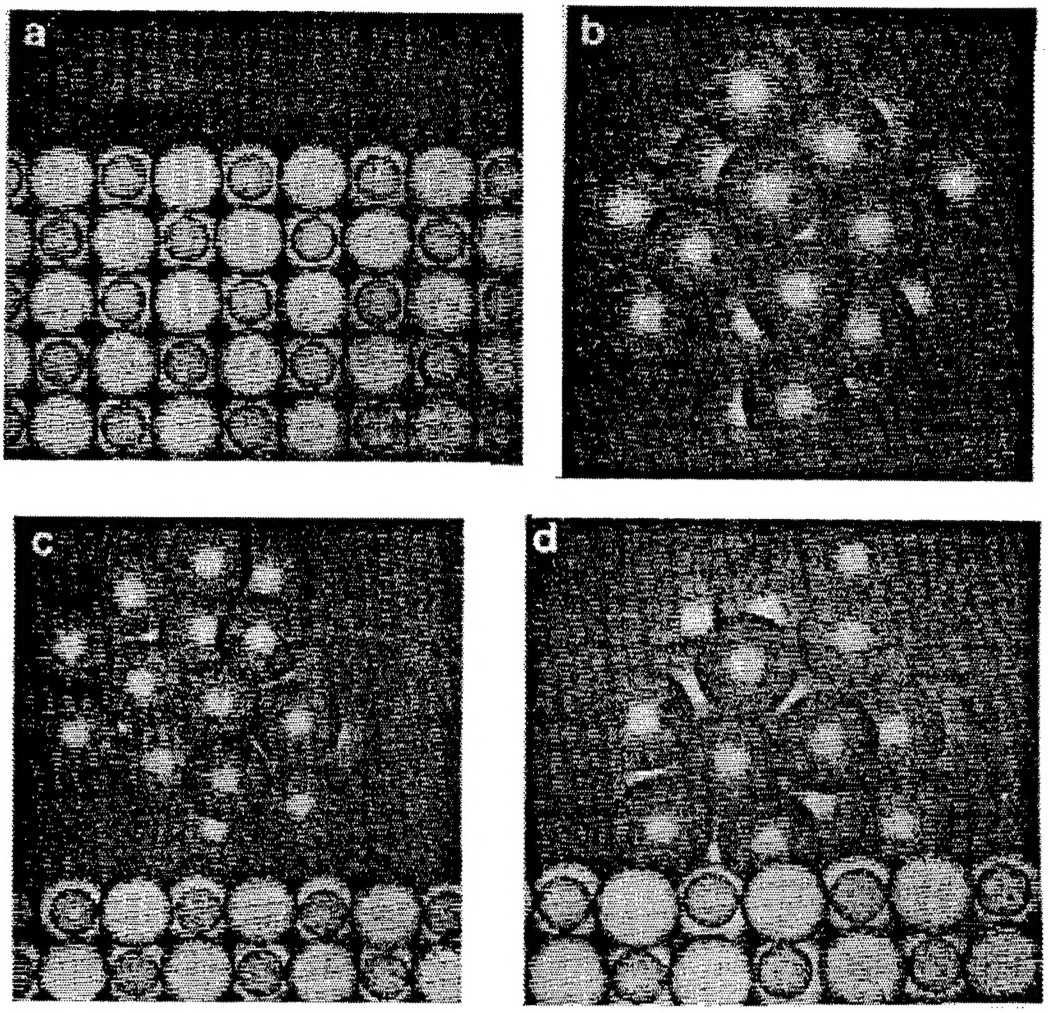

Figure 9. Computer Graphic Images of MgO (100) Plane (a), Au_{32} Cluster (b), and Process for Fixation of Au_{32} Cluster on MgO (100) Plane (c),(d)

Research on dynamic behaviors of functional materials using MD and computer graphics is branching into studies of molecular-sieve materials such as ion-exchange zeolites, metallosilicates, and VPI-5 and of sintering behaviors of ultrafine particles.

- END -